A SPATIO-TEMPORAL ASSESSMENT OF URBAN FLOODING WITHIN THE UNITED STATES

by

AMANDA JEAN SCHROEDER

(Under the Direction of J Marshall Shepherd)

ABSTRACT

Urbanization leads to drastic changes in land cover, which has major effects on local hydrology. Recently documented urban flooding has highlighted the need for more research on the unique interplay between hydrometeorology and the built environment, so this dissertation explored three major components of the urban water cycle that affect the development and magnitude of flash floods: atmospheric contributors, hydrologic response, and land use/land cover characteristics. To explore the atmospheric component, quantitative analyses were performed on thermodynamic variables from forty urban flood events. Spatio-temporal hydroclimatological trends and characteristics associated with urban flooding events for several cities were examined to address the hydrologic response and land use/land cover aspect. Finally, the three components (atmospheric, hydrologic, and land use/land cover) were combined via an observational case study of a historic flood in Oklahoma City to identify what urban-atmospheric-hydrologic interactions played a role in the evolution of the event. Additionally, various observational networks, including the unique, intra-urban Oklahoma City Micronet, were examined to identify optimal observing methodology.

Results showed that detailed assessments of the atmospheric *and* surface/subsurface conditions (from both a hydrologic and land use perspective) are crucial to obtain accurate assessments of the potential for, and resultant magnitude of, urban flash floods. When assessing the atmospheric conditions prior to a heavy rain event, the precipitable water (PW) anomaly with respect to the local PW climatology, as well as the warm cloud depth (WCD), MUCAPE, and wind shear are key. From a hydrologic and land use perspective, results illustrated that urban basins experienced a higher percentage of flood events during abnormally dry conditions and were more "flashy". Finally, from an observational perspective, gage-biased radar mosaic QPE provided the best continuous representation of the rainfall distribution over the area but were not adequately able to capture all details of the observed distribution from the Oklahoma City Micronet, illustrating the need to include *both* in situ and remotely sensed observing networks for an improved characterization of urban rainfall.

INDEX WORDS: urban flood, flash flood, urban hydrology, hydrometeorology, Oklahoma City

A SPATIO-TEMPORAL ASSESSMENT OF URBAN FLOODING WITHIN THE UNITED STATES

by

AMANDA JEAN SCHROEDER

BS, University of Oklahoma, 2008

MS, University of Oklahoma, 2010

A Dissertation Submitted to the Graduate Faculty of The University of Georgia in Partial Fulfillment of the Requirements for the Degree

DOCTOR OF PHILOSOPHY

ATHENS, GEORGIA

2015

A SPATIO-TEMPORAL ASSESSMENT OF URBAN FLOODING WITHIN THE UNITED STATES

by

AMANDA JEAN SCHROEDER

Major Professor:	J Marshall Shepherd
Committee:	Thomas Mote
	Lan Mu
	Todd Rasmussen
	Jeffrey B Basara

Electronic Version Approved:

Julie Coffield
Interim Dean of the Graduate School
The University of Georgia
May 2015

DEDICATION

This dissertation is dedicated to my husband, Chris, and two children, Laura and Anthony. Without their continued support, patience, and encouragement, this body of work would not have been possible. I am eternally grateful to have been blessed with such a wonderful family.

ACKNOWLEDGEMENTS

I would like to acknowledge the National Aeronautics and Space Administration Precipitation Measurement Mission Program for their support of this dissertation through a NASA ROSES grant. Additionally, I would also like to acknowledge my committee members for their insight, guidance, and support throughout this process. Finally, I would like to acknowledge the staff at the National Weather Service Weather Forecast Office in Fort Worth, Texas for their patience and support during the completion of this dissertation.

TABLE OF CONTENTS

Page

ACKNOWLEDGEMENTS v

LIST OF TABLES viii

LIST OF FIGURES x

CHAPTER

1 INTRODUCTION AND LITERATURE REVIEW 1

1.1 Introduction 1

1.2 Research Objectives 4

1.3 Significance of Research 8

1.4 References 9

2 INSIGHTS INTO ATMOSPHERIC CONTRIBUTORS TO URBAN FLASH FLOODING ACROSS THE UNITED STATE USING AN ANALYSIS OF RAWINSONDE DATA AND ASSOCIATED CALCULATED PARAMETERS 15

2.1 Introduction 17

2.2 Data and Methods 20

2.3 Results 23

2.4 Conclusions 29

2.5 References 32

3 HYDROCLIMATOLOGICAL TREND ANALYSIS OF FLOODS USING DAILY MAXIMUM DISCHARGE 45

3.1 Introduction....47

3.2 Study Area 49

3.3 Data....50

3.4 Methods 53

3.5 Results....56

3.6 Conclusions....65

3.7 References....67

4 ATMOSPHERIC AND HYDROLOGIC CONTRIBUTORS TO THE 14 JUNE 2010 FLASH FLOOD EVENT IN OKLAHOMA CITY....96

4.1 Introduction....98

4.2 Data....101

4.3 Methods 105

4.4 Results....108

4.5 Conclusions....119

4.6 References....121

5 SUMMARY AND CONCLUSIONS 163

5.1 Overview....163

5.2 Summary....165

5.3 Conclusions....170

LIST OF TABLES

Page

Table 1.1: Scales of horizontal motion in the atmosphere (adapted from Wallace and Hobbs (2006)) 12

Table 2.1: List of forty urban flash flood event cases used in this study 35

Table 2.2: Strength of PW anomaly for each event used in this study 36

Table 2.3: Statistical analysis of important surface and moisture parameters, vertical levels, stability parameters, and upper level wind changes for the events used in this study 37

Table 3.1: City population statistics for the cities used in this study (U.S. Census Bureau 2011 and Texas Almanac 2014) 70

Table 3.2: City geographical statistics for the cities used in this study (NCDC 2014 and http://ggweather.com/normals/index.htm) 71

Table 3.3: Information for the USGS sites used in the study 72

Table 3.4: Land use/land cover percentage breakdown for each basin 73

Table 3.5: Information for the NWS COOP sites used in this study 74

Table 3.6: Categorical information for each location analyzed in this study 75

Table 3.7: Mann-Kendall test results comparing flood occurrence during months with below normal rainfall to flood occurrence during months with observed rainfall greater than or equal to that month's 30-yr.normal rainfall value at that location 76

Table 3.8: Mann-Kendall test results from the urban vs. rural comparison of flood occurrence during months with 0-75% normal rainfall 77

Table 3.9: Mann-Kendall test results comparing urban flood days and rural flood days during months with greater than 75% of normal rainfall for the 3 cities examined in this study 78

Table 4.1: Statistical analysis of important surface and moisture parameters, vertical levels, stability parameters, and upper level wind changes for the events used in Chapter 2 with the addition of the values from the June 2010 OKC event examined in the current Chapter 125

LIST OF FIGURES

Page

Figure 1.1: Schematic diagram of the urban water cycle (Gessner et. al 2014) 13

Figure 1.2: Schematic chart illustrating the components addressed in this dissertation....14

Figure 2.1: Estimated rainfall rate (mm) for the September 2013 Colorado flood event over the period September 8 to September 17 using the TRMM multi-satellite precipitation analysis 38

Figure 2.2: Locations of the upper air sites used for the various urban flash flood cases .39

Figure 2.3: PW value for 12 UTC on 11 September 2013 superimposed on the PW climatology plot for Denver, CO 40

Figure 2.4: Skew-t Log P diagram of the upper-air sounding from the Wilmington, OH site for 1200 UTC on 1 March 1997.....41

Figure 2.5: PW value for 1200 UTC on 1 March 1997 superimposed on the PW climatology plot for Wilmington, OH 42

Figure 2.6: Box-and-whisker plot of -10°C height based off of the 40 flash flood cases examined.....43

Figure 2.7: Skew-T Log P diagram of the composite sounding of temperature and dewpoint calculated using 36 of the flash flood cases examined in this study.....44

Figure 3.1: Schematic illustrating the changes to the hydrologic cycle with increasing urbanization (Burian and Pomeroy 2010).....79

Figure 3.2: Weather fatality statistics for the United States (NWS 2015).....80

Figure 3.3: Rating curve for the USGS site located at White Rock Creek at Greenville Ave. in Dallas, TX (USGS 2015) 81
Figure 3.4: USGS sites, COOP sites, and basin boundaries for the DFW area comparison and the associated NLCD 2011 land cover characteristics 82
Figure 3.5: USGS sites, COOP sites, and basin boundaries used in the Austin area comparison and the associated NLCD 2011 land cover characteristics 83
Figure 3.6: NLCD 2011 land cover classification legend 84
Figure 3.7: DFW area basins used in the study and flood LSR/SHAVE reports associated with those basins that correspond to the time period examined 85
Figure 3.8: Austin area basins used in the study and flood LSR/SHAVE reports associated with those basins that correspond to the time period examined....86
Figure 3.9: Double-y bar graph for Dallas, TX, the urban location (left) and Greenville, TX, the rural comparable (right) that shows the annual rainfall anomaly and annual flood occurrence for each location 87
Figure 3.10: Double-y bar graph for Fort Worth, TX, the urban location (left) and Greenville, TX, the rural comparable (right) that shows the annual rainfall anomaly and annual flood occurrence for each location 88
Figure 3.11: Double-y bar graph for Austin, TX, the urban location (left) and Llano, TX, the rural comparable (right) that shows the annual rainfall anomaly and annual flood occurrence for each location....89
Figure 3.12: Flood occurrence distribution via monthly percent of normal categorical rainfall for Dallas FAA/White Rock Creek at Dallas, TX, the urban Dallas representative (left) and Greenville/Cowleech Fork of the Sabine River at

Greenville, TX, the rural comparison site (right) from October 2001 through December 2014 90

Figure 3.13: Flood occurrence distribution via monthly percent of normal categorical rainfall for Joe Pool Lake/Walnut Creek near Mansfield, TX, the urban Fort Worth representative (left) and Greenville/Cowleech Fork of the Sabine River at Greenville, TX, the rural comparison site (right) from October 2001 through December 2014 91

Figure 3.14: Flood occurrence distribution via monthly percent of normal categorical rainfall for Austin Bergstrom/Onion Creek at Austin, TX, the urban Austin representative (left) and Llano/Sandy Creek at Kingsland, TX, the rural comparison site (right) from October 2001 through December 2014 92

Figure 3.15: Seasonal distribution of flood occurrence for White Rock Creek at Greenville Ave, Dallas, TX (left) and Cowleech Fork of the Sabine River at Greenville, TX, the rural comparison site (right) from October 2001 through December 2014 93

Figure 3.16: Seasonal distribution of flood occurrence for Walnut Creek near Mansfield, TX, the urban Fort Worth representative (left) and Cowleech Fork of the Sabine River at Greenville, TX, the rural comparison site (right) from October 2001 through December 2014 94

Figure 3.17: Seasonal distribution of flood occurrence for Onion Creek at US Hwy 183 in Austin, TX, (left) and Sandy Creek at Kingsland, TX, the rural comparison site (right) from October 2001 through December 2014 95

Figure 4.1: Map of Oklahoma City, OK (generated from http://viewer.nationalmap.gov/viewer/).....126
Figure 4.2: NLCD 2011 land use/land cover characteristics for the Oklahoma City metropolitan area (MRLC 2014) 127
Figure 4.3: OKCW Mesonet site, located near N. Portland Ave. and Black Gold Dr. in the western portion of Oklahoma City.....128
Figure 4.4: Distribution of OKCNET sites (red circles indicate traffic light sites and blue triangles indicate Oklahoma Mesonet sites associated with the OKCNET network; *courtesy of the Oklahoma Climatological Survey*). 129
Figure 4.5: a) "Bird's eye view" and b) street view of KCB103, the OKCNET site located at Robert S. Kerr Ave. and N. Robinson Ave. in downtown Oklahoma City (*courtesy of the Oklahoma Climatological Survey*).....130
Figure 4.6: Area of responsibility (shaded in green) for the ABRFC (ABRFC 2011)....131
Figure 4.7: 24-hr. total gage biased radar estimated rainfall for the ABRFC area for time ending 14 June 2010 at 0000 UTC (http://www.srh.noaa.gov/abrfc/arc_search.php).....132
Figure 4.8: 24-hr. total gage biased radar estimated rainfall for the ABRFC area for time ending 15 June 2010 at 0000 UTC (http://www.srh.noaa.gov/abrfc/arc_search.php).....133
Figure 4.9: Model Builder created for the construction of the difference maps used in this study to compare the various observing systems.....134
Figure 4.10: May 2010 Palmer Drought indices for the contiguous United States divided into climate division (a) Palmer Z-Index, (b) Palmer Drought Severity Index, (c)

Palmer Hydrological Drought Index (NCDC 2013: http://www.ncdc.noaa.gov/oa/climate/research/prelim/drought/palmer.html)....135
Figure 4.11: Palmer Z-Index maps for the contiguous United States divided into climate division for a) January 2010, b) February 2010, c) March 2010, and d) April 2010 (NCDC 2013: http://www.ncdc.noaa.gov/oa/climate/research/prelim/drought/palmer.html)....136
Figure 4.12: a) 2-inch FWI departure from the long-term average for 2010 for the central climate division and b) time series of the 2-inch FWI for the central climate division for 2010 and the long-term average (Oklahoma Mesonet 2013).....137
Figure 4.13: a) 10-inch FWI departure from the long-term average for 2010 for the central climate division and b) time series of the 10-inch FWI for the central climate division for 2010 and the long-term average (Oklahoma Mesonet 2013)138
Figure 4.14: USGS streamgage sites utilized in the Oklahoma City 14 June 2010 flood event (NWS AHPS 2015 http://water.weather.gov/ahps2/index.php?wfo=oun) 139
Figure 4.15: USGS rating curve for the USGS gage located on the North Canadian River at Britton Rd. in Oklahoma City, OK (USGS 2013) 140
Figure 4.16: Discharge data from 1 January 2010 through 1 July 2010 for the USGS gage site located on the North Canadian River at Britton Rd. in Oklahoma City, OK (USGS 2013).....141
Figure 4.17: Upper air analysis at 1200 UTC on 14 June 2010 (top) 500 mb (middle) 700 mb and (bottom) 850 mb (SPC 2012 http://www.spc.noaa.gov/obswx/maps/) ..142
Figure 4.18: North American Regional Reanalysis (NARR) displaying composite maps of (a) 850 mb specific humidity, (b) 700 mb specific humidity, (c) 850 mb winds,

and (d) 300 mb winds from 14 June 2010 (Image provided by NOAA/ESRL Physical Science Division, Boulder, CO from their website at http://www.esrl.noaa.gov/psd//).....143
Figure 4.19: Sounding from the NWS Weather Forecast Office in Norman, OK (OUN) for 1200 UTC on 14 June 2010 (University of Wyoming 2013).....144
Figure 4.20: Annual climatology of precipitable water (PW) values for the Oklahoma City area (NWS UNR 2013) with the PW value for 1200 UTC on 14 June 2010 superimposed on the graph 145
Figure 4.21: KTLX reflectivity and OK Mesonet 10 m winds at 0500 UTC (12:00 a.m. CDT) on 14 June 2010.....146
Figure 4.22: KTLX velocity and OK Mesonet 10 m winds at 0500 UTC (12:00 a.m. CDT) on 14 June 2010.....147
Figure 4.23: KTLX reflectivity and OK Mesonet 10 m winds at 0900 UTC (4:00 a.m. CDT) on 14 June 2010.....148
Figure 4.24: KTLX velocity and OK Mesonet 10 m winds at 0900 UTC (4:00 a.m. CDT) on 14 June 2010 149
Figure 4.25: KTLX reflectivity and OK Mesonet 10 m winds at (a) 1000 UTC (5:00 a.m. CDT), (b) 1100 UTC (6:00 a.m. CDT), (c) 1200 UTC (7:00 a.m. CDT), (d) 1300 UTC (8:00 a.m. CDT), (e) 1400 UTC (9:00 a.m. CDT), (f) 1500 UTC (10:00 a.m. CDT), (g) 1600 UTC (11:00 a.m. CDT), (h) 1700 UTC (12:00 p.m. CDT) on 14 June 2010 150
Figure 4.26: KTLX velocity and OK Mesonet 10 m winds at (a) 1000 UTC (5:00 a.m. CDT), (b) 1100 UTC (6:00 a.m. CDT), (c) 1200 UTC (7:00 a.m. CDT), (d) 1300

UTC (8:00 a.m. CDT), (e) 1400 UTC (9:00 a.m. CDT), (f) 1500 UTC (10:00 a.m. CDT)), (g) 1600 UTC (11:00 a.m. CDT), (h) 1700 UTC (12:00 p.m. CDT) on 14 June 2010 151

Figure 4.27: Schematic diagram that displays what led to the evolution of the 14 June 2010 Oklahoma City flood event 152

Figure 4.28: Schematic of a typical meso-high event that leads to flash flooding (Maddox et. al 1979) 153

Figure 4.29: Spatial interpolation of OK Mesonet pressure reduced to sea level with plotted OK Mesonet 10 m winds and accumulated rainfall since midnight (mm) at 1600 UTC (11:00 a.m. CDT) on 14 June 2010 154

Figure 4.30: Rainfall distribution (inches) of the combined OKCNET and Oklahoma Mesonet observations 155

Figure 4.31: Precipitation frequency curves for north Oklahoma City, OK (NOAA HDSC 2015) 156

Figure 4.32: 24-hr. rainfall accumulation difference from the ABRFC's raw radar QPE 24-hr. rainfall accumulation minus the ABRFC's gage-biased QPE 24-hr. rainfall accumulation ending at 12z on 14 June 2010 157

Figure 4.33: 24-hr. rainfall accumulation difference from the Oklahoma Mesonet 24-hr. rainfall accumulation minus the ABRFC's gage-biased QPE 24-hr. rainfall accumulation ending at 12z on 14 June 2010 158

Figure 4.34: 24-hr. rainfall accumulation difference from the combined Oklahoma Mesonet/OKCNET 24-hr. rainfall accumulation minus the ABRFC's gage-biased QPE 24-hr. rainfall accumulation ending at 12z on 14 June 2010 159

Figure 4.35: 24-hr. rainfall accumulation difference from the ABRFC's raw radar QPE 24-hr. rainfall accumulation minus the ABRFC's gage-biased QPE 24-hr. rainfall accumulation ending at 12z on 15 June 2010 160
Figure 4.36: 24-hr. rainfall accumulation difference from the Oklahoma Mesonet 24-hr. rainfall accumulation minus the ABRFC's gage-biased QPE 24-hr. rainfall accumulation ending at 12z on 15 June 2010 161
Figure 4.37: 24-hr. rainfall accumulation difference from the combined Oklahoma Mesonet/OKCNET 24-hr. rainfall accumulation minus the ABRFC's gage-biased QPE 24-hr. rainfall accumulation ending at 12z on 15 June 2010 162

CHAPTER 1

INTRODUCTION AND LITERATURE REVIEW

1.1 Introduction

Extreme rainfall events that lead to flooding have caused infrastructural and property damage, as well as loss of life (Davis 2001). In a review conducted by Kunkel et al. (1999), flood-related damages and deaths were shown to have increased over the previous several decades. Even recently, the annual hazard statistics for the United States (US) show that floods were the second deadliest weather-related hazard in 2013 and were the single deadliest convective weather-related hazard over the 30-year period from 1984-2013 (NWS 2015a), illustrating that this deadly trend continues. In a study that investigated the synoptic and mesoscale environments associated with deadly flooding events in the US, Ashley and Ashley (2008) demonstrated that 58% of the fatalities were associated with flash floods, thus illustrating the danger associated with such fast-acting weather events.

A flash flood is defined here as a rapid inundation of water into a relatively small area that begins within six hours of a causative event, which is typically intense rainfall but can also be ice jams or dam failures (AMS 2015; NWS 2015b). Furthermore, Davis (2001) delineates flash flooding from slow-rise stream flooding (i.e. riverine flooding) based on the rate of rise in water levels for affected streams or urban drainage systems. These types of floods tend to evolve on the same time and space scales as the intense

precipitation that led to the flooding in the first place. However, predicting the heavy rains that give rise to flash flood events can be a considerable challenge because extreme rainfall events can be caused by multiple storm types. Forecasting floods, especially flash floods, is a complex undertaking but is vital for the protection of life and property. Even so, when heavy rains that cause flash floods are forecast well and detected with enough advance notice to allow for adequate lead time, public response to the threat obviously remains a problem (Davis 2001).

The flash flood challenge is further complicated, in part, because floods are not solely a meteorological phenomena; they result when favorable meteorological *and* hydrological conditions coexist (Davis 2001). Doswell et al. (1996) pointed out that there are several important hydrologic components that play a role in whether flooding will occur and to what degree. Some of these additional ingredients include: antecedent precipitation/soil moisture, size of the drainage basin, topography of the basin, and land use/land cover characteristics of the area. Likewise, Winkler (1988) found that the potential for any given storm to give rise to flash flooding depends on numerous factors like topography, rainfall rate, rainfall duration, land cover, and time of year.

Changes in surface characteristics have led to urban areas possessing different climates when compared to nearby rural areas (Voogt and Oke 1997), and changes in land use/land cover affect local hydrologic systems as well (Miller et al. 2014). The replacement of pervious soils with impervious surfaces like roads, parking lots, and roofs reduces infiltration of water into subsurfaces, while artificial drainage replacing natural pathways accelerates runoff (Konrad 2003). As a result, these combined processes lead to considerable alterations to an area's hydrologic response to rainfall (Miller et al. 2014).

Figure 1.1 (Gessner et al. 2014) illustrates many of the components of the urban water cycle.

One altered process related to urban hydroclimates is hydrometeorological extremes, flooding, in particular (Shepherd et al. 2011). Rapid population growth in urban areas has led to increased urbanization, which often increases an area's flood risk (Chang and Franczyk 2008, Wheater and Evans 2009). Therefore, altered hydrologic system components due to changes in surface characteristics have led to diverse flooding situations in urban areas. Usual consequences of urban development are increased peak discharge and frequency of floods (Konrad 2003).

With the urban population only expected to continue to climb (UN 2008), all of these issues combine to further illustrate the need for additional research in this area. This dissertation directly addressed three of the main components that contribute to urban flood events: atmospheric conditions, hydrologic conditions, and land surface aspects. It should be noted that for this dissertation, only flash floods where the causative event was heavy rainfall were directly examined.

This dissertation addressed urban flooding in multiple ways (Fig. 1.2). The first quantified the atmospheric contributors that result in heavy rainfall episodes that often lead to major urban flash flood events. This was assessed via rawinsonde analyses of forty past flood events that affected numerous urban areas across the US, and therefore took a broad, geographic scale approach. Secondly, spatio-temporal trends of urban flooding, from a hydroclimatological perspective, and characteristics associated with urban flooding events for several cities within the state of Texas were examined, which, to-date, has not been undertaken. This was done using a partial duration series approach

that analyzed daily maximum discharge, where National Weather Service (NWS) flood stage, US Geological Survey (USGS) rating curves, NWS local storm reports (LSRs), and the new and unique National Severe Storms Laboratory (NSSL) Severe Hazards Analysis and Verification Experiment (SHAVE) data were incorporated to select and validate thresholds. Doing so draws the geographic extent of the analysis into a more regional focus. Finally, a record-breaking flood event that affected Oklahoma City in 2010 was explored to gain a better understanding of the hydrometeorological factors that led to the flood and whether urban-atmospheric-hydrologic interactions played some role. Additionally, various observational networks were examined in order to assess whether or not optimal observing methodologies exist. This analysis included the high-density, intra-urban Oklahoma City Micronet (OKCNET) observation network, which, to-date, had not been included into a detailed, hydrometeorological study of urban flash floods that specifically addressed optimal observing methodologies. This final assessment brings the spatial extent down to the mesoscale to get an even finer resolution perspective on flash flooding.

1.2 Research objectives

To date, no study has evaluated the possible contributions of the urban landscape to the spatio-temporal pattern of a major flood event within a large-scale meteorological environment conducive to flooding, and doing such work was recently recommended by Shepherd et al. (2011). Therefore, the overarching goal of this dissertation was to gain a better understanding of the conditions, both atmospheric and hydrologic, that can lead to urban flash flood events, with a secondary goal aimed at identifying optimal observing

networks for continued assessment of urban flash floods. The specific objectives are as follows:

Objective 1

(1) What do the atmospheric profiles leading up to major urban flood events across the United States look like? (2) What are the key atmospheric contributors that can lead to such events?

To address these research questions, rawinsonde analyses of forty past flood events that affected numerous urban areas across the US was conducted. Lamb (2001) pointed out that moisture provides the source material for precipitation to form and is an important fraction of the energy that drives the convective cells responsible for the heavy rainfall. As such, the atmospheric profile portrayed from these events was expected to be very moist, despite the large geographic reach and variable climate regimes included in the study. Additionally, it was hypothesized that commonalities in the atmospheric profiles associated with major urban flood events exist, and anomalously high values of particular atmospheric moisture variables, such as precipitable water and mixing ratio, were likely present. Other atmospheric components likely played a role in the urban flood events examined as well, and this study dove into additional areas beyond moisture including instability and wind shear.

Objective 2

(1) What are the flooding trends for various urban areas within the state of Texas and how do they compare to nearby rural areas? (2) Does variability in flood trends exist among the various cities? (3) What factors could contribute to the urban flood trends exposed?

To address these research questions, a detailed hydroclimatological trend analysis was performed that incorporated hydrologic, land use/land cover, and meteorological information. An upward trend in urban floods was anticipated, especially when compared with neighboring rural locations, and annual and seasonal differences likely exist as well. Possible causes may include: variable rainfall amounts, variable land use/land cover, urban growth, and/or increased precipitation. Furthermore, it was expected that flood occurrence for all locations were closely tied to rainfall as well.

Additionally, this analysis will evaluate the influence of urban terrain on the "meso-urban" scale for both precipitation and land surface hydrology (i.e. runoff). The term "meso-urban" is proposed as a new scale to capture the spatio-temporal scales of influence that urban areas exert on the regional hydroclimate. Previous studies (Mote et al. 2007; Hand and Shepherd 2009) have indicated that the typical regions associated with urban-enhanced precipitation is anywhere from 25 to 75 km downwind of the central business district (CBD). This proposed scale would be near the typical boundary between the meso-alpha and meso-beta scales of horizontal motion (Table 1.1).

Objective 3

(1) What were the hydrometeorological and land cover factors associated with the 14 June 2010 Oklahoma City flood? (2) What were the spatio-temporal characteristics of this extreme urban flood? (3) How does the diagnosis of an extreme urban flood vary as a function of the spatio-temporal complexity of available observing methodologies?

These final research questions were addressed via an examination of the antecedent conditions and evolution of the OKC flood using a variety of atmospheric, hydrologic, and land use data, as well as a detailed statistical comparison of the observing systems. It was expected that some aspects of the synoptic/mesoscale factors contributing to the event were relatively unique, and that enhancement of precipitation in and downwind of Oklahoma City was possible. Also, it was expected that much of the area affected by heavy rainfall had impervious surface land cover, which would enhance runoff, significantly contributing to the flood event. Finally, the different datasets incorporated into the rainfall analysis of the event were expected to expose various elements of the event and provide for a unique, in-depth analysis. The combination of NWS radar data and in situ data from the Oklahoma City Micronet (OKCNET) and the Oklahoma Mesonet likely provide enhanced resolution of the flood event, yet the inclusion of land use/land cover data likely enhanced the results beyond the capability of the meteorological data alone.

1.3 Significance of research

For the 10-year period (2001-2010) average, floods were the third-deadliest weather-related hazard in the US, and for 2010, floods were the deadliest weather-related hazard (NWS 2012). More than half of US residents live in urban areas (FHWA 2012), so an assessment of the trends in urban flooding is imperative. Because many floods are a result of heavy rains, understanding the atmospheric contributors to these events, such as those explored in Objective 1, will help meteorologists in the future by adding valuable information about specific variables and common values to look for prior to the onset of heavy rain events that may lead to flash flooding.

Impervious surface coverage common in cities puts urban areas at increased risk for floods, and due to a high percentage of US residents already residing in urban areas, and that percentage expected to increase over the coming decades, countless numbers of people are at risk. The knowledge gained from Objective 2 regarding the flooding trends for specific cities within the state of Texas, along with the anticipated growth of these cities, could provide insight into future flooding scenarios for the cities used in this study and add perspective for other cities within the same geographic region. Specifically, the information gained from this study has the potential to help local emergency managers by providing information on the flooding trends for particular areas, which could allow them to be more proactive when floods are forecast.

The final objective of this study, Objective 3, could provide unique insight into a specific observed urban flash flood event through the coupled analysis of high spatial and temporal resolution in situ data and robust radar mosaic data. Further information can also be gained through the utilization of land cover information for a more thorough

understanding of the unique interplay between the atmosphere and the land surface as well. Additionally, the results from this study could provide additional insight into which combination of observing methodologies can provide the most thorough depiction of the rainfall distribution, and therefore more accurately assess potential flood threat areas. Finally, this approach has the potential to provide additional insight into the event, as well as the antecedent conditions the preceded the event, and understanding the details of such can aid urban planners, emergency managers, weather forecasters, and water resource management when preparing for future events.

1.4 References

American Meteorological Society (AMS) cited 2015: Meteorology glossary: American Meteorological Society glossary of meteorology. [Available online at http://glossary.ametsoc.org/wiki/Flash_flood.]

Ashley, S. T. and W. S. Ashley, 2008: The storm morphology of deadly flooding events in the United States. *Int. J. of Climatolo*., **28**, 493-503.

Chang, H. and J. Franczyk, 2008: Climate change, land use change, and floods: toward and integrated assessment. *Geog. Compass*, **2**(5), 1549-1579.

Davis, R. S., 2001: Flash flood forecast and detection methods. *Severe Convective Storms*, C. A. Doswell, III, Ed., Amer. Meteor. Soc., 481-525.

Doswell, C. A., III, H. E. Brooks, R. A. Maddox, 1996: Flash flood forecasting: an ingredients-based methodology. *Wea. Forecasting*, **11**, 560-581.

Federal Highway Administration Office of Planning, Environment, and Realty, cited 2012: Census Issues: Census 2000 Population Statistics - U.S. Population Living in Urban vs. Rural Areas. [Available online at http://www.fhwa.dot.gov/planning/census_issues/metropolitan_planning/cps2k.cfm.]

Gessner, M. O., R. Hinkelmann, G. Nutzmann, M. Jekel, G. Singer, J. Lewandowski, T. Nehls, M. Barjenbruch, 2014: Urban water interfaces. *J. Hydro*., **514**, 226-232.

Hand, L. M. and J. M. Shepherd, 2009: An investigation of warm-season spatial rainfall variability in Oklahoma City: Possible linkages to urbanization and prevailing wind. *J. Appl. Meteor. Climatolo*., **48**, 251-269.

Konrad, C. P., 2003: Effects of urban development on floods. United States Geological Survey Fact Sheet FS-076-03. [Available online at http://pubs.usgs.gov/fs/fs07603/pdf/fs07603.pdf].

Kunkel, K. E., R. A. Pielke, and S. A. Changnon, 1999: Temporal fluctuations in weather and climate extremes that cause economic and human heath impacts: A review. *Bull. Amer. Meteor. Soc*., **80**, 1077-1098.

Lamb, D., 2001: Rain production in convective storms. *Severe Convective Storms*, C. A. Doswell, III, Ed., Amer. Meteor. Soc., 299-321.

Miller, J. D., H. Kim, T. R. Kjeldsen, J. Packman, S. Grebby, and R. Dearden, 2014: Assessing the impact of urbanization on storm runoff in a peri-urban catchment using historical change in impervious cover. *J. Hydro*., **515**, 59-70.

Mote, T. L., M. C. Lacke, and J. M. Shepherd, 2007: Radar signatures of the urban effect on precipitation distribution: A case study for Atlanta, GA. *Geophys. Res. Lett*., **34**, L20710, doi:10.1029/2007/GL031903.

National Weather Service, cited 2012: Summary of natural hazard statistics for 2010 in the United States [Available online at http://www.nws.noaa.gov/os/hazstats/sum10.pdf.]

National Weather Service, cited 2015a: Summary of natural hazard statistics for 2013 in the United States. [Available online at http://www.nws.noaa.gov/om/hazstats/sum13.pdf.]

National Weather Service, cited 2015b: Glossary. [Available online at http://w1.weather.gov/glossary/index.php?letter=f.]

Shepherd, J. M., M. Carter, M. Manyin, D. Messen, S. Burian, 2010: The impact of urbanization on current and future coastal precipitation: a case study for Houston. *Environment and Planning B: Planning and Design*, **37**(2), 284-304.

Shepherd, J. M, T. Mote, J. Dowd, M. Roden, P. Knox, S. C. McCutcheon, and S. E. Nelson, 2011: An overview of synoptic and mesoscale factors contributing to the disastrous Atlanta flood of 2009. *Bull. Amer. Meteor. Soc*., **92**, 861-870.

Voogt, J. A. and T. R. Oke, 1997: Complete urban surface temperature. *J. Appl. Meteor*., **36**, 1117-1132.

Wallace, J. M. and P. V. Hobbs, 2006: *Atmospheric Science: An Introductory Survey*, 2nd Ed., Academic Press, 376.

Wheater, H. and E. Evans, 2009: Land use, water management, and future flood risk. *Land Use Policy*, **26**, S251-S264.

Winkler, J., 1998: Climatological characteristics of summertime extreme rainstorms in Minnesota. *Ann. Assoc. Amer. Geograph*., **78**, 57-73.

Table 1.1: Scales of horizontal motion in the atmosphere (adapted from Wallace and Hobbs (2006)).

Spatial Thresholds	**Scale**
20,000 km	Planetary
2,000 km	Synoptic
200 km	Meso-α
25-75 km	***Meso-urban***
20 km	Meso-β
2 km	Meso-γ
200 m	Micro-α
20 m	Micro-β
2 m	Micro-γ
2 mm	Micro-δ
Air molecule	Molecular

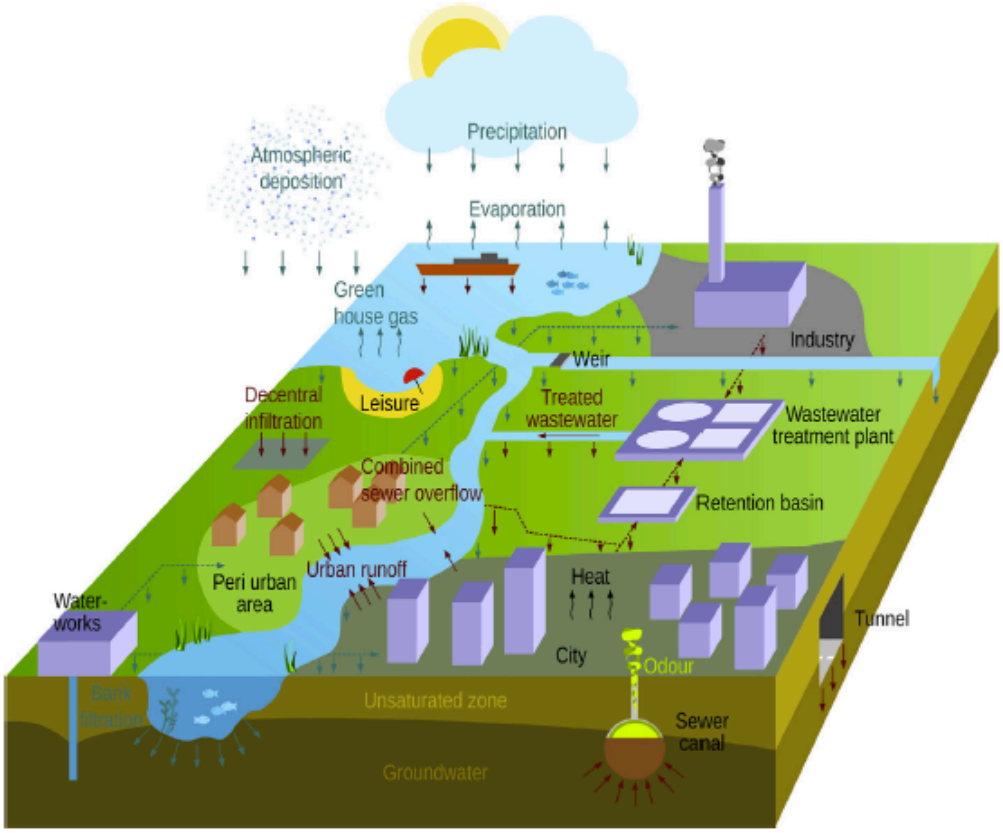

Figure 1.1: Schematic diagram of the urban water cycle (Gessner et. al 2014).

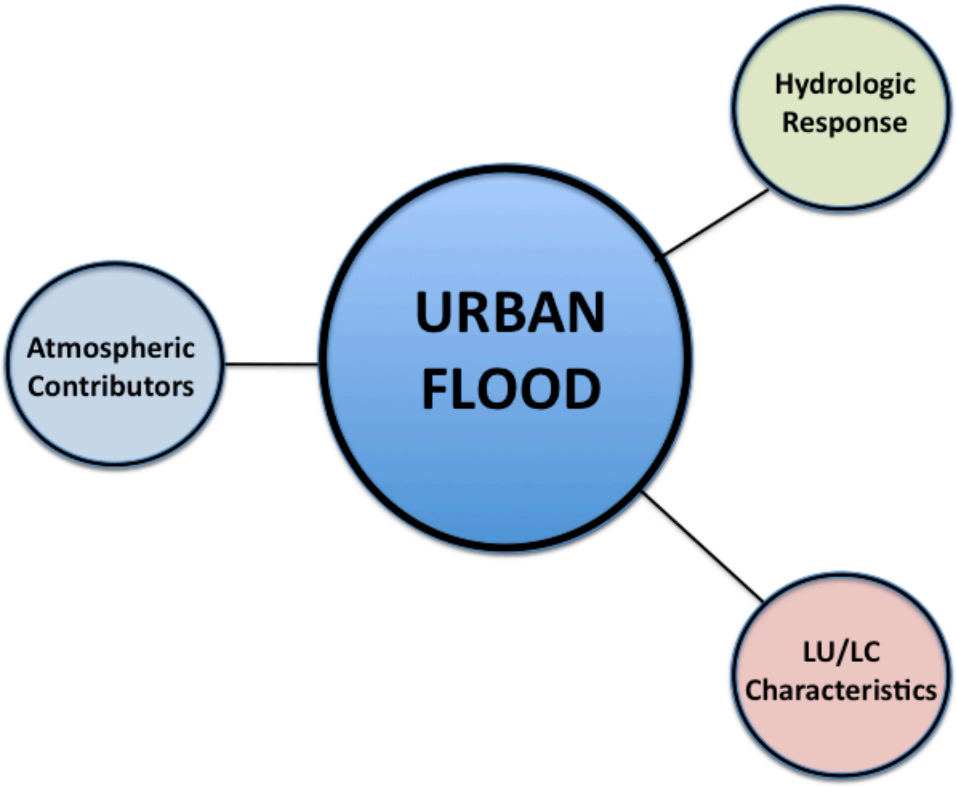

Figure 1.2: Schematic chart illustrating the components addressed in this dissertation.

CHAPTER 2

INSIGHTS INTO ATMOSPHERIC CONTRIBUTORS TO URBAN FLASH FLOODING ACROSS THE UNITED STATES USING AN ANALYSIS OF RAWINSONDE DATA AND ASSOCIATED CALCULATED PARAMETERS[1]

[1] Schroeder, A., J. Basara, J. M. Shepherd, and S. Nelson. Submitted to. *Journal of Applied Meteorology and Climatology,* 1/30/15.

Abstract

Flooding is routinely one of the most deadly weather related hazards in the United States (US), which highlights the need for more hydrometeorological research related to forecasting these deadly events. Building upon previous literature, we have conducted a synergistic study to analyze hydrometeorological aspects of major urban flood events in the US from 1977 through 2014 caused by locally heavy precipitation. Primary datasets include upper-air soundings and climatological precipitable water (PW) distributions. A major finding of this work is that major urban flood events are associated with extremely anomalous PW values, many of which exceeded the 99th percentile of the associated climatological dataset and all of them were greater than 150% of climatological mean values. However, of the forty cases examined in this study, only fifteen had PW values that exceeded 50.4 mm (2 inches) illustrating the importance of including the location-specific PW climatology in a PW analysis relevant to the potential for flash floods. Additionally, these events revealed that, despite geographic location and time of year, most had a warm cloud depth (WCD) of at least 6 km, which is defined here as the layer between the lifted condensation level (LCL) and the height of the -10°C level. A "composite" flood sounding was also calculated and revealed a characteristically tropical structure, despite cases related to tropical cyclones being excluded from the study.

2.1 Introduction

Floods were the second deadliest United States (US) weather-related hazard in 2013, only behind heat-related deaths. Furthermore, floods were the third costliest US weather-related hazard that year at approximately $2.3 billion (NWS 2015a). In a study that investigated the synoptic and mesoscale environments associated with deadly flooding events for a 10-year period in the US, Ashley and Ashley (2008) demonstrated that 58% of the fatalities were associated with flash flooding events, thus further illustrating the high danger associated with such events. Forecasting floods, especially flash floods, is a complex undertaking but is vital for the protection of life and property. In this study, the focus is on flash floods, which is defined as a rapid inundation of water into a relatively small area that begins within 6 hours of a causative event, which is typically intense rainfall, a dam failure or an ice jam (AMS 2015; NWS 2015b). In the fundamental study from Maddox et al. (1979) that examined 151 flash flood events in the US, the authors discussed four typical atmospheric patterns and identified general thresholds for K-Index, Lifted Index, and precipitable water (PW) values for each of the four typical patterns. Numerous studies reference this work with complementary research describing case studies in Minneapolis, MN (Schwartz et al. 1990), Milwaukee, WI (Roebber and Eise 2001), Las Vegas, NV (Li et al. 2003), and Nashville, TN (Durkee et al. 2012). Also, Changnon and Kunkel (1999), Shepherd et al. (2011), and Basara et al. (2011) focused on Chicago, Atlanta, and Oklahoma City, respectively, and highlighted extreme precipitable water values during flash flood events, as well as other contributing factors.

In September 2013, the National Weather Service (NWS) described flooding in and around Boulder, CO as "biblical" when multiple days of heavy rainfall led to widespread flooding across the area. A new 24-hour rainfall record was set for Boulder when 230.6 mm (9.08 inches) fell between 00Z 12 September 2013 and 00Z 13 September 2013, shattering the previous record of 121.9 mm (4.80 inches) on 31 July 1919 (NCAR/UCAR 2014; NWS 2014). In mountainous regions, satellite-derived rainfall estimates can be useful, and Figure 2.1 illustrates this by displaying the rainfall rate distribution over the period of 8 September to 17 September 2013 from the National Aeronautics and Space Administration (NASA) Tropical Rainfall Measuring Mission (TRMM) satellite-based dataset for this particular event. Coincidently, the maximum PW value for this event was 36.5 mm (1.44 in), which significantly exceeded the 99th-percentile threshold for this location and time of year.

The primary hypothesis for the current study is that *local* anomalously high PW values accompany flash flood events and can offer predictive insight. By combining a PW analysis with an assessment of other pertinent thresholds related to flash flooding, forecasters can have enhanced situational awareness of impending flash flood potential.

Additionally, a secondary hypothesis posits that soundings will be characterized as having maritime tropical environments, illustrating the important role warm rain processes play in flash flood events. A complementary study for this hypothesis comes from Elsner et al. (1989) who described warm-topped convection contributing to the Milwaukee, WI flash flood event in 1986. Such results support the notion of tropical-like airmasses being common for flash flood events due to convection having warmer cloud temperatures. Additionally, a Smith et al. (2010) study examined three different flood

scenarios in the Delaware River Basin and found that, while orographic effects played a significant role in three different causative categories (tropical cyclones, late winter-early spring extratropical systems, and warm-season convective systems), deep atmospheric moisture and the strong low-level transport of that moisture were common to all three categories. They utilized National Lightning Detection Network (NLDN) data to examine convective intensity, and found that for all three events, lightning strikes were low or non-existent, further alluding to the tropical nature of all of the studied event types.

The current study also extends the Maddox et al. (1979) analysis by expanding beyond general guidelines for PW values and examining location-specific precipitable water climatologies and anomalies for given events. This is critical given PW values vary substantially throughout the US; one value for a certain location may be extreme, but for another location may be below the mean for that time of year. Additionally, this study presents evidence of links between flash floods and other variables obtained from sounding analyses including: mixing ratio, warm cloud depth (WCD), wind shear, and various instability parameters. Finally, this study provides a composite sounding created from the case studies examined in this paper.

As with Doswell et al. (1996) that examined an ingredients-based approach to flash flood forecasting, the authors herein acknowledge that there are important hydrologic components such as antecedent precipitation/soil moisture, size of the drainage basin, and topography of the basin, that are not addressed in this study. Additionally, the differences between flood responses for specific types of land use are not explored. It should also be noted that the current study only examines meteorological floods on the local-scale caused by significant rainfall and not floods related to ice jams,

dam breaks, river floods, or tidal floods. Details regarding those types of floods can be obtained from Andersen and Shepherd (2013). The current study is similar to Smith et al. (2010), which examined only flood events caused by typical meteorological flood-generating mechanisms. At the same time, this study does not include cases related to land falling tropical cyclones, which were studied by Smith et al. (2010).

Further, this study focuses solely on flooding that occurred in urban areas, which are defined here as cities with populations of greater than 50,000 residents at the time of the event. Also, for cases where multiple locations were affected, the largest city was used to identify the case presented, thus primarily highlighting only major urban centers. Additionally, urban flood events were chosen simply due to an increased likelihood of the flood event being reported and because floods in urban areas have significant socio-economic impacts. The study does not dissect the differences between urban and rural flash flood events because the scope of the methodology is focused on high-impact urban flash flood cases. In fact, it is quite likely that the results of this study are applicable to rural areas in the vicinity of study cities. Cities are simply the organizing framework and have a larger vulnerability to flash flooding (Ashley and Ashley 2008b, Shepherd et al. 2011). Finally, the authors acknowledge that the case list is not exhaustive, only a representative sample.

2.2 Data and Methods

Several data sources were utilized in this study. The first was National Weather Service sounding data obtained from: (a) the University of Wyoming Department of Atmospheric Science (University of Wyoming 2014) and processed sounding data files

(via the NSHARP software package) obtained from the Storm Prediction Center (SPC). The second primary data source is calculated precipitable water (PW) climatologies obtained from the National Weather Service (NWS) Weather Forecast Office (WFO) in Rapid City, SD (NWS UNR 2014). The University of Wyoming dataset and the NWS WFO Rapid City, SD PW climatology dataset are both available via internet-based interfaces where user-defined downloads can be created. The sounding data for two days prior to a particular event through two days after the event, as well as the PW climatologies associated with the upper air sites used for each event analyzed were downloaded. Additionally, online event synopses from the local NWS offices for the various events were consulted, when available.

The case list for this study was built through several means. First, exhaustive online searches were performed to identify well-documented urban flood cases within the US that occurred from 1977 through 2014. Additionally, Science and Operations Officers (SOOs) within the National Weather Service (NWS) were contacted regarding urban flood case suggestions from their respective County Warning Areas (CWAs). While nearly 100 cases were identified, several limiting factors existed that diminished the case list size for this paper. Many suggested cases could not be used due to the following criteria: (1) the flood was directly related to a tropical cyclone, (2) the flood-affected city was not close enough to an upper air (UA) site (within 400 km), (3) the flood-affected city did not meet the established population threshold (> 50K), and/or (4) the sounding data was unavailable for unknown reasons. Table 2.1 lists the cases used in the study, and Figure 2.2 shows the locations of the UA sites used for the various cases.

PW was calculated following the NWS-Rapid City methodology whereby:

$$e = e_o * \exp[(17.67 * T_d) / (T_d + 243.5)] \quad (1)$$

$$\rho_{vapor} = [(e / (R_v * T)] * 10^5 \quad (2)$$

$$PW_{layer} = \overline{\rho_{vapor}} * Z * 10^{-3} \quad (3)$$

$$PW_{sfc-300mb} = \sum PW_{layer} \quad (4)$$

where: e is vapor pressure [hPa], e_o is 6.112 hPa, T_d is dewpoint [°C], ρ_{vapor} is vapor density [g m^{-3}], R_v, the gas constant for water vapor, is 461.5 J kg^{-1} K^{-1}, and T is temperature [K].

The majority of the remaining variables utilized in this study were computed using NSHARP, an interactive skew-t and hodograph software program. The only additional variable that required computation was the height of the -10°C level, and was computed via linear interpolation using the raw UA sounding data.

To construct the composite sounding, the most recent sounding closest to the onset of the event was identified for each group of soundings pulled for all cases so that only one was used per case to calculate the composite. Next, a linear interpolation of all observed sounding data at 25 hPa intervals was performed. Next, the composite mean sounding was then constructed from the interpolated temperature and dewpoint values. Wind profiles were not included due to the variability among sites used in the study. Four cases (Fort Collins, July 1997; Las Vegas, July 1999; Amarillo, July 2010; Boulder, September 2013) utilized in the sounding parameters assessment were not included in the composite sounding because low-level data for the respective soundings were not

available due to the elevation above sea-level of the UA sites used for those particular cases.

Jessup and DeGaetano (2008) examined the flood checklist employed by NWS forecasters at the Binghamton, NY WFO (BGM) that utilized thresholds for multiple variables, including precipitable water. Like the current study, the closest station was chosen in the upwind direction prior to the event. Composites of temperature and dewpoint were also calculated. However, several methodological differences exist between the methodology used in the Jessup study and that applied herein. For example, Jessup and DeGaetano (2008) included wind profiles in their calculations while the current study did only for the individual cases but not for the composite sounding construction. Also, the individual composite soundings calculated in the Jessup and DeGaetano (2008) study utilized data from only one upper air station, which was appropriate due to the relatively small study area. However, the current study calculated a single composite for all events studied within the study area's geographic extent. Jessup and DeGaetano (2008) also removed urban floods because they assumed relatively small impact, but the current study explicitly sought only urban events. Finally, and of particular significance, the current study examines a broader set of geographical and climate regimes.

2.3 Results

Flood cases occurred during all seasons, but 24 of 40 cases (60%) occurred during the summer months of June, July, and August (JJA). This concurs with the Maddox et al. (1979) study, as well as the more recent Jessup and DeGaetano (2008) study that both

documented a peak in the annual distribution of floods during the summer months. Of the 40 urban flood cases used in the current study, 30 cases (75%) had PW values above 2 standard deviations (SD) from the mean, and 22 of those 30 (73%) were above the 99th percentile. Further still, 6 of those 22 (27%) were at or near the maximum value for that particular location and time of year, including the catastrophic September 2013 Boulder, CO flood event. The 10 remaining cases had PW values above the 75th percentile, but below 2 SD. Table 2.2 further illustrates these results by displaying the type of anomaly and which events fell into each category. The PW threshold value evaluated in the Jessup and DeGaetano (2008) study was 150% of normal, and the current study illustrates that a threshold of 150% of normal PW values for a location is a valid threshold, as all 40 of the cases studied here were above that threshold as well (i.e. the 75th percentile). Additionally, it should be noted that 25 (63%) of the 40 cases examined in the current study had PW values less than 50.8 mm (2 inches), the common value often used by forecasters across the US to hone in on days when flash flooding could be a possibility for their area. *These results clearly identify the need to account for how PW compares to the PW climatology for that particular location and time of year.* Had only the 50.8 mm (2 inch) value been used as the point of heightened awareness, 63% of the devastating floods examined in the current study may have been missed if such a PW was a prime identifier used to alert forecasters to flash flooding possibilities.

One of the most extreme examples of PW from the case list was from the flood event that affected Boulder, CO and the Front Range of the Rocky Mountains in September 2013. During the seven-day period from 9 September through 15 September, approximately 430 mm (17 inches) of rain fell over Boulder, CO (NCAR/UCAR 2014).

Numerous swift water rescues were performed in and around the area and major roads were washed away, making some small mountain communities inaccessible. Multiple fatalities resulted from this flood event including two teenagers who were swept away by floodwaters in northwestern portions of the city of Boulder (Denver Post 2014). The UA site used for this event was located in Denver (DNR), approximately 40 km SE of Boulder. The maximum event PW value of 36.5 mm (1.44 in) came from the 00Z 11 September 2013 sounding and significantly exceeded the previous maximum PW value for this location and time of year (Fig. 2.3)

Another extreme case came from the Louisville, KY flood that occurred on 1 March 1997. This flood event set the 24-hour rainfall record for KY at 266.2 mm (10.48 in.), which was reported at the WFO in Louisville. The Louisville metro area sustained approximately $200 million in damages from the flood and 2 interstate highways were closed during the event. Unfortunately, a teenage boy lost his life when his van was swept off the road by a swollen creek in one of the suburbs of the city (NWS LMK 2012). Located approximately 240 km NE of Louisville, KY, the Wilmington, OH UA site was used in this study as a proxy for the event due to its proximity to the flood-affected city and the prevailing wind direction. Figure 2.4 is the sounding from the Wilmington, OH UA site for 1200 UTC on 1 March 1997, and Figure 2.5 illustrates the PW value for the event (1.42 inches) superimposed on the PW climatology plot for this location. As of 2013, this case provided the maximum PW value for this location and time of year.

Additional moisture parameters were analyzed for this study including: surface dewpoint and relative humidity, as well as various mixing ratio depth calculations. The

average surface dewpoint was 19.6°C (67.3°F) with a standard deviation of 3.7°C (6.6°F), and the average surface relative humidity was 85% with a standard deviation of 12%. While 8 of the 40 cases displayed surface relative humidity values less than 75%, all 8 of those cases had surface dewpoints of at least 19°C (66°F). Additionally, three cases yielded surface dewpoints less than 15.5°C (60°F), but all of those cases had surface relative humidity values of at least 83%.

While considering the more widely used dewpoint and relative humidity values does provide some insight into the low-level moisture for the events, a more robust method for diagnosing moisture may be to examine the various mixing ratio calculations, simply because mixing ratio is the conserved variable and the other two variables are not. With the average 0 to 1 km mean mixing ratio being 14.60 g/kg (standard deviation of 2.70 g/kg) and the average 0 to 3 km mean mixing ratio being 11.99 g/kg (standard deviation of 1.83 g/kg), ample low level moisture was present for the cases examined in this study. Doswell et al. (1996) and Shepherd et al. (2001) state the importance of low-level moisture in minimizing evaporation of precipitation below the cloud base, which is critical for high precipitation efficiency, and these results illustrate that the low-levels were relatively saturated during each case, minimizing the impact of evaporation below cloud base.

While ample atmospheric moisture is critical, more ingredients are needed to create flash flood producing rainfall events, so the statistical details for each of these calculations can be obtained from Table 2.3. As such, the details of the vertical profiles from each of the forty cases were examined to gather additional clues about the atmospheric instability, vertical wind profile, heights of various temperature thresholds,

and certain commonly used indices. While this study does not explicitly perform a vertical moisture flux calculation, which Doswell et al. (1996) explains is very important when analyzing flash flood producing rainfall events, the current study does indirectly account for this by considering lapse rates and mixing ratio values. Not surprisingly, all of the lapse rate calculations were nearly moist-adiabatic, and, as stated previously, the lower-level mixing ratio values were around 14 g kg^{-1}. Reduced lapse rates allow raindrops more time to grow via collision-coalescence processes, thus increasing precipitation efficiency, and high mixing ratio values depict the available moisture present in the atmosphere necessary for precipitation generation (Vitale and Ryan 2013).

Multiple studies have highlighted the absence of strong vertical wind shear for many flash flood-producing heavy rainfall events (Maddox et al. 1979; Zapotocny and Byrd 2002; Basara et al. 2011). The results of this study demonstrate that weak to moderate shear values were present for the 40 cases analyzed with an average wind speed increase of approximately 5 kts (2.5 ms^{-1}) for the 700 to 925 hPa level (or lowest mandatory level observed, if 925 was below ground level due to terrain) and 11 kts (5 ms^{-1}) for the 500 to 925 hPa level (or lowest mandatory level observed, if the 925 or 850 levels were below ground level due to terrain). For the directional change, the average for the 700 to 925 hPa level was veered by 44° and was veered by 67° for the 500 to 925 hPa level.

The stability of each of the cases was evaluated by examining most unstable convective available potential energy (MUCAPE), most unstable convective inhibition (MUCIN), downdraft convective available potential energy (DCAPE), various lapse rates, and the K Index. Results show that most cases exhibited “tall, skinny” CAPE

profiles (with an average value of 1817 J kg^{-1}) and little to no CIN and had lapse rates near 6°C km^{-1}. Instability profiles like these have updrafts that lead to a longer residence time for the raindrops, allowing them to grow more effectively via the collision-coalescence process (Vitale and Ryan 2013). Additionally, K Index values were indicative of thunderstorm activity with an average value of 37.3.

One of the most critical statistical results from the current study was the warm cloud depth (WCD), which is defined here as the layer between the lifted condensation level (LCL) and the height of the -10°C level, the same definition as used in the Vitale and Ryan (2013) study. The WCD and -10°C level were calculated in addition to the melting level (height of the 0°C isotherm) because supercooled water is typically present when temperatures are above -10°C, yet below 0°C (WDTB 2014). Warm rain precipitation processes governed by collision-coalescence instead of the Bergeron process, which requires the presence of ice in the cloud, is dominant if water is still in liquid form (Vitale and Ryan 2013). Because warm rain processes are typically more efficient rainfall producers, examining all details related to such processes was important. Figure 2.6 presents the box-and-whisker plot for the height of the -10°C level. The average height of the -10°C level for the 40 cases examined was 6213 m AGL (20383 ft AGL) with a standard deviation of 466 m AGL (1529 ft AGL). The highest -10°C level of 6782 m AGL (22252 ft AGL) came from the 13 September 1978 flood case over Little Rock, AR. The lowest height of the -10°C level was 5021 m AGL (16471 ft AGL) came from the 18 December 2009 over Charleston, SC. These statistics include cases from all seasons and multiple cases from areas with complex terrain. It is interesting to note that none of the extremes of the height of the -10°C level came from areas of highest terrain.

Despite the removal of events caused by tropical cyclones, the composite sounding calculated from the cases (Fig. 2.7) used in this study exhibits characteristics of soundings typically associated with convection in tropical environments (UCAR 2015). Jessup and DeGaetano (2008) calculated composite soundings in a similar manner for their study that examined flood events in the CWA for the NWS WFO in Binghamton, NY (BGM) and yielded similar results in sounding shape (see Figures 10 and 11 in Jessup and DeGaetano 2008). They also noted that the flash flood events examined in their paper tended to have low to moderate CAPE values when compared to other precipitating events, demonstrating a preference for collision-coalescence warm rain processes. Davis (2001) points out that the potential for high rainfall rates, one of the key ingredients needed for flash floods, is greater for cloud systems with deep warm cloud layers because cloud droplets have more time to interact and thus lead to a better precipitation efficiency when the collision-coalescence process is dominant. Such results further support the tropical characteristics of the composite sounding calculated for the current study.

2.4 Conclusions

From 1977-2014, 40 urban flash flood cases within the U.S. were identified and examined. Nearly two-thirds of the cases occurred during the summer months of JJA. Additionally, approximately 75% of the urban flash flood cases were associated with PW values that were at least 2SD above the mean for that location and time of year, and all 40 of were above the 75th percentile (150% of the mean). As mentioned earlier, this compares favorably to many previous studies, including the results obtained from the

Jessup and DeGaetano (2008) study that examined common thresholds and composite soundings for flash flood events created for the BGM CWA. Importantly, our results expand the findings to broader geographical and climate regimes rather than one CWA. A key point from the current research is that a universal threshold is not an appropriate way to analyze PW. With only 15 of the 40 cases (38%) examined in the current study having PW values that exceeded 50.8 mm (2 inches), the common "broad brush" value often used by forecasters to heighten their awareness of flash flooding potential, over half of the devastating floods examined in this study would have been missed by forecasters had PW been a primary indicator for heightened flash flood potential. This clearly demonstrates the need to include the climatology for the location in question to attain proper perspective of the degree to which the value is anomalous. However, as Doswell et al. (1996) states, it is the assembly of multiple ingredients that is important. While the PW anomaly is a strong indicator to alert forecasters to the potential for a heavy rainfall event, that variable alone is not sufficient to produce a flash flood event for any location. Current results have shown that instability and wind shear also play an important role. Commonalities emerged from the 40 cases studied including: WCD values near 6 km, MUCAPE between 1000 and 2200 J kg^{-1} K, and weak to moderate speed and directional wind shear. Given the tropical-like presentation of the composite sounding computed from these case studies, these values compare well to other studies mentioned previously.

The calculated composite sounding created from our cases resembled a tropical atmospheric sounding, despite cases directly associated with tropical cyclones being removed from the dataset. This sounding shape is similar to the composite sounding appearance obtained by Schumacher and Johnson (2009) who analyzed 6 different heavy

rainfall events that resulted in flash flooding. The biggest difference between the two composites was the depth of moisture, with the moisture for the current study extending farther into the midlevels of the atmosphere than the composite sounding from the Schumacher and Johnson (2009) study.

Based on the results from the current study, PW anomalies are one of the necessary conditions needed for urban flash flood events. Because forecasting and detecting flash floods is one of the greatest challenges facing forecasters due to the fact that key meteorological and hydrological situations must coexist in order to yield a flash flood event (Davis 2001), any detailed insight into the subject can help with the forecast process. While other key ingredients are needed to produce a flash flood, the findings from this study could improve situational awareness and aid forecasters attempting to recognize scenarios in which urban flash flood events caused by extreme rainfall could occur. This would, in turn, help better prepare the public and potentially save lives and property, the primary mission of the National Weather Service.

In the future, the authors plan to add additional cases to the list to make the results more robust with a larger population sample size. Additionally, using the results from the current study, the authors plan to perform an analysis for a particular UA location, calculating the variables outlined here and comparing those values to flash flood reports, further exploring the usefulness of the results in operational meteorology. Also, a flash flood index could potentially be constructed using both results and would be calculated for observed soundings to help identify regions where some of the atmospheric ingredients common to flash flood events have come together. An additional prospect for future work would be to conduct an analysis similar to the one conducted by Smith et al.

(2010) that utilized the NLDN. This could be applied to the cases studied here using the correlation that deep tropical-like systems are not electrified because of a lack of glaciation.

2.5 References

American Meteorological Society (AMS) cited 2015: Meteorology glossary: American Meteorological Society glossary of meteorology. [Available online at http://glossary.ametsoc.org/wiki/Flash_flood.]

Andersen, T. K. and J. M. Shepherd, 2013: Floods in a changing climate. *Geog Compass*, **7**(2) 95-115.

Ashley, S. T. and W. S. Ashley, 2008: Flood fatalities in the United States. *J. Appl. Meteor. Climatolo.*, **47**, 805-818.

Basara, J. B., B. G. Illston, G. D. McManus, 2011: Atmospheric contributors to the 14 June 2010 Flash Flood in Oklahoma City. International Symposium on Earth-Science Challenges, September 14-16, 2011, Norman, Oklahoma. 79.

Changnon, S. A. and K. E. Kunkel, 1999: Record flood-producing rainstorms of 17-18 July 1996 in the Chicago metropolitan area, Part I: synoptic and mesoscale features. *J. App. Meteor.*, **38**, 257-265.

UCAR COMET, cited 2015: Skew-t Mastery. (Convection > Severe T-storms > Type II Sounding…under Ch. 4 "Forecast Applications")

Davis, R. S., 2001: Flash flood forecast and detection methods. *Severe Convective Storms, Meteor. Monogr.,* No. 50, Amer. Meteor. Soc., 481–525.

Denver Post, cited 2014: Colorado flooding: two new fatalities announced, one is Lyons man Gerald Boland. [Available online at http://www.denverpost.com/breakingnews/ci_24131875/larimer-county-adds-1-number-people-presumed-killed.]

Doswell, C. A., III, H. E. Brooks, R. A. Maddox, 1996: Flash flood forecasting: an ingredients-based methodology. *Wea. Forecasting*, **11**, 560-581.

Durkee, J. D, L. Campbell, K. Berry, D. Jordan, G. Goodrich, R. Mahmood, and S. Foster, 2012: A synoptic perspective of the record 1-2 May 2010 mid-south heavy precipitation event. *Bull. Amer. Meteor. Soc.*, **5**, 611-620.

Elsner, J. B., W. H. Drag, and J. K. Last, 1989: Synoptic weather patterns associated with the Milwaukee, Wisconsin flash flood of 6 August 1986. *Wea. Forecasting*, **4**, 537-554.

Jessup, S. M. and A. T. DeGaetano, 2008: A statistical comparison of the properties of flash flooding and nonflooding precipitation events in portions of New York and Pennsylvania. *Wea. Forecasting*, **23**, 114-130.

Li, J., R. A. Maddox, X. Gao, S. Sorooshian, and K. Hsu, 2003: A numerical investigation of the storm structure and evolution during the July 1999 Las Vegas flash flood. *Mon. Wea. Rev*., **131**, 2038-2059.

Maddox, R. A., C. F. Chappell, and L. R. Hoxit, 1979: Synoptic and meso-alpha aspects of flash flood events. *Bull. Amer. Meteor. Soc., **60,*** 115–123.

National Weather Service, cited 2014: September 11-18, 2013 floods. [Available online at http://www.crh.noaa.gov/images/bou/precip/Sep2013Flood.pdf.]

National Weather Service, cited 2015a: Summary of natural hazard statistics for 2013 in the United States. [Available online at http://www.nws.noaa.gov/om/hazstats/sum13.pdf.]

National Weather Service, cited 2015b: Glossary. [Available online at http://w1.weather.gov/glossary/index.php?letter=f.]

National Weather Service Weather Forecast Office: Louisville, KY (LMK), cited 2012: The flood of March 1997. [Available online at http://www.crh.noaa.gov/lmk/?n=flood97.]

National Weather Service Weather Forecast Office: Rapid City, SD (UNR), cited 2014: Precipitable water plots. [Available online at http://www.crh.noaa.gov/unr/?n=pw.]

NCAR/UCAR, cited 2014: Inside the Colorado deluge. [Available online at http://www2.ucar.edu/atmosnews/perspective/10250/inside-colorado-deluge.]

Roebber, P. J. and J. Eise, 2001: The 21 June 1997 flood: storm-scale simulations and implications for operational forecasting. *Wea. Forecasting*, **16**, 197-218.

Schumacher, R. S. and R. H. Johnson, 2009: Quasi-stationary, extreme-rain-producing convective systems associated with midlevel cyclonic circulations. *Wea. Forecasting*, **24**, 555-574.

Schwartz, B. E., C. F. Chappell, W. E. Togstad, and X. Zhong, 1990: The Minneapolis flash flood: meteorological analysis and operational response. *Wea. Forecasting*, **5**, 3-21.

Shepherd, J. M., B. S. Ferrier, and P. S. Ray, 2001: Rainfall morphology in Florida convergence zones: a numerical study. *Mon. Wea. Rev*., **129**, 177-197.

Shepherd, J. M, T. Mote, J. Dowd, M. Roden, P. Knox, S. C. McCutcheon, and S. E. Nelson, 2011: An overview of synoptic and mesoscale factors contributing to the disastrous Atlanta flood of 2009. *Bull. Amer. Meteor. Soc*., **92**, 861-870.

Smith, J. A., M. L. Baeck, G. Villarini, and W. F. Krajewski, 2010: The hydrology and hydrometeorology of flooding in the Delaware River Basin. *J. of Hydromet*., **11**, 841-859.

UCAR COMET MetEd, cited 2015: Forecast Applications. *Skew-t Mastery*. [Available online at http://www.meted.ucar.edu/mesoprim/skewt/.]

University of Wyoming, College of Engineering, Dept. of Atmospheric Science, cited 2014: Weather. [Available online at http://weather.uwyo.edu/upperair/sounding.html.]

Vitale, J. D. and T. Ryan, 2013: Operational recognition of high precipitation efficiency and low-echo-centroid convection. *J. Operational Meteor*., **1**, 128-143.

WDTB, cited 2014: Introduction to the Top-Down Methodology, Topic 6, Lesson 1, AWOC Winter Weather Track. Warning Decision Training Branch, Norman, OK. [Available online at www.wdtb.noaa.gov/courses/winterawoc/IC6/lesson1/player.html.]

Zapotocny, C. M. and S. F. Byrd, 2002: An examination of the eastern Nebraska and western Iowa flash flood event of 6-7 August 1999. *Natl. Wea. Dig.*, **26**, 7-26.

Table 2.1: List of forty urban flash flood event cases used in this study.

Event #	Date/Time	Upper Air Site	Flood Location
1	3/1/97 12:00	Wilmington, OH	Louisville, KY/Cincinnati, OH
2	3/12/12 0:00	Lake Charles, LA	Lafayette, LA
3	3/19/06 0:00	Fort Worth, TX	Dallas, TX
4	3/29/07 18:00	Fort Worth, TX	Tarrant Co., TX (Fort Worth)
5	5/2/10 0:00	Nashville, TN	Nashville, TN
6	5/6/95 0:00	Fort Worth, TX	Dallas/Ft. Worth, TX
7	5/9/95 12:00	Slidell, LA	SE Louisiana (Slidell/New Orleans)
8	5/25/13 0:00	Corpus Christi, TX	San Antonio, TX
9	6/9/08 0:00	Davenport, IA	Madison/Milwaukee, WI
10	6/13/08 12:00	Springfield, MO	Springfield, MO
11	6/14/10 12:00	Norman, OK	Oklahoma City, OK
12	6/18/07 0:00	Fort Worth, TX	Haltom City/Gainesville/Sherman, TX
13	6/20/12 0:00	Chanhassen, MN	Duluth, MN
14	6/25/14 12:00	Fort Worth, TX	Fort Worth, TX
15	6/26/02 12:00	White Lake, MI	Fort Wayne, IN
16	7/6/02 12:00	Corpus Christi, TX	San Antonio/New Braunfels, TX
17	7/7/10 12:00	Amarillo, TX	Amarillo, TX
18	7/8/99 12:00	Desert Rock, NV	Las Vegas, NV
19	7/8/04 0:00	Sterling, VA	Baltimore, MD
20	7/12/00 12:00	Springfield, MO	Springfield, MO
21	7/16/01 0:00	Bismarck, SD	Rapid City, SD
22	7/18/96 12:00	Davenport, IA	Chicago, IL
23	7/22/10 12:00	Davenport, IA	Milwaukee, WI
24	7/23/06 0:00	Greensboro, NC	Charlotte, NC
25	7/29/97 0:00	Denver, CO	Ft. Collins, CO
26	7/29/04 0:00	Fort Worth, TX	Dallas, TX
27	7/30/07 12:00	Greensboro, NC	Winston-Salem, NC
28	8/6/11 0:00	Greensboro, NC	Charlotte, NC
29	8/7/99 0:00	Omaha, NE	Omaha, NE
30	8/8/07 12:00	Upton, NY	New York City
31	8/8/13 0:00	Nashville, TN	Nashville, TN
32	8/28/12 12:00	Charleston, SC	Charleston, SC
33	9/1/03 12:00	Wilmington, OH	Indianapolis, IN
34	9/11/13 12:00	Denver, CO	Boulder, CO
35	9/13/77 12:00	Topeka, KS	Kansas City
36	9/13/78 12:00	North Little Rock, AR	SW Little Rock, AR
37	9/22/09 0:00	Peachtree City, GA	Atlanta, GA
38	10/5/98 0:00	Topeka, KS	Kansas City
39	10/18/98 0:00	Del Rio, TX	San Antonio, TX
40	12/18/09 12:00	Charleston, SC	Charleston, SC

Table 2.2: Strength of PW anomaly for each event used in this study.

Max. PW Anomaly	**Event Number**
At/near max. value	1, 2, 5, 25, 33, 34
At/above 99th %	3, 6, 7, 11, 13, 18, 20, 23, 24, 26, 28, 35, 36, 37, 39
Above 2SD	4, 9, 14, 17, 21, 22, 29, 30, 38
Above 75th %	8, 10, 12, 15, 16, 19, 27, 31, 32, 40

Table 2.3: Statistical analysis of important surface and moisture parameters, vertical levels, stability parameters, and upper level wind changes for the events used in this study.

	Average	Standard Deviation	Max	Min
Surface T [°C]	22.3	4.7	31.4	9.0
Surface Td [°C]	19.6	3.7	25.5	6.4
Surface RH [%]	85	12	100	53
Surface - 850 hPa mean mixing ratio (g kg^{-1})	14.05	2.36	18.21	7.59
0 - 1 km mean mixing ratio (g kg^{-1})	14.60	2.70	19.45	7.60
0 - 3 km mean mixing ratio (g kg^{-1})_	11.99	1.83	14.61	6.78
Melting Level [m AGL]	4108	502	4791	2734
Height of -10 °C Level [m AGL]	6213	466	6782	5021
WCD (m)	5866	522	6680	4691
LCL [m AGL]	346.27	299.95	1262.93	17.02
MUCAPE	1817	1155	5146	76
MUCIN	-16	23	0	-85
700-500 hPa lapse rate [°C/km]	5.95	0.79	7.47	3.61
850-500 hPa lapse rate [°C/km]	6.17	0.54	7.23	4.79
0-3 km lapse rate [°C/km]	5.97	0.93	7.79	3.79
3-6 km lapse rate [°C/km]	5.94	0.72	7.56	3.86
K Index	37.3	4.1	44.5	26
700 hPa wind speed [kts]	24	16	70	3
Wind speed change btw 700 and lowest MAN hPa level [kts]	5	14	52	-20
Wind speed change btw 500 and lowest MAN hPa level [kts]	11	16	64	-13
Wind direction change btw 700 and lowest MAN hPa level [deg]	44	50	200	-16
Wind direction change btw 500 and lowest MAN hPa level [deg]	67	57	210	-45

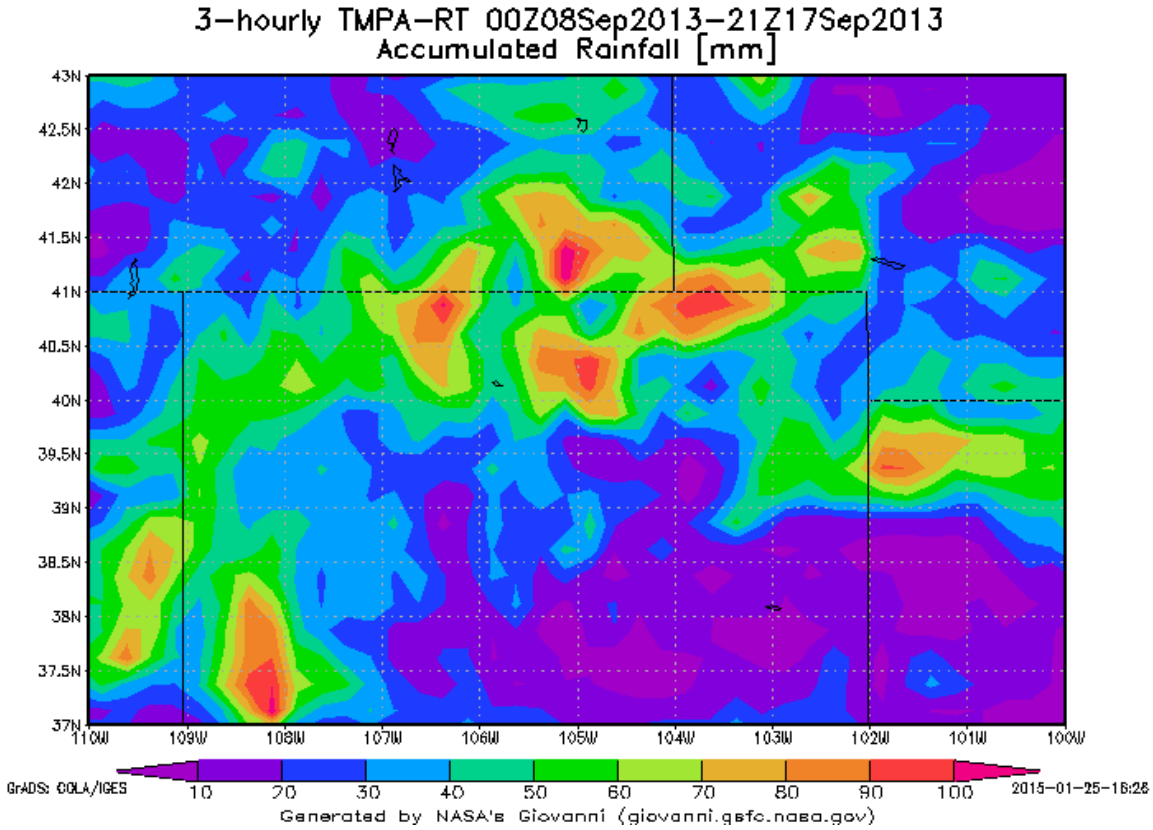

Figure 2.1: Estimated rainfall rate (mm) for the September 2013 Colorado flood event over the period September 8 to September 17 using the TRMM multi-satellite precipitation analysis.

Figure 2.2: Locations of the upper sites used for the various urban flash flood cases.

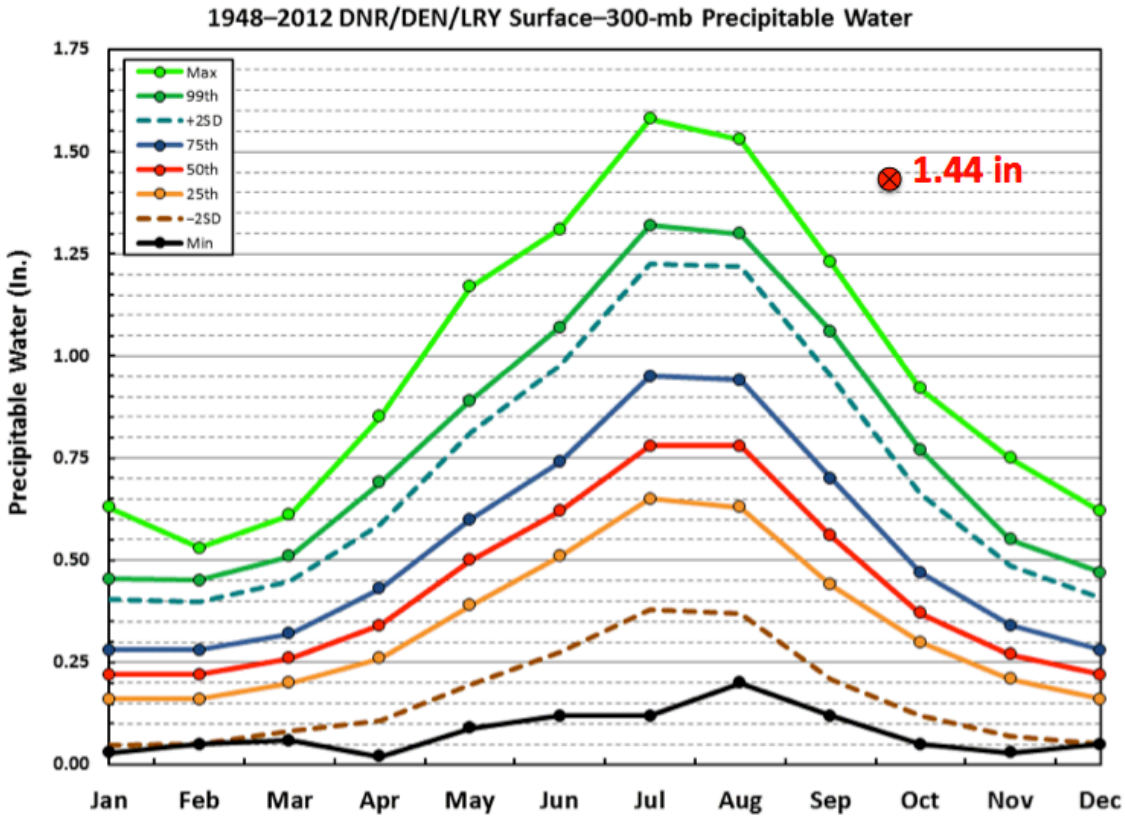

Figure 2.3: PW value for 12 UTC on 11 September 2013 superimposed on the PW climatology plot for Denver, CO.

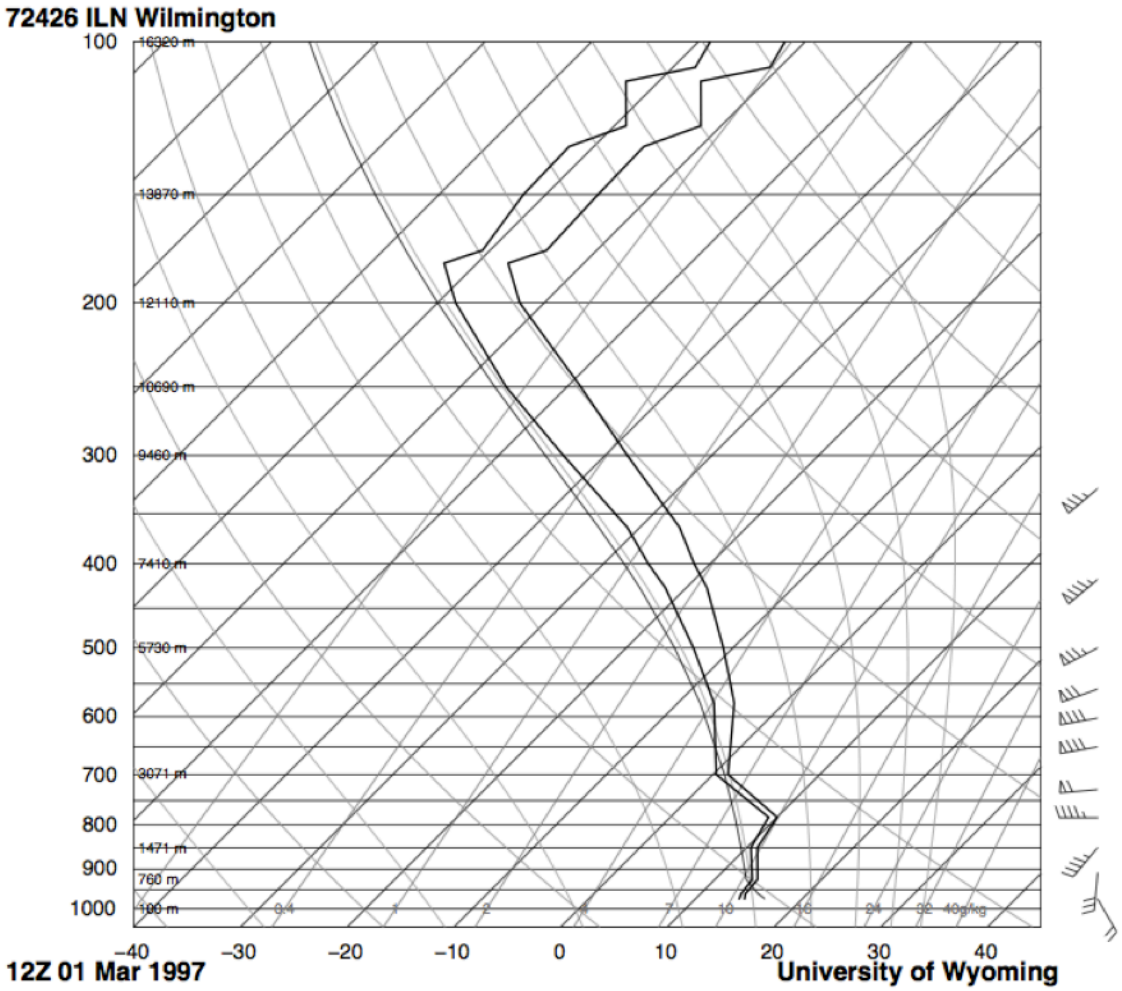

Figure 2.4: Skew-t Log P diagram of the upper-air sounding from the Wilmington, OH site for 1200 UTC on 1 March 1997.

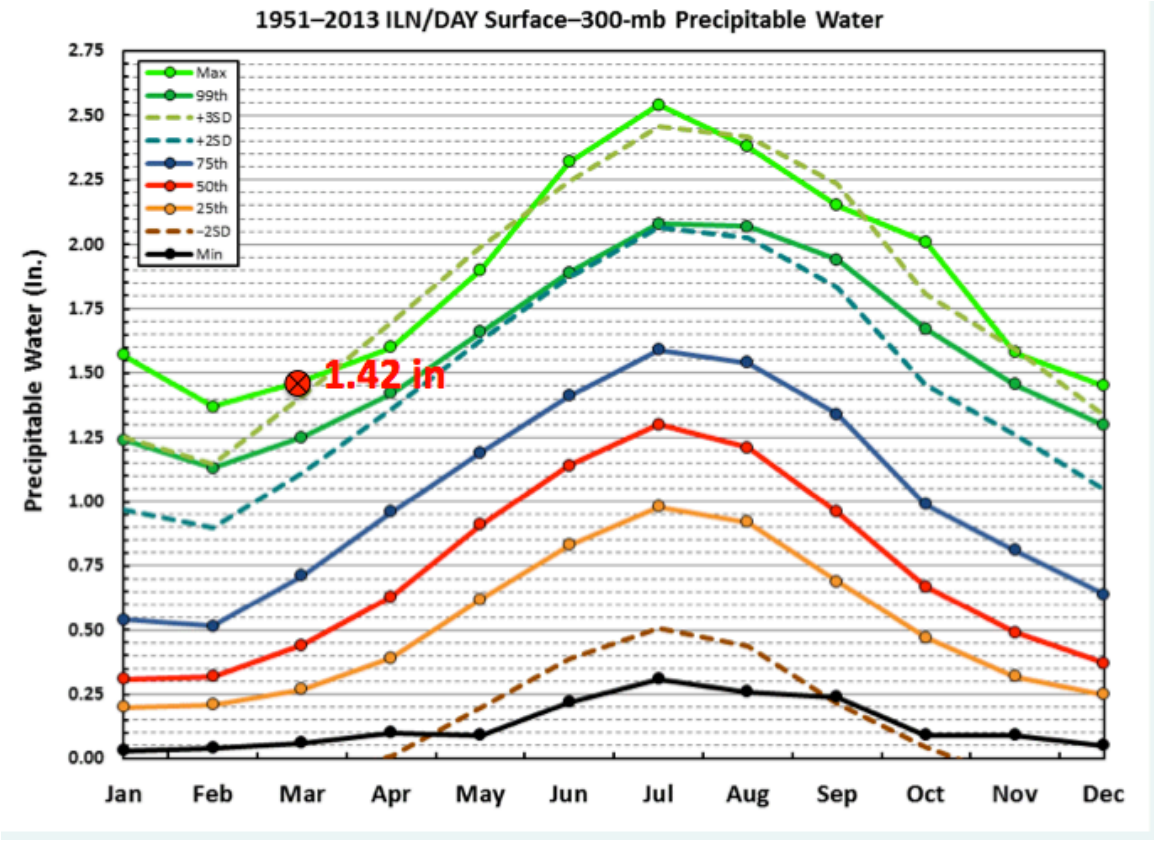

Figure 2.5: PW value for 1200 UTC on 1 March 1997 superimposed on the PW climatology plot for Wilmington, OH.

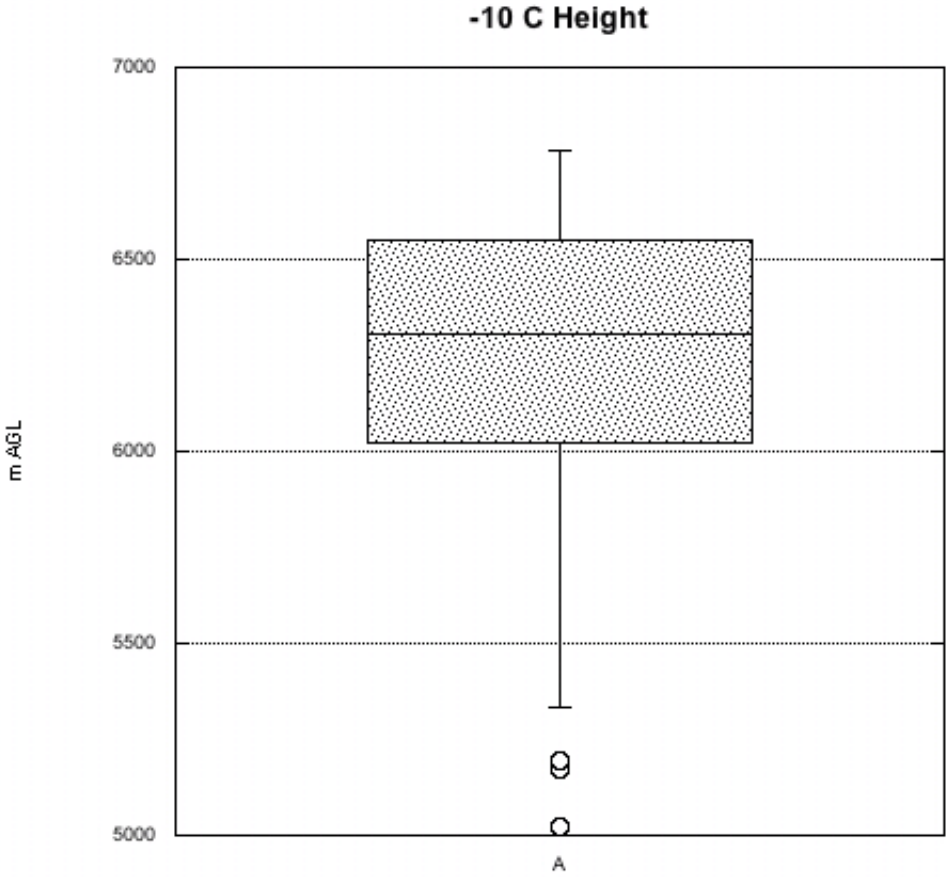

Figure 2.6: Box-and-whisker plot of -10°C height based off of the 40 flash flood cases examined.

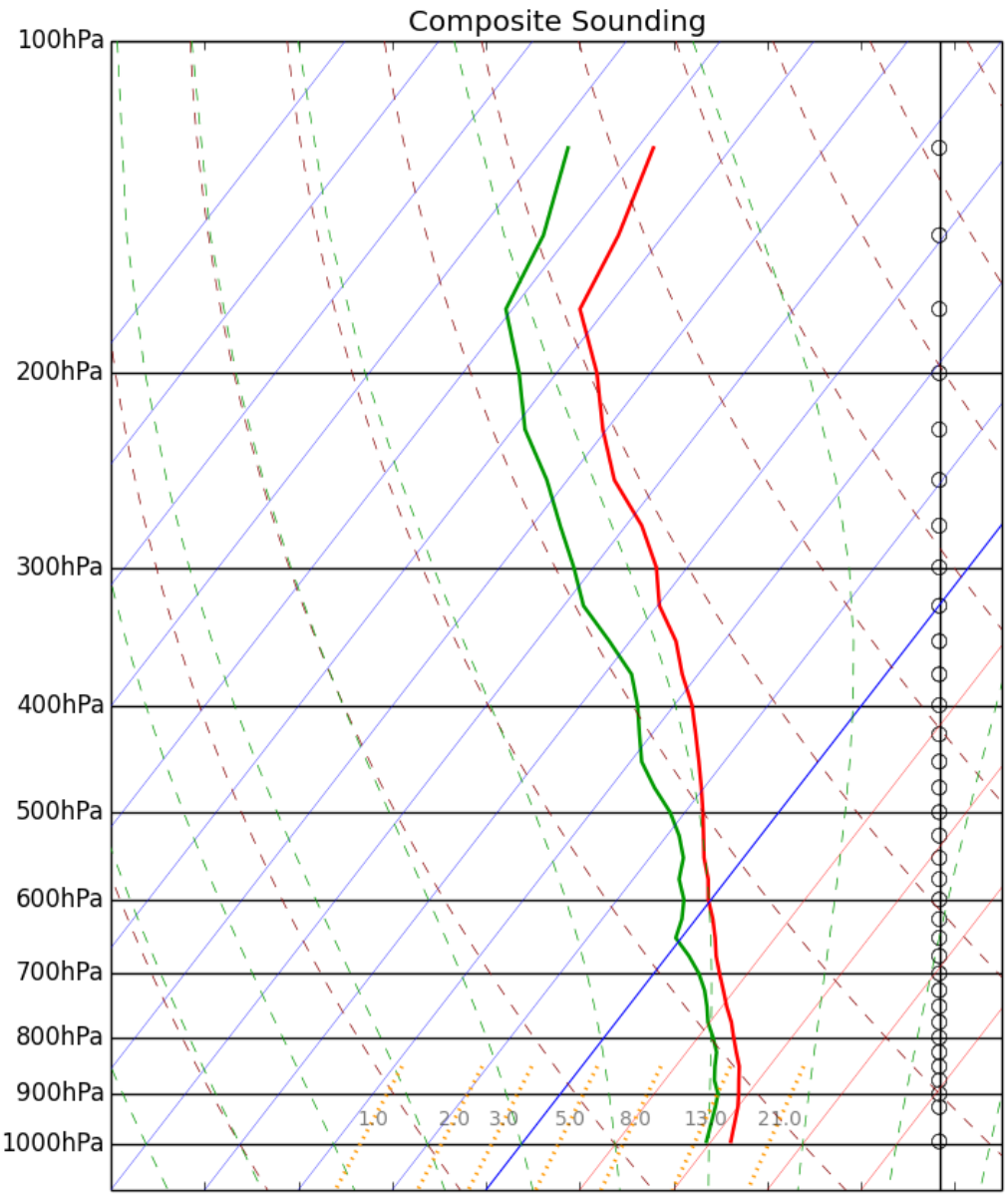

Figure 2.7: Skew-T Log P diagram of the composite sounding of temperature and dewpoint calculated using 36 of the flash flood cases examined in this study.

CHAPTER 3

HYDROCLIMATOLOGICAL TREND ANALYSIS OF FLOODS USING DAILY MAXIMUM DISCHARGE[2]

[2] Schroeder, A. and J. M. Shepherd. To be submitted to *Journal of Hydrometeorology*.

Abstract

Recently documented urban flooding in the United States (U.S.) and globally has highlighted the need for more research on the unique interplay between hydrometeorology and the built environment. Current and future rainstorms may overwhelm current stormwater management and planning frameworks, which can lead to major flash floods. The current study incorporates 13 years of daily maximum discharge for five watersheds in Texas to quantify the flood trends for three urban basins and two nearby rural basins from 2001 through 2014. A partial duration series (PDS) approach identifies floods for each location. Rainfall data were also utilized to compare with the trends in flood occurrence. Results showed that the urban basins experienced a high percentage of flood events during abnormally dry conditions, but their rural counterparts did not. Likewise, the urban basins experienced more flood events during the summer months, which is the climatological peak for flash floods, and display faster response and recovery times than their rural counterparts. Finally, multiple right-tailed Mann-Kendall tests were run on the data and revealed varying degrees of statistical significance.

3.1 Introduction

The development of urban areas leads to drastic changes in land cover and land use, which has major effects on the local hydrologic cycle (Hollis 1975). The removal of vegetation during urbanization decreases interception capacity, and the compaction of soils and introduction of impervious surfaces like asphalt, concrete, and roofs reduce infiltration and storage capacity. These altered components of the hydrologic cycle combine with altered drainage systems to increase the time to peak and volume of runoff within urban areas (Burian and Pomeroy 2010). Furthermore, surface runoff in urban areas has a higher velocity than in rural areas because impervious surfaces are smoother than surfaces with abundant vegetative cover. The increased velocity and runoff volumes result in faster concentration of flow and an increased peak rate of flow (Urbonas and Roesner 1993), This manifests itself as increased flashiness of runoff response for urban areas (Leopold 1968; Burian and Pomeroy 2010). As urbanization progresses, these anthropogenic inputs and deviations from natural flow increase, further magnifying the runoff response changes for the area (Burian and Pomeroy 2010). Figure 3.1 (Burian and Pomeroy 2010) illustrates the differences between these rural and urban processes.

In a study by Villarini et al. (2009), annual peak discharges from two North Carolina watersheds were examined over several decades, and the results illustrated not only an increase in flood magnitude during the period of rapid urbanization from the 1960s through the 2000s but also that urbanization had a significant impact on the upper tail end of the flood peak distribution. Additionally, in a 2014 study (Miller et al.) that performed a 50-year assessment of two catchments of similar size but with varying degrees of urbanization, the transition from rural to peri-urban had a greater effect on the

runoff response than did the transition from peri-urban to urban. They also concluded that it was the combination of increased impervious surface and altered drainage systems that led to flashier responses and higher peak flows than a change in land cover alone.

Hollis (1975) states that the effect of urbanization is greatest for small floods, and that the urbanization footprint is diminished as the size of the flood and recurrence interval increases. Kunkel et al. (1999) note that excess precipitation is the primary cause of hydrologic floods; however, other factors contributed to the events such as antecedent soil moisture and the physical characteristics (i.e. size, topography, control structures, etc.) of the basin itself. Additionally, Reynolds et al. (2008) concluded that a primary issue associated with the urban hydrologic cycle is that the urban land surfaces distribute stormwater through associated conveyance systems at a higher volume and at a faster rate, which can lead to overwhelming the system capacity, thus causing flooding problems for the city.

In a review conducted by Kunkel et al. (1999), indications were that flood-related damages and deaths had increased over the past several decades. Furthermore, the annual hazard statistics for the US support this claim by Kunkel et al. (1999) and suggest the trend continues (Fig. 3.2). Floods were the second deadliest weather-related hazard in 2013 and were the single deadliest convective weather-related hazard over the 30-year period from 1984-2013 (NWS 2015). With the urban population only expected to continue to climb (UN 2008), all of these variables combine to further illustrate the need for additional research in this area.

While the previous chapter in this dissertation focused mainly on the atmospheric component of the hydrologic cycle, this chapter focused primarily on runoff, yet another

altered component of the hydrologic cycle for urban areas (Cech 2005). Studies conducted by Lins and Michaels (1994) and Lettenmaier et al. (1994) revealed upward trends in streamflow for the US consistent with the upward trends in precipitation found by Karl et al. (1995a,b). The goal of this objective was to use a variety of hydrological and meteorological datasets to quantify urban flooding trends for various US cities in the state of Texas. The urban/rural basins were examined within the meso-urban to meso-alpha scale framework. The proposed research questions are:

- What are the flooding trends for various urban areas within the state of Texas, and what factors could contribute to the trend? Do the trends differ for the various cities?
- Has urban flooding increased in this area, and if so, what possible explanations were uncovered with this analysis?

An upward trend in urban flooding events was anticipated, and possible causes may include: urban growth (i.e. increased impervious surface area and population growth) and/or increased extreme precipitation.

3.2 Study area

The study area for this objective was focused around selected metropolitan areas within the state of Texas. The primary areas of interest were the Dallas/Fort Worth and Austin metropolitan areas. Careful attention was applied in order to select metropolitan areas that vary in population, as well as size. Tables 3.1 and 3.2 illustrate some of the

statistics for the cities used in this study. Note that the population statistics were for the cities themselves, not the entire metropolitan areas associated with those cities.

3.3 Data

Several different types of datasets were used in this study, but the primary datasets included: streamgage data from the United States Geological Survey (USGS) and rainfall data from the National Weather Service (NWS) cooperative observer network (COOP). In addition to the USGS and NWS COOP data, National Severe Storms Laboratory (NSSL) Severe Hazards Analysis and Verification Experiment (SHAVE) flood reports and NWS local storm reports (LSRs) were incorporated into the study, as well as basin boundary shapefiles from the NWS National Operational Hydrologic Remote Sensing Center (NOHRSC) and land cover data from the National Land Cover Database 2011 (NLCD 2011), available through the Multi-Resolution Land Characteristics (MRLC) Consortium.

Peak daily discharge, i.e. streamflow, data were used to assess flooding trends for Dallas, Fort Worth, and Austin, TX, as well as neighboring rural locations for comparison purposes. Sites within this national dataset directly measure gage height, i.e. stage, every 15 minutes. Discharge is also available in near real-time via the rating curve created and maintained for each individual location, coupled with the near real-time gage height measurements. Figure 3.3 provides the rating curve from the USGS site located at White Rock Creek at Greenville Ave. in Dallas, TX, one of the locations used in this study. Archives containing daily values of maximum, minimum, and mean discharge and stage data were available for the sites chosen for study, and all USGS data, including

rating curves, are readily available online through the USGS WaterWatch website (USGS 2015).

In order to truly address the *urban* flood signature from the discharge data, comparisons between urban and rural basins were necessary. As stated earlier, this analysis was within the meso-urban to meso-alpha scale framework because the urban basins examined were within the 25-75 km distance from the respective city center, but the distance between the urban basins and their comparative rural counterparts were all 80-130 km away. To accomplish the comparative analyses, an urban basin and a nearby rural basin of similar size and topography were identified for each city. Table 3.3 provides information for each USGS site used in the study. Note that the rural comparison location, Greenville, TX, was used as the rural comparison location for both of the urban locations within the DFW metropolitan area. Additionally, National Land Cover Database (NLCD) 2011 data were incorporated (MRLC 2015) along with the basin boundaries (NOHRSC 2015) to illustrate the land cover associated with each basin. Both of these GIS datasets are available online. Figures 3.4 and 3.5 show the land use/land cover characteristics of each basin, along with the USGS and COOP site locations, and Figure 3.6 provides the detailed legend associated with the NLCD 2011 dataset. Additionally, Table 3.4 shows the land use/land cover categorical percentage breakdown for each basin.

The USGS sites chosen for study did not record rainfall, so rainfall data were obtained from nearby NWS COOP sites to assess local rainfall trends during the study period. One COOP site was paired with each USGS site to accomplish this. Observed rainfall totals, as well as the 1981-2010 normal rainfall values for each COOP site were

obtained from the National Climatic Data Center (NCDC) data archive website. When choosing a COOP site, proximity to the USGS site representing that area was a high priority, as well as the data completeness and quality. Table 3.5 provides some of the details associated with the COOP sites utilized.

To help with verification of the flood events that were identified in the discharge analysis, local storm reports (LSRs) issued by the National Weather Service (NWS) and Severe Hazards Analysis and Verification Experiment (SHAVE) data were utilized. SHAVE is a relatively new and unique project that blends high-resolution radar data with geographic information and weather report information obtained through surveys for the contiguous US. This annual project, managed by NOAA's National Severe Storms Laboratory (NSSL) and Cooperative Institute for Mesoscale Meteorological Studies (CIMMS), has been conducted every May through August since 2006, and flash flood assessments have been a part of this program since 2008 (Ortega et al. 2009; SHAVE 2011). *The SHAVE dataset has only recently become available to scientists outside of the governing organizations; therefore, the addition of this dataset to the current study adds a rather unique perspective to the analysis.*

According to past literature, there appears to be a difference in opinion regarding what a 'flood' actually entails. Literature suggests that there are hydrological floods and damaging floods; just because a hydrological flood occurred does not necessarily mean it was also a damaging flood (Pielke 1999, Pielke and Downton 2000, Barredo 2009). Therefore, for this particular study, hydrological floods are what were specifically assessed due to the nature of the datasets utilized to identify flood events. However, some

damaging floods were also accounted for by the inclusion of the SHAVE and LSR datasets.

3.4 Methods

Data from Dallas, Fort Worth, and Austin, TX were used for urban flooding trend assessment. The time period from October 2001 through December 2014 and was solely dictated by the USGS daily maximum discharge data availability, which was the variable chosen for evaluation in order to have the analysis directly capture the degree of flooding over the specified time period. In addition to the period of record limitations, percentage of missing data issues had to be addressed as well. Finally, in order for an urban vs. rural comparison to take place, USGS sites and COOP sites from the Greenville, TX area (the rural comparison location for both DFW locations) and the Llano, TX area (the rural comparison location for Austin, TX) were brought into the analysis.

Changes to the stream channel occur over time, and these changes will have an effect on the discharge and stage at a particular location along the channel (Booth 1990). Additionally, Kunkel et al. (1999) noted that major levee system development has greatly influenced the river stages over time by forcing the river to remain in its channel, thus forcing the stage to rise. Thus, the sites and data collection methods used for the study need to be carefully documented to ensure the capture of true flood signatures. Unlike many other previous flood studies, the current study provided unique insight into flooding trends because of the use of daily maximum discharge over the traditional daily mean discharge. The daily maximum value is the maximum observed discharge value for a given calendar day and can be directly related to the magnitude of a flood peak.

Unfortunately, using the daily maximum value instead of the daily mean value severely limited the period of record and the number of urban areas available for study because archives of daily maximum discharge were only available since the early 2000s for this study area and were only archived for certain sites, whereas the daily mean value had been recorded for several decades and for thousands of locations across the country. *However, using this rather "new" variable adds a novel aspect to the current study because it captures the true magnitude of the flood peaks themselves and does not infer flood trends from a dampened signal.*

According to Madsen et al. (1997b), there are two main methods for assessment of at-site modeling of extreme hydrologic events: annual maximum series (AMS) and partial duration series (PDS), also known as peaks-over-threshold (POT). The AMS approach to assess hydrologic extremes only records the single largest event in any given year, regardless of whether the second largest event in that year exceeds the largest events for other years. However, the PDS approach includes all peaks over a designated threshold level (Stedinger et al. 1993). To identify the flood occurrences for each location during the 13-year study period, a partial duration series (PDS) approach was taken for this analysis. This approach was chosen over the more traditional annual maximum series approach to account for the possibility of multiple flood peaks during a given year. Additionally, for quantile estimation, Madsen et al. (1997a) shows evidence that PDS should be the preferred method for at-site modeling of extreme hydrologic events because heavy-tailed distributions are the most common in hydrologic applications.

The first step in the process was to identify valid USGS sites that could be used in the study, both an urban representative and a nearby rural one, for each metropolitan area.

Careful attention was paid to ensure that the basins used for direct comparison were similar in drainage area, as well as selecting watersheds that were headwater basins in order to eliminate outside water routing influences. Once sites were selected, the most appropriate discharge value that would identify the flood peaks for each USGS site was determined. To do this, the most recent rating curve was incorporated and compared with the NWS designated flood stage for each location to identify the corresponding discharge value. Once an individual discharge value was obtained for each USGS location, Perl scripts parsed through the data and output files containing only data from dates where the designated discharge value was met or exceeded for each site. To identify the floods themselves, entries spanning consecutive calendar days were designated as one singular event. It should be noted as well that by choosing to perform this PDS approach and keeping the same discharge threshold value throughout the entire study period, stationarity assumptions are brought into the picture, which is not typically a valid assumption over a long time period because stream channel changes occur over time and can alter the relationship between stage and discharge. However, the period of record was relatively short compared to longer-term studies, so this assumption was deemed acceptable.

With the flood events identified, the results were compared to NWS LSRs and SHAVE reports that fell in and near each basin during the time period evaluated to further validate the appropriateness of the discharge value selected for each site. Figures 3.7 and 3.8 display these findings for each urban area examined in the study. By comparing the identified floods and their corresponding daily maximum streamflow/stage values for the various locations used in the study to the flood reports documented in the

SHAVE and the LSR databases, validation of the threshold used for PDS could be quantified. Unfortunately, the SHAVE dataset has only been incorporating flood events into its database since 2008, and the project only operates during the warm season, further limiting the number of events applicable to the current study. For this reason, LSRs were also brought into the analysis to help assess the validity of the thresholds employed.

Because the occurrence of floods is tied to how much rainfall an area receives, rainfall data was brought into the analysis. To incorporate rainfall into the analysis, the first step was to identify the nearest COOP site to each USGS site. This process was also complicated by period of record and missing data limitations, but a valid COOP site was eventually identified for each USGS site. The monthly rainfall data were downloaded from the NCDC website for each location, as well as each site's corresponding updated rainfall normals (1981-2010). Next, a direct comparison between observed rainfall and normal was performed, for each month and year in the analysis and used for comparison purposes to identify "wet" and "dry" years for each location.

Finally, once trends were established for the various sites in this study, statistical testing was utilized to quantify the validity of the results. Because the nature of the data being used does not exhibit a normal distribution, the Mann-Kendall test was used to quantify the statistical significance of any trends that emerged.

3.5 Results

To assess the flooding and rainfall trends for each location, several methods were employed. First, the annual rainfall anomaly, defined here as the annual observed rainfall

minus the 30-yr. normal for that particular location, was calculated for each COOP site. Next, annual flood event occurrence counts were tabulated for each USGS site. Double-y bar graphs were then created to depict each area's annual flood occurrence along with its annual rainfall anomaly. Figs. 3.9-3.11 show these results, with the urban location and comparable rural location displayed side-by-side for each urban area analyzed. While the period of record for the majority of this study spanned from October 2001 through December 2014, the analysis depicting the annual breakdown of rainfall and flood occurrence only spanned from 2002 through 2014 because the complete annual cycle for 2001 was not available for all necessary data.

When the annual distribution of flood occurrence compared to annual rainfall anomaly for Dallas was compared with that of Greenville, several key things stood out. First of all, there were multiple years in the Dallas flood occurrence vs. rainfall analysis that depicted a high number of floods occurring during relatively "dry" years. However, the Greenville area flood occurrence vs. rainfall analysis, the rural comparison site for Dallas, did not exhibit these qualities. For example, the three "wettest" years (according to the annual rainfall anomaly) for Dallas were 2004, 2007, and 2009, but the years with the highest number of flood occurrence were 2003, 2004, and 2007. While two of those years (2004 and 2007) were one of the three "wettest" years for this period of record, 2003 was one of the three "driest" for Dallas, yet was one of the years with the highest number of flood events. This outcome was not the case for Greenville, TX, the rural comparison site. All of the years with the highest number of flood occurrences happened during years with near or above normal annual precipitation, and this location

experienced the least number of floods during years that received much below normal precipitation.

When the Fort Worth comparison was assessed, it showed similar qualities to that presented in the Dallas flood occurrence vs. rainfall analysis. For example, the top 3 years with the highest number of flood occurrences for Fort Worth (2004, 2009, and 2012) were not the 3 "wettest" years in the period of record. Similar to Dallas, one of the years with the highest number of flood occurrences (2012) was during a year with much below normal annual precipitation. Keep in mind that the total number of flood events for the Fort Worth urban location was significantly less than those for the Dallas and Greenville locations, so the dampened signal could be a product of sample size. The Dallas and Greenville locations recorded over 50 floods during the study period, but the Fort Worth representative only had a dozen.

Shifting south towards the Austin, TX area, the urban location exhibited trends similar to the urban locations highlighted from the DFW metroplex. For example, the 3 years with the highest number of floods (2002, 2004, and 2014) were again not the same as the 3 "wettest" for the period of record (2002, 2004, and 2007). Actually, one of the most flood prone years, 2014, was one of the drier ones for the period of record with below normal annual precipitation. For the Llano, TX comparison, the rural comparison site for the Austin area, exhibited similar trends to the Greenville, TX comparison, the rural comparison site for the DFW urban locations. Like Greenville, the number of floods for any given year appeared to be directly tied to how anomalous the annual observed precipitation was for that year. Actually, for the Llano location, there were no floods identified during years with below normal precipitation. However, like the Fort Worth

urban location, it should be pointed out that neither the Austin or Llano location recorded more than a dozen floods during this 13-year study period. Without a large enough sample size, definitive trends are unlikely to present themselves.

To stratify the analysis further, comparisons between monthly rainfall and flood occurrence were performed in order to tease out more information from the trends that were emerging. To do this, monthly percent-of-normal observed rainfall was calculated for each month in the period of record, which spanned from October 2001 through December 2014. This calculation was done to normalize the rainfall distribution for the study period and make direct comparisons between the urban and rural sites possible. Pie charts were created for each location to illustrate the number of flood occurrences for each monthly percent of normal rainfall category. Figs. 3.12-3.14 display those results, and Table 3.6 provides further details of the categorical breakdown for each location as well.

Some rather interesting features stood out when performing the urban vs. rural monthly percent of normal comparison for the DFW metro area locations. For the Dallas to Greenville comparison, the sum of the bottom 2 categories for each location showed that Dallas had a higher percentage of floods (16% of its total number of flood occurrences for the period or record) that occurred during months with 0-75% of the monthly normal precipitation, i.e. the “driest” months, than did the Greenville location (only 11%). Likewise, the comparison between the Fort Worth location and Greenville location showed the same results with 16% of the floods for Walnut Creek having occurred during months when only 0-75% of the monthly normal precipitation was observed.

However, this finding was not reciprocated in the Austin area urban vs. rural comparison. Neither the urban or rural location near Austin had any floods recorded during months when 0-75% of the normal precipitation was observed. Like mentioned earlier, a factor that likely contributed to this result for the Austin area was a low number of flood occurrences for the entire study period. The urban site for Austin (Onion Creek) only recorded 13 total floods from October 2001 through December 2014, and the rural location (Sandy Creek) only recorded 8 floods during the same time period.

An assessment of flood occurrence for the monthly percent of normal breakdown for the "wet" end of the spectrum (percentage of flood occurrence during months with greater than 125% of normal precipitation) unsurprisingly demonstrated that all locations had at least 50% of their observed flood occurrence happen during months where at least 125% of normal rainfall was observed. Konrad (2003) noted that the effects of urban development on the hydrologic response within a basin are most pronounced from moderate storms following dry periods. For storms that occur during wet periods, the soils in rural basins become saturated and additional rainfall creates runoff in much the same manner as it does in an urban basin. Therefore, the results here that indicate all locations (urban and rural) experienced a rather large percentage of flood occurrence during "wet" months is not surprising.

An assessment of the seasonal variability of the flood trends was also performed to examine how each location's flood occurrence varied by season. March, April, and May were categorized as the spring months, and June, July, and August were grouped as summer months. Likewise, September, October, and November were tagged as the fall

months, and December, January, and February were deemed as winter months. Pie charts were created that illustrate this breakdown for each location (Figs. 3.15-3.17).

In the pivotal Maddox et al (1979) study that examined 151 flood cases across the US, the results illustrated that most flash floods occurred during summer months of June, July, and August. While all of the locations examined in the current study were relatively small in size, the urban locations had vastly different surface characteristics because of the varied land use. As expected, these locations would likely be more "flashy" than their rural counterparts, and as such, show a higher percentage of flood occurrence during the summer months, which Maddox et al. (1979) pointed out as the climatological peak in flash floods. For the DFW metro area comparisons, that was what the seasonal analysis showed. The urban Dallas location, White Rock Creek, had 19% of the floods for the study period occur during the summer months of June, July, and August (JJA), but the rural counterpart location, Cowleech Fork of the Sabine River at Greenville, only had 10% of the floods occur during JJA. For the urban Fort Worth site, Walnut Creek, the percentage was even higher, with 25% of the floods there occurring during the summer months. This finding compares favorably to the previous chapter's results as well, which demonstrated that nearly two-thirds of the urban flash flood cases examined occurred during JJA.

The same cannot be said for the Austin area urban vs. rural seasonal comparison. Sandy Creek, the rural counterpart for the Austin area, had half of it's floods occur during the months of JJA, but only 23% of the floods at the Onion Creek USGS site, the designated urban location for Austin, were during this time of year. Like the monthly percent-of-normal analysis, the small sample size for each of these locations likely played

a role in the results for the Austin area comparison, but without further data, this cannot be guaranteed.

Finally, Mann-Kendall tests were computed to assess inferences on independent samples that compare the means of two populations, and the statistical significance of the results can be gleamed through the examination of the p-value for each test (Weiss 2008). This method was chosen because the data were not normally distributed. The first null hypothesis tested was that an equal number of flood occurrences would be observed in "wet" months and "dry" months, and this test was performed for each location. A "wet" month was defined as a month where the observed rainfall was greater than or equal to that month's 30-yr. normal value, and a "dry" month was a month where the observed rainfall was less than the 30-yr. normal. Table 3.7 displays the results from these tests, and the results indicated that the null hypothesis could be rejected. All but 1 location (Llano/Sandy Creek) was significant to at least the 90^{th} percentile.

The second set of Mann-Kendall tests performed compared urban and rural flood occurrences during the "driest" months (defined here as months with observed rainfall less than or equal to 75% of the 30-year normal). The null hypothesis for this test was that there were an equal number of floods for urban locations and their rural counterparts. Table 3.8 displays the results from this test, which indicated that the null hypothesis could not be rejected because all of the p-values were too high. This result is likely at least due in part to the small number of flood events that were recorded for this "driest" month category for all locations. Additionally, the total number of flood occurrences for each urban vs. rural comparison were not similar either. For example, the Greenville/Cowleech location recorded 59 floods during the entire period of record, but

Joe Pool/Walnut only recorded 12. Given the trends that emerged from the previous sections, it was assumed that the urban locations experienced a higher percentage of floods than the rural locations during months that received only 0-75% of that location's 30-year normal rainfall. These Mann-Kendall test results show that for the Dallas FAA/White Rock vs. Greenville/Cowleech comparison, that assumption would be accurate (given the positive Z statistic), but the relationship was not strong enough to show statistical significance (because of the high p-value). The reverse can be inferred from the test performing the Joe Pool/Walnut vs. Greenville/Cowleech comparison because the Z statistic was negative, which means that the rural location (Greenville/Cowleech) actually experienced more floods during the "driest" months than the Fort Worth urban location. However, given the lack of similarity in the total number of flood events for the period of record, this may or may not be a relevant result. Therefore, obtaining a longer period of record, therefore increasing the sample size and number of flood events recorded, could have substantial implications on the results. For the Austin comparison, the results merely show that the two are equal, and this is not surprising because neither one of these locations experienced any flood events during their "driest" months (i.e. months where only 0-75% of the 30-year normal rainfall was observed).

The third and final set of Mann-Kendall tests examined the relationship between the number of flood days for the urban basins compared to the number of flood days for the rural basins. This approach was entirely different from any of the other analyses performed in the study because all other analyses used the number of flood events, not number of flood days. This test was run in order to gain insight into the "flashiness" of

the basins. The null hypothesis for this test was that the urban location and the rural location had the same number of flood days for months with observed rainfall that exceeded 75% of normal. The null hypothesis could be rejected for 2 of the 3 urban vs. rural comparisons, and the results are displayed in Table 3.9. The results for the Dallas FAA/White Rock vs. Greenville/Cowleech indicated that Greenville/Cowleech had more flood days than Dallas FAA/White Rock and was significant to the 95th confidence interval. Because the total number of flood events for each of these locations was relatively similar for the entire period of record, it can be inferred that the urban basin (White Rock) was significantly more "flashy" than it's rural counterpart because it had a similar number of flood events yet significantly fewer flood days. It could also be deduced that the rural basin took longer to peak and longer to recover from the flood events that affect that area, and conversely, that there was a quick response and recovery from flood events for the urban basin.

This test had a similar result for the Joe Pool/Walnut vs. Greenville/Cowleech comparison, where the null hypothesis could be rejected. These results were significant to the 99th confidence interval, as the p-value was less than 0.0001. This indicated that the rural location (Greenville/Cowleech) had significantly more flood days than the Fort Worth urban location (Joe Pool/Walnut). However, it should be noted that the total number of flood events for the entire period of record for each of these locations was not similar; Walnut Creek had 12 flood events while Cowleech Fork had 68. Therefore, you cannot legitimately infer the same results for this comparison as was made claim to for the Dallas/White Rock vs. Greenville/Cowleech comparison. Furthermore, the test result for the Austin/Onion vs. Llano/Sandy was not statistically significant, as the p-value was

0.7387, and an inverse relationship actually ensued, because the Z statistic was negative, indicating the urban location had more flood days that its rural counterpart.

3.6 Conclusions

Urban flooding trends were assessed for 3 urban locations in the state of Texas: Dallas, Fort Worth, and Austin, TX. The study period spanned from October 2001 through December 2014 and captured numerous floods during this time period. In order to properly address the urban flooding trends, nearby rural basins of similar size were used in order to compare the urban vs. rural flood trends over the 13-year study period. Daily maximum discharge data from the USGS and rainfall data from NWS COOP sites were analyzed to identify flooding and rainfall trends. To assess the flooding trends, PDS was performed and used NWS flood stage values coupled with the most recent rating curve for each location to identify flood events. Incorporating flood reports from the SHAVE dataset, as well as NWS LSRs further validated the thresholds used for each basin. Additionally, NLCD 2011 data were compared to the basin boundary shapefiles to assess the land use and land cover characteristics of each basin, which helped verify which basins were urban and which were not.

The annual analysis revealed that the rural locations' flood occurrences were tied to how anomalously wet that year was. However, that trend was not equaled for the urban locations because the urban basins experienced a high percentage of flood events during abnormally dry years, but their rural counterparts did not. By stratifying the analysis into months instead of years, it was revealed that urban locations had a higher percentage of floods occur during months when only 0-75% of normal rainfall was observed than did

the rural locations. Additionally, when the seasonal breakdown of flood occurrence was examined, it was revealed that the urban locations had a higher percentage of floods occur during the climatological summer months of JJA, which compared favorably to the results from the previous chapter of this dissertation and to Maddox et al. (1979).

Finally, various Mann-Kendall tests were conducted on the analyzed data in order to assess statistical significance. It was concluded that it was statistically significant to the 90^{th} percentile that 5 of the 6 locations experienced more flood events as the monthly % of normal rainfall increased. However, when the test was run comparing urban and rural flood occurrence during months that experienced only 0-75% of normal rainfall, the test failed for all comparisons, so no statistical significance could be concluded for that comparison. This was likely due in part to the small number of flood events that occurred for all locations in the "driest" category. However, when the urban vs. rural Mann-Kendall test comparing the number of flood days instead of the number of flood events was run, some statistical significance could be concluded for 2 of the comparisons: Dallas FAA/White Rock vs. Greenville/Cowleech and Joe Pool/Walnut vs. Greenville/Cowleech. Because the Dallas FAA/White Rock vs. Greenville/Cowleech comparison also had a similar number of total flood events for the period of record, this Mann-Kendall result suggests that the urban basin (White Rock Creek) was more "flashy" than the rural basin (Cowleech Fork) because it had a faster response and recovery than the rural location.

More than half of US residents live in urban areas (FHWA 2012), so an assessment of the trends in urban flooding is imperative. The increased impervious surface percentage common in cities puts urban areas at increased risk for flooding events

due to a high percentage of US residents already residing in urban areas and that percentage expected to increase over the coming decades. The knowledge gained from this study regarding the flooding trends for specific cities along with the anticipated growth of these cities could provide insight into future flooding scenarios for the cities used in this study.

3.7 References

Barredo, J., 2009: Normalized flood losses in Europe: 1970-2006. *Nat. Hazards Earth Syst. Sci*., **9**, 97-104.

Booth, D. B., 1990: Stream channel incision following drainage-basin urbanization. *J. Amer. Water Resource Assoc*., **26**(3), 407-417.

Burian, S. and C. Pomeroy, 2010: Urban impacts on the water cycle and potential green infrastructure Implications. *Urban Ecosystem Ecology, Agronomy Monogr.*, No. 55, J. Aitkenhead-Peterson and A. Volder, Eds., Amer. Soc. Agronomy., 277-296.

Cech, T. V., 2005: Principles of water resources: history, development, management, and policy. 2nd ed. John Wiley and Sons, Inc. Hoboken, NJ.

Federal Highway Administration Office of Planning, Environment, and Realty, cited 2012: Census Issues: Census 2000 Population Statistics - U.S. Population Living in Urban vs. Rural Areas. [Available online at http://www.fhwa.dot.gov/planning/census_issues/metropolitan_planning/cps2k.cfm.]

Hollis, G. E., 1975: The effect of urbanization on floods of different recurrence interval. *Water Resources Res*., **11(3)**, 431-435.

Karl, T. R., R. W. Knight, N. Plummer, 1995a: Trends in high-frequency climate variability in the twentieth century. *Nature*, **377**, 217-220.

Karl, T. R., R. W. Knight, D. R. Easterling, R. G. Quayle, 1995b: Trends in U.S. climate during the twentieth century. *Consequences*, **1**, 3-12.

Konrad, C. P., 2003: Effects of urban development on floods. United States Geological Survey Fact Sheet FS-076-03. [Available online at http://pubs.usgs.gov/fs/fs07603/pdf/fs07603.pdf].

Kunkel, K. E., R. A. Pielke, and S. A. Changnon, 1999: Temporal fluctuations in weather and climate extremes that cause economic and human heath impacts: A review. *Bull. Amer. Meteor. Soc*., **80**, 1077-1098.

Leopold, L. B., 1968: Hydrology for urban planning – A guidebook on the hydrologic effects of urban land use. USGS Circ. 554. USGS, Washington, DC.

Lettenmaier, D. P., E. F. Wood, J. R. Wallis, 1994: Hydroclimatological trends in the continental United States. *J. Climate,* **7**, 586-607.

Lins, H. F. and P. J. Michaels, 1994: Increasing U.S. streamflow linked to greenhouse forcing. *Eos. Trans. Amer. Geophys. Union*, **75**, 281-285.

Madsen, H., C. P. Pearson, and D. Rosbjerg, 1997b: Comparison of annual maximum series and partial duration series methods for modeling extreme hydrologic events 2, Regional modeling. *Water Resources Res*, **33**, 759-769.

Miller, J. D., H. Kim, T. R. Kjeldsen, J. Packman, S. Grebby, and R. Dearden, 2014: Assessing the impact of urbanization on storm runoff in a peri-urban catchment using historical change in impervious cover. *J. Hydro*., **515**, 59-70.

Multi-Resolution Land Characteristics Consortium, cited 2015: National Land Cover Database 2011 (NLCD 2011). [Available online at http://www.mrlc.gov/nlcd2011.php.]

National Climatic Data Center, cited 2015: Cooperative observer network (COOP). [Available online at http://www.ncdc.noaa.gov/data-access/land-based-station-data/land-based-datasets/cooperative-observer-network-coop.]

National Operational Hydrologic Remote Sensing Center, cited 2015: GIS Data Sets. [Available online at http://www.nohrsc.noaa.gov/gisdatasets/.]

National Weather Service, cited 2015: Natural hazard statistics. [Available online at http://www.nws.noaa.gov/om/hazstats.shtml.]

National Climatic Data Center, cited 2014: Data Tools: 1981-2010 Normals. [Available online at http://www.ncdc.noaa.gov/cdo-web/datatools/normals]

Ortega, K. L., T. M. Smith, K. L. Manross., K. A. Scharfenberg, A. Witt, A. G. Kolodziej, J. J. Gourley, 2009: The Severe hazards analysis and verification experiment. *Bull. Amer. Met. Soc*., **90**, 1519-1530.

Pielke, R. A. 1999: Nine fallacies of floods. *Climate Change*, **42**, 413-438.

Pielke, R. A. and M. W. Downton, 2000: Precipitation and damaging floods: trends in the United States, 1932-1997. *J. of Climate*, **13**, 3625-3637.

Reynolds, S., S. Burian, M. Shepherd, and M. Manyin, 2008: Urban induced rainfall modifications on urban hydrologic response. *Reliable Modeling of Urban Water Systems*, W. James et al., Eds., Computational Hydraulics International, 99-122.

Severe Hazards Analysis and Verification Experiment, cited 2011: Severe hazards analysis and verification experiment: NOAA hazardous weather testbed – experimental warning program. [Available online at http://ewp.nssl.noaa.gov/projects/shave/.]

Stedinger, J. R., R. M. Vogel, and E. F. Georgiou, 1993: Frequency analysis of extreme events. *Handbook of Hydrology*, D. R. Maidment, Ed., McGraw Hill, Inc., 18.1-28.66.

Texas Almanac, cited 2014: City Population History from 1850-2000. [Available online at http://www.texasalmanac.com/sites/default/files/images/CityPopHist%20web.pdf.]

United Nations, cited 2008: United Nations expert group meeting on population distribution, urbanization, internal migration, and development. [Available online at http://www.un.org/esa/population/meetings/EGM_PopDist/P01_UNPopDiv.pdf.]

United States Census Bureau, cited 2011: State and county quickfacts. [Available online at http://quickfacts.census.gov/qfd/index.html.]

United States Geological Survey, cited 2015: WaterWatch. [Available online at http://waterwatch.usgs.gov/index.php?r=tx&m=real.]

Urbonas, B. R. and L. A. Roesner, 1993: Hydrologic design for urban drainage and flood control. *Handbook of Hydrology*, D. R. Maidment, Ed., McGraw Hill, Inc., 28.1-28.52.

Villarini, G., J. A. Smith, F. Serinaldi, J. Bales, P. D. Bates, and W. F. Krajewski, 2009: flood frequency analysis for nonstationary annual peak records in an urban drainage basin. *Adv. in Water Resources*, **32**, 1255-1266.

Weiss, N. A, 200: *Introductory Statistics, 8th ed.*, Pearson Addison-Wesley, 486-571.

Table 3.1: City population statistics for the cities used in this study (U.S. Census Bureau 2011 and Texas Almanac 2014).

City, State	Pop. (2010)	Pop. Change (from 2000 to 2010)	Pop. Density (persons per km^2)	Land Area (km^2)
Austin, TX	790,390	+20.1%	1,024	771.6
Dallas, TX	1,197,833	+ 0.1 %	1,358	881.9
Fort Worth, TX	742,066	+ 34.9 %	843.2	880.1

Table 3.2: City geographical statistics for the cities used in this study (NCDC 2014 and http://ggweather.com/normals/index.htm).

City, State	Elevation (m-above SL)	Normal (1981-2010) Jan. Min/Aug. Max Temp (°C)	Normal (1981-2010) Annual Precipitation (mm (in))	Normal (1981-2010) Annual Snowfall (mm (in))
Austin, TX (Bergstrom Int'l Airport)	146.3	2.4/35.6	816.7 (32.15)	N/A
Dallas, TX (FAA Airport)	134.1	2.9/35.8	954.3 (37.57)	38.1 (1.5)
Fort Worth, TX (NWS WFO)	209.4	1.9/34.9	960.1 (37.80)	53.3 (2.1)

Table 3.3: Information for the USGS sites used in the study.

USGS Site	County	Basin Size (km^2 (mi^2))	Flood Stage (ft)	Estimated Flood Discharge (cfs)
Cowleech Fk Sabine Rvr at Greenville TX	Hunt	210 (81)	14	550
White Rock Crk at Dallas	Dallas	171 (66)	84	4400
Walnut Crk near Mansfield	Tarrant	163 (63)	22	3300
Sandy Crk near Kingsland	Llano	896 (346)	12	13000
Onion Crk at US Hwy 183 Austin	Travis	831 (321)	17	7000

Table 3.4: Land use/land cover percentage breakdown for each basin.

LU/LC Category	White Rock Creek Percentage	Walnut Creek Percentage	Cowleech Fork Percentage	Onion Creek Percentage	Sandy Creek Percentage
Open Water	< 1	1	1	< 1	< 1
Developed, Open Space	15	11	7	14	1
Developed, Low Intensity	26	10	2	8	< 1
Developed, Medium Intensity	34	6	< 1	6	< 1
Developed, High Intensity	19	2	< 1	2	< 1
Barren Land (Rock/Sand/ Clay)	< 1	1	< 1	1	< 1
Deciduous Forest	2	19	14	11	6
Evergreen Forest	< 1	< 1	1	19	31
Mixed Forest	0	0	< 1	0	< 1
Shrub/Scrub	0	< 1	< 1	21	47
Grassland/ Herbaceous	2	35	44	15	16
Pasture/Hay	< 1	14	18	1	< 1
Cultivated Crops	1	2	11	1	< 1
Woody Wetlands	< 1	< 1	< 1	1	< 1
Emergent Herbaceous Wetlands	< 1	< 1	< 1	< 1	0

Table 3.5: Information for the NWS COOP sites used in this study.

NWS COOP Site	County	1980-2010 Annual Rainfall Normal (mm (in.))	Paired USGS site	Distance from Paired USGS site (km)
Greenville, TX	Hunt	1134 (44.65)	Cowleech Fk Sabine Rvr at Greenville TX	5.4
Dallas FAA Airport	Dallas	954.3 (37.57)	White Rock Crk at Dallas	12.1
Joe Pool Lake	Tarrant	1040 (40.93)	Walnut Crk near Mansfield	16.6
Llano, TX	Llano	703.6 (27.70)	Sandy Crk near Kingsland	32.1
Austin Bergstrom	Travis	816.6 (32.15)	Onion Crk at US Hwy 183 Austin	1.2

Table 3.6: Categorical information for each location analyzed in this study.

% Normal Monthly Rainfall Category	White Rock Creek # of Flood Events	Cowleech Fork # of Flood Events	Walnut Creek # of Flood Events	Onion Creek # of Flood Events	Sandy Creek # of Flood Events
</= 25%	1	1	1	0	0
25-75%	8	7	1	0	0
75-100%	7	12	0	0	1
100-125%	5	9	1	0	0
125-175%	20	20	2	1	0
>/= 175%	18	19	7	12	7
POR Total	59	68	12	13	8

Table 3.7: Mann-Kendall test results comparing flood occurrence during months with below normal rainfall to flood occurrence during months with observed rainfall greater than or equal to that month's 30-yr.normal rainfall value at that location.

COOP site/USGS site	**Z Statistic**	**p-value**
Joe Pool/Walnut	1.499	0.0669
Dallas FAA/White Rock	5.165	< 0.0001
Greenville/Cowleech	4.18	< 0.0001
Austin/Onion	1.765	0.0388
Llano/Sandy	0.807	0.2099

Table 3.8: Mann-Kendall test results from the urban vs. rural comparison of flood occurrence during months with 0-75% normal rainfall.

urban COOP site/USGS site vs. rural COOP site/USGS site	**Z Statistic**	**p-value**
Joe Pool/Walnut vs. Greenville/Cowleech	-0.723	0.7651
Dallas FAA/White Rock vs. Greenville/Cowleech	0.188	0.4256
Austin/Onion vs. Llano/Sandy	0.0	0.5

Table 3.9: Mann-Kendall test results comparing urban flood days and rural flood days during months with greater than 75% of normal rainfall for the 3 cities examined in this study.

urban COOP site/USGS site vs. rural COOP site/USGS site	**Z Statistic**	**p-value**
Joe Pool/Walnut vs. Greenville/Cowleech	5.026	< 0.0001
Dallas FAA/White Rock vs. Greenville/Cowleech	2.158	0.0155
Austin/Onion vs. Llano/Sandy	-0.639	0.7387

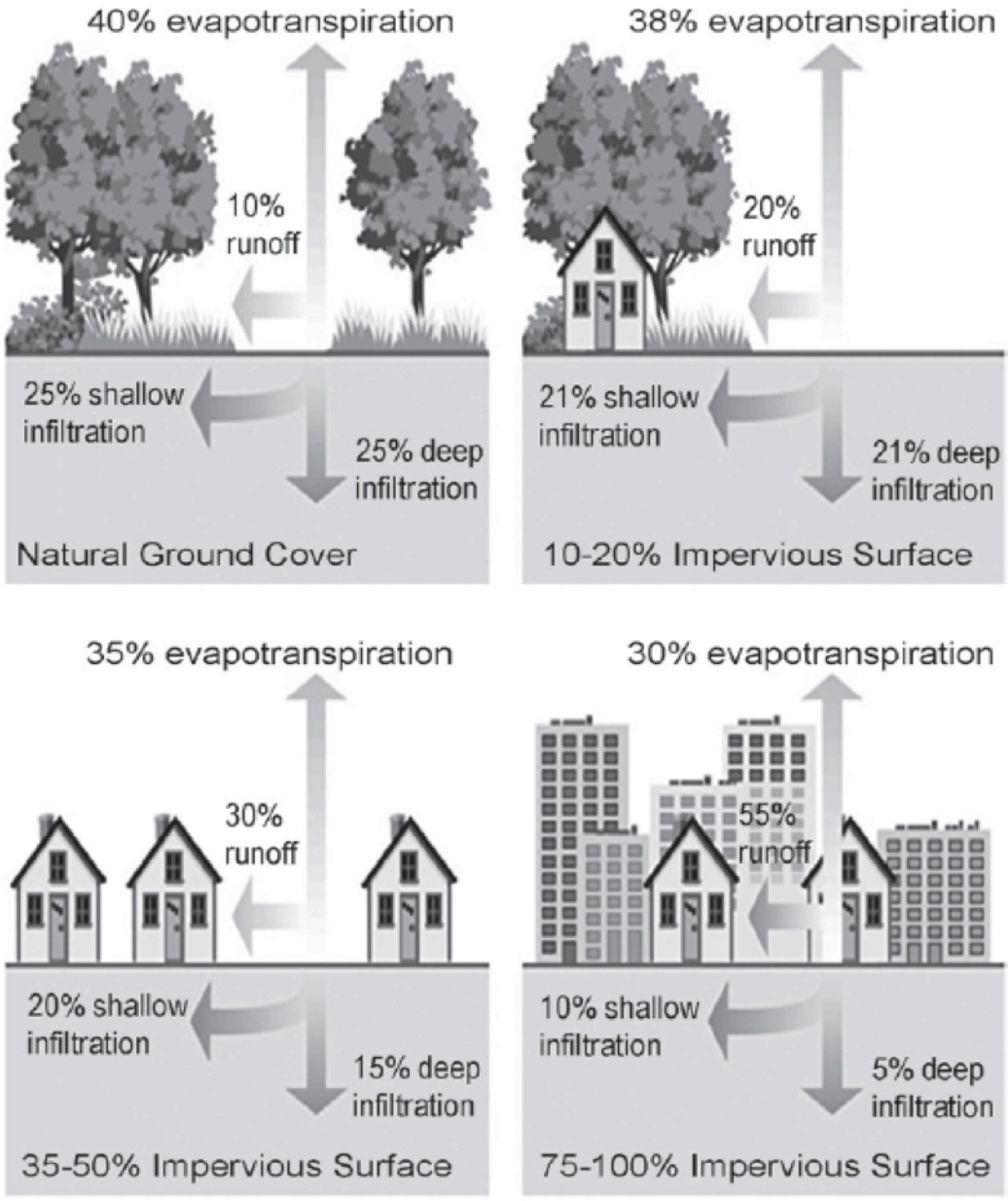

Figure 3.1: Schematic illustrating the changes to the hydrologic cycle with increasing urbanization (Burian and Pomeroy 2010).

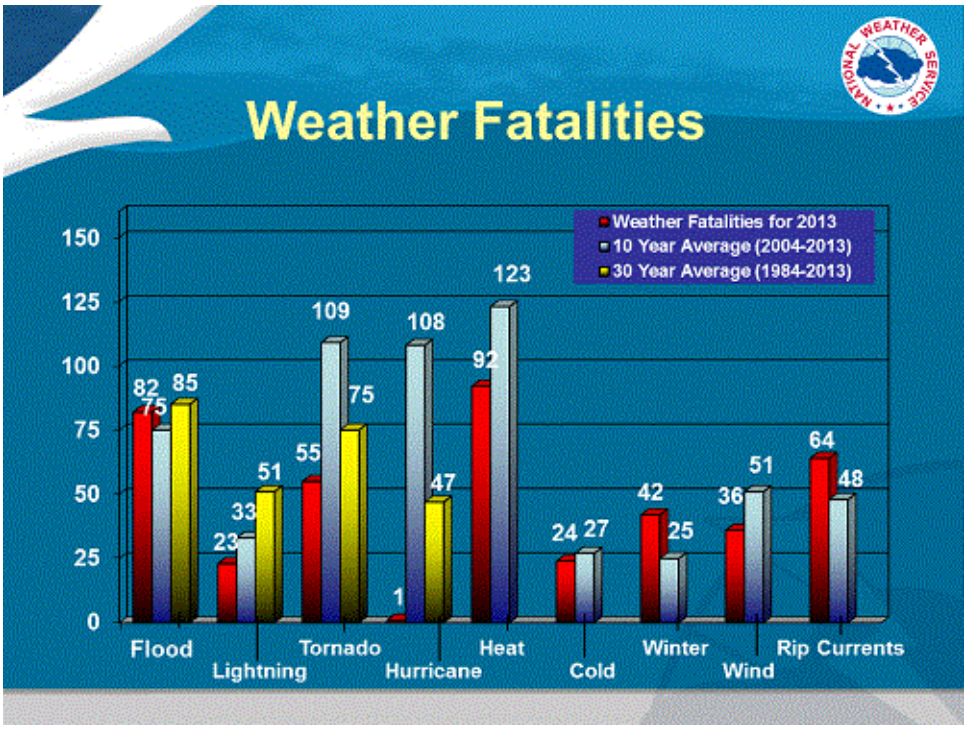

Figure 3.2: Weather fatality statistics for the United States (NWS 2015).

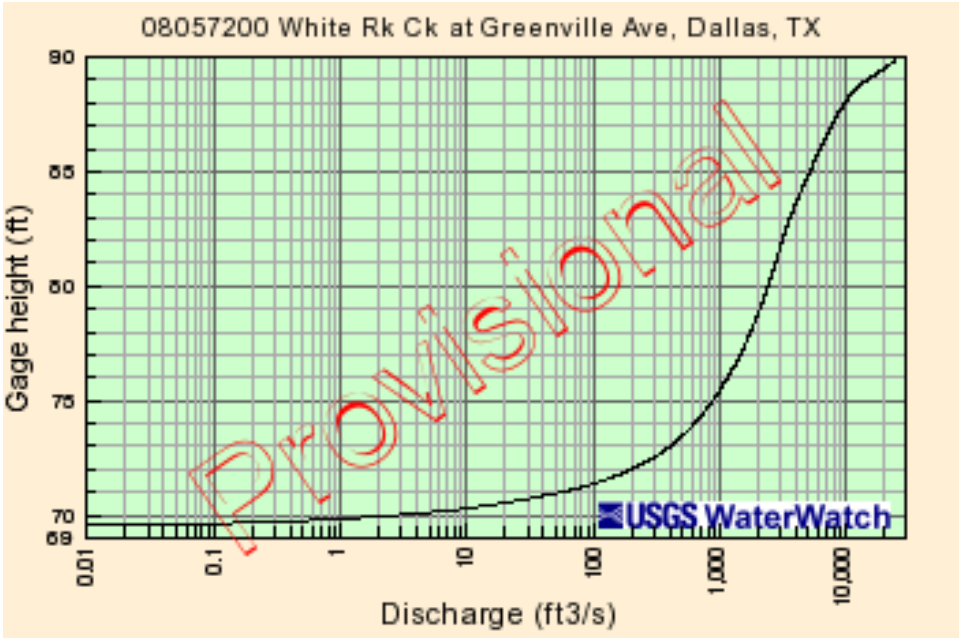

Figure 3.3: Rating curve for the USGS site located at White Rock Creek at Greenville Ave. in Dallas, TX (USGS 2015).

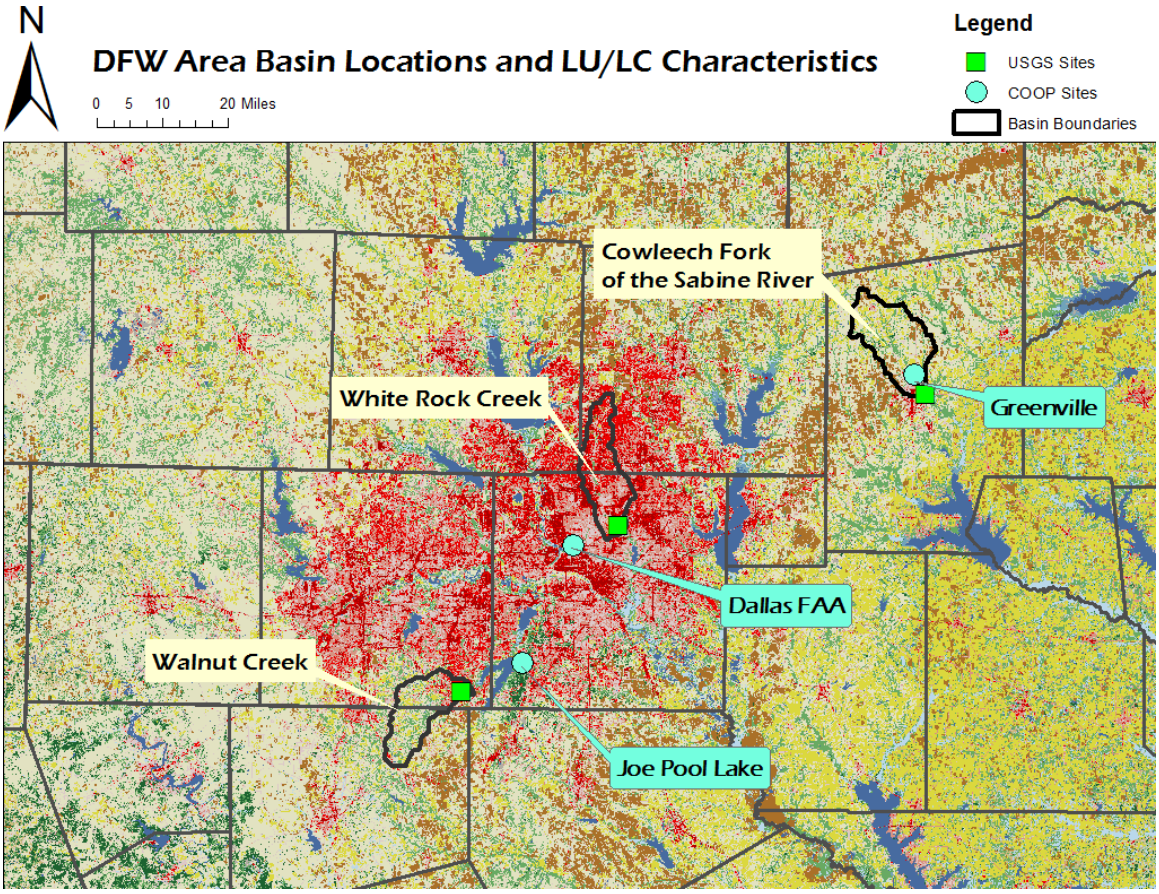

Figure 3.4: USGS sites, COOP sites, and basin boundaries for the DFW area comparison and the associated NLCD 2011 land cover characteristics.

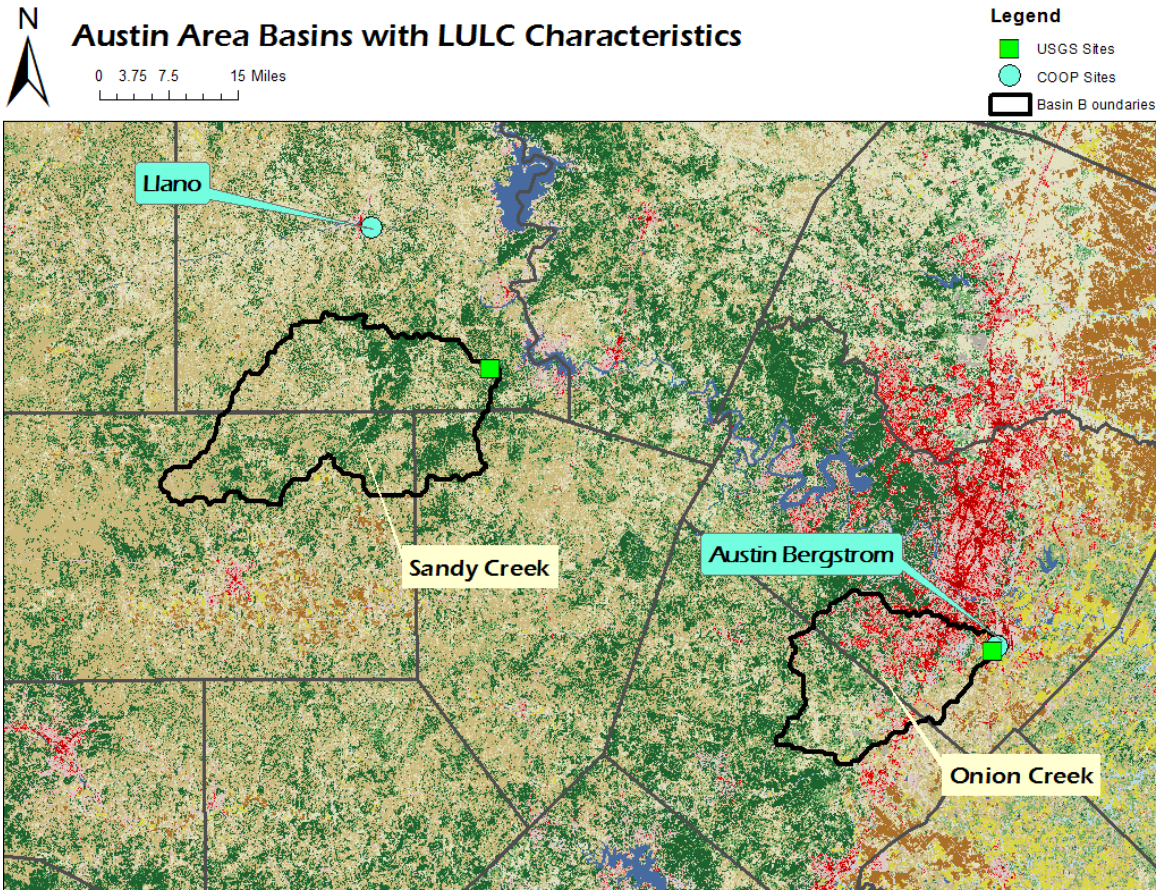

Figure 3.5: USGS sites, COOP sites, and basin boundaries used in the Austin area comparison and the associated NLCD 2011 land cover characteristics.

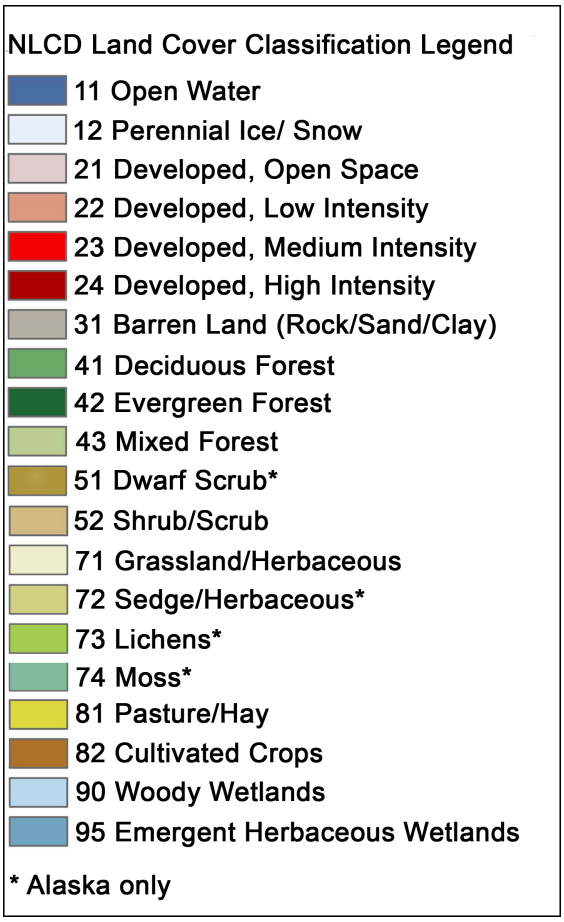

Figure 3.6: NLCD 2011 land cover classification legend (MRLC 2015).

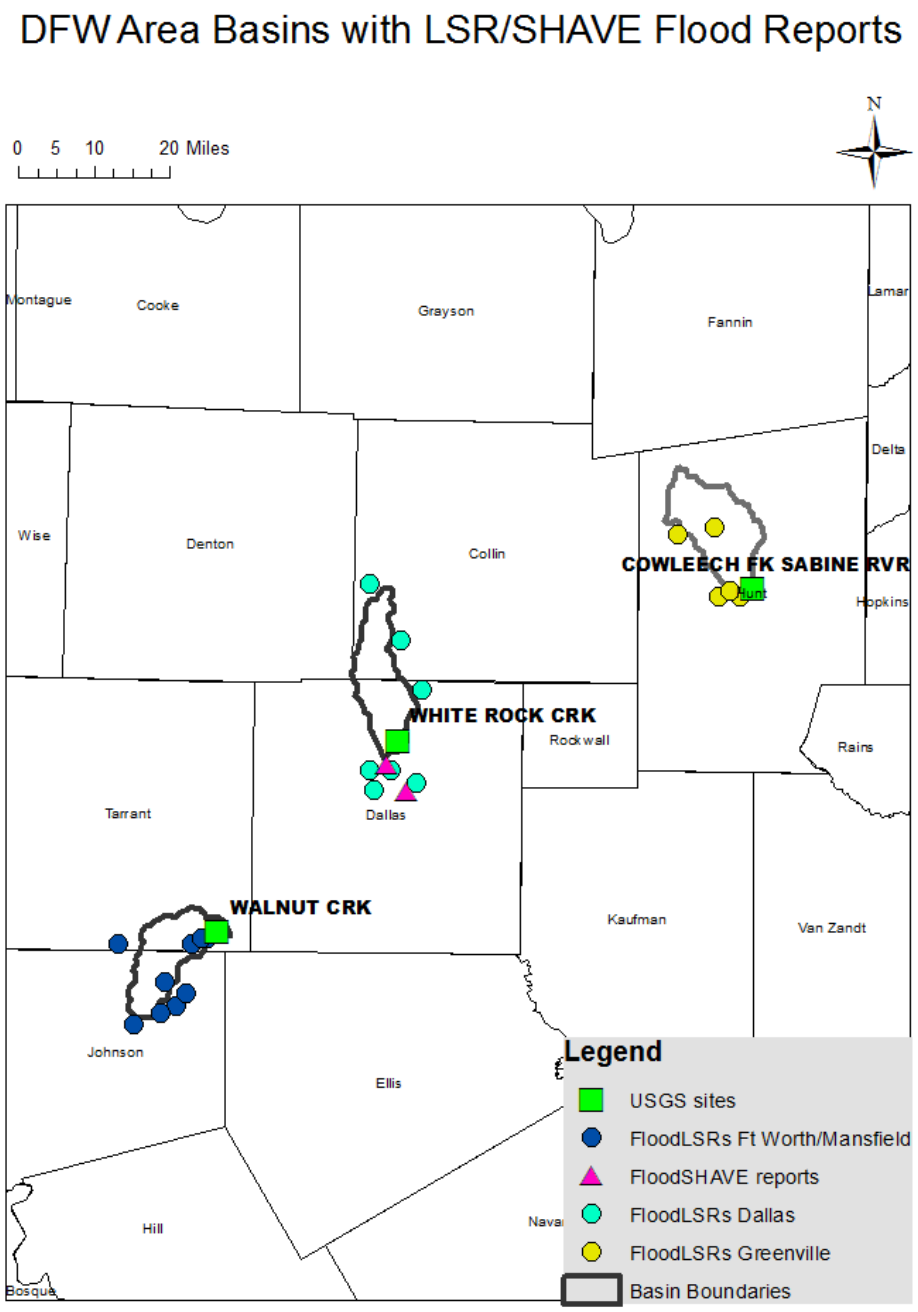

Figure 3.7: DFW area basins used in the study and flood LSR/SHAVE reports associated with those basins that correspond to the time period examined.

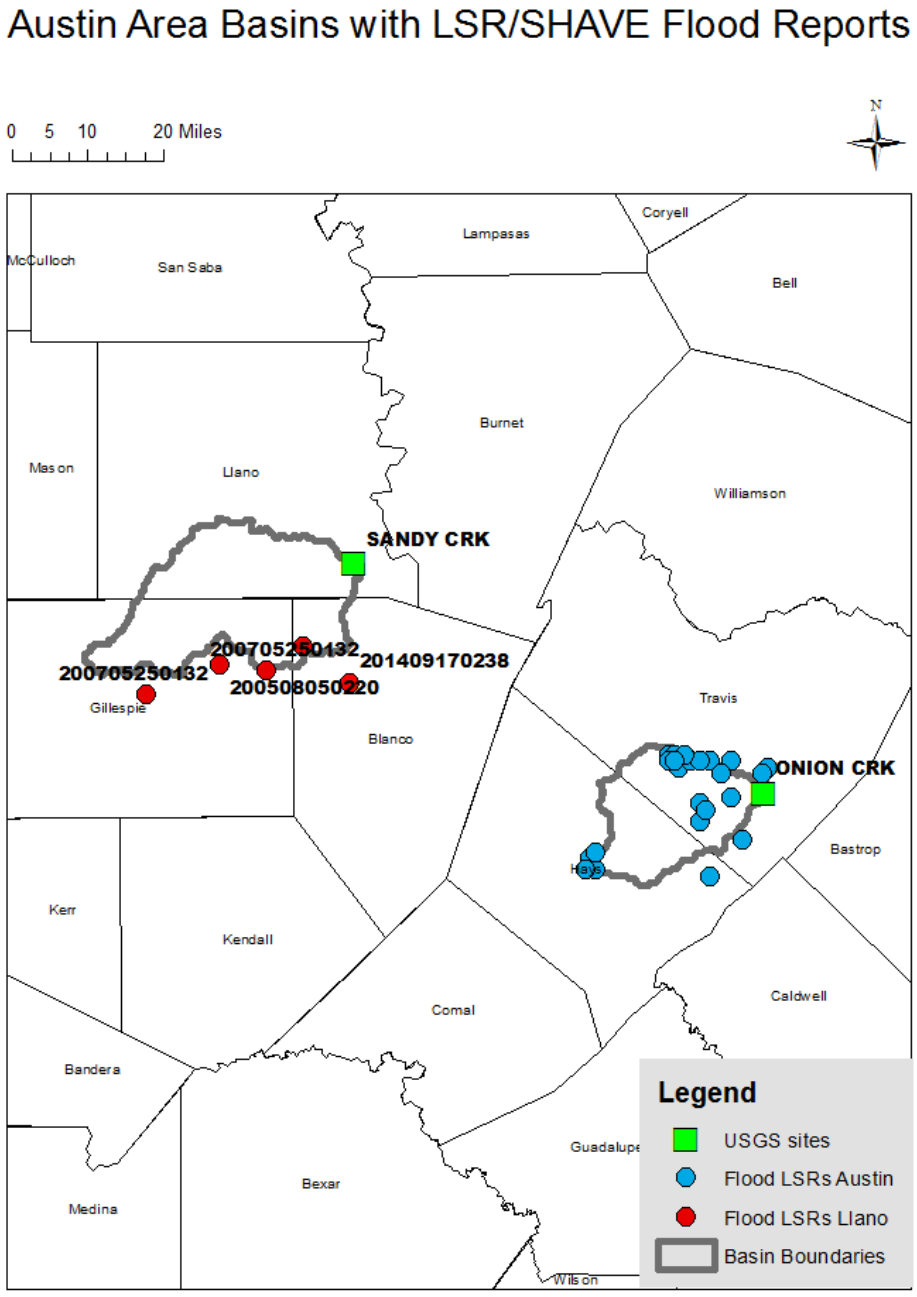

Figure 3.8: Austin area basins used in the study and flood LSR/SHAVE reports associated with those basins that correspond to the time period examined.

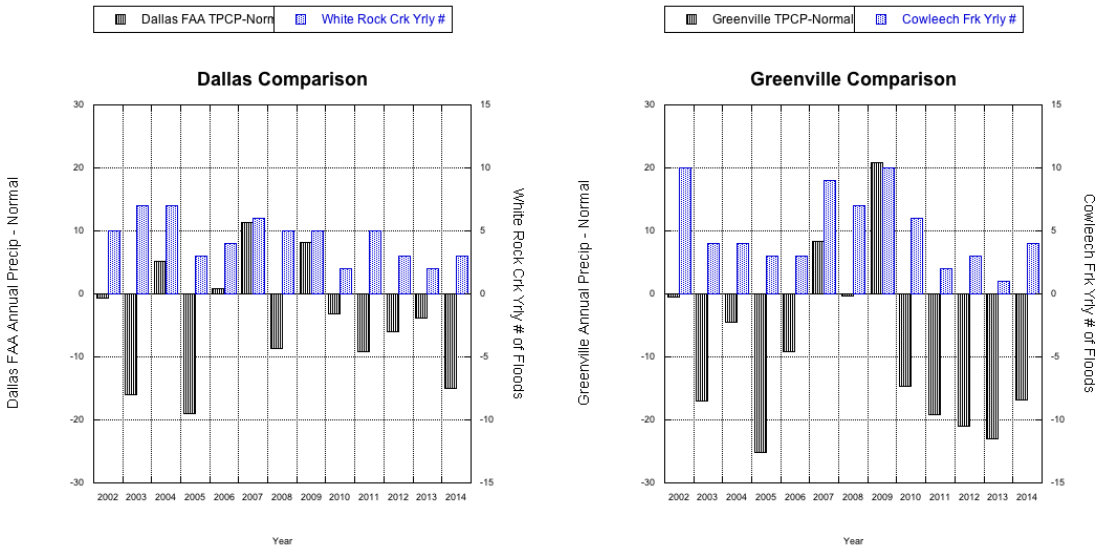

Figure 3.9: Double-y bar graph for Dallas, TX, the urban location (left) and Greenville, TX, the rural comparable (right) that shows the annual rainfall anomaly and annual flood occurrence for each location.

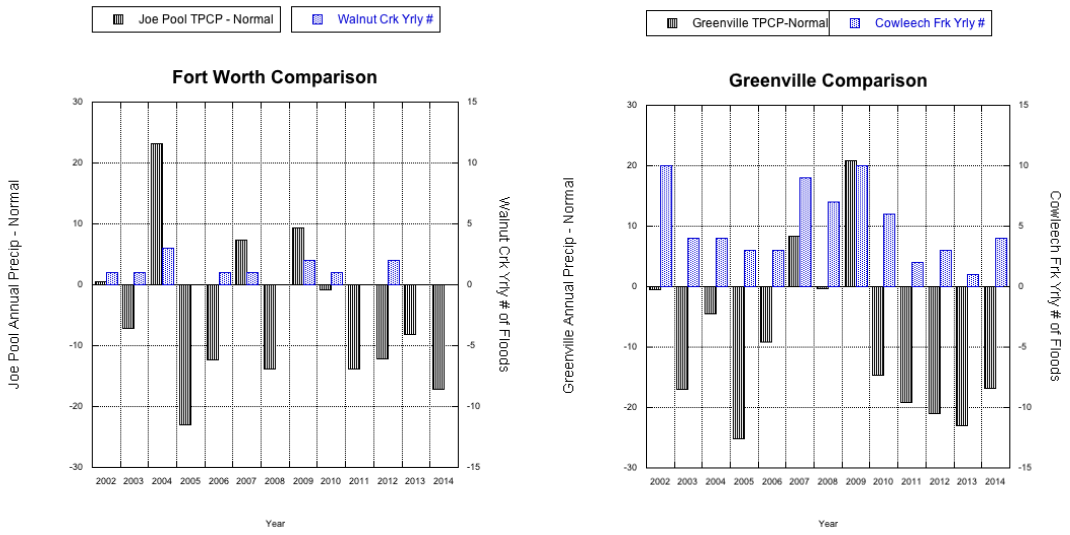

Figure 3.10: Double-y bar graph for Fort Worth, TX, the urban location (left) and Greenville, TX, the rural comparable (right) that shows the annual rainfall anomaly and annual flood occurrence for each location.

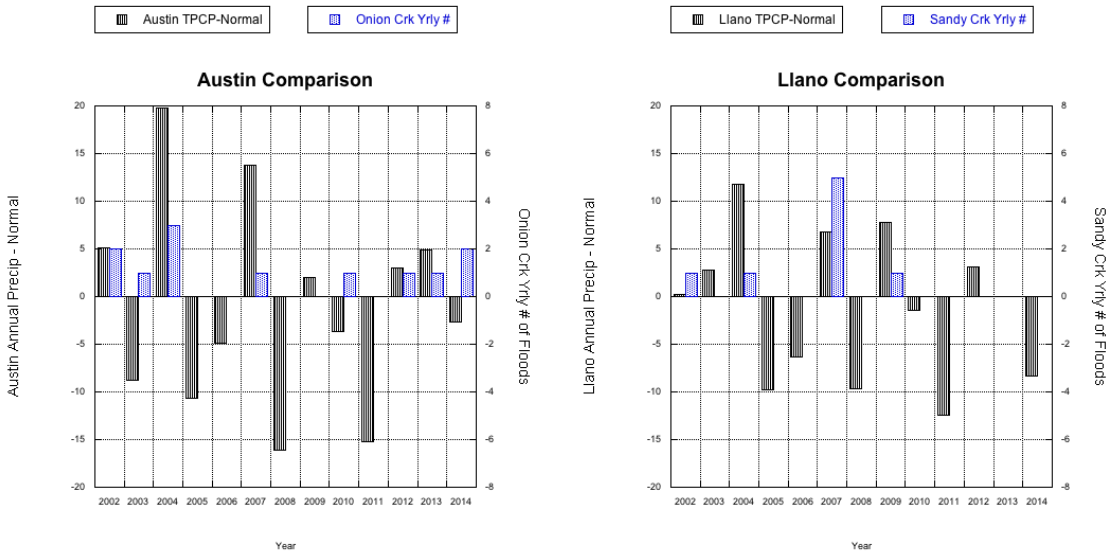

Figure 3.11: Double-y bar graph for Austin, TX, the urban location (left) and Llano, TX, the rural comparable (right) that shows the annual rainfall anomaly and annual flood occurrence for each location.

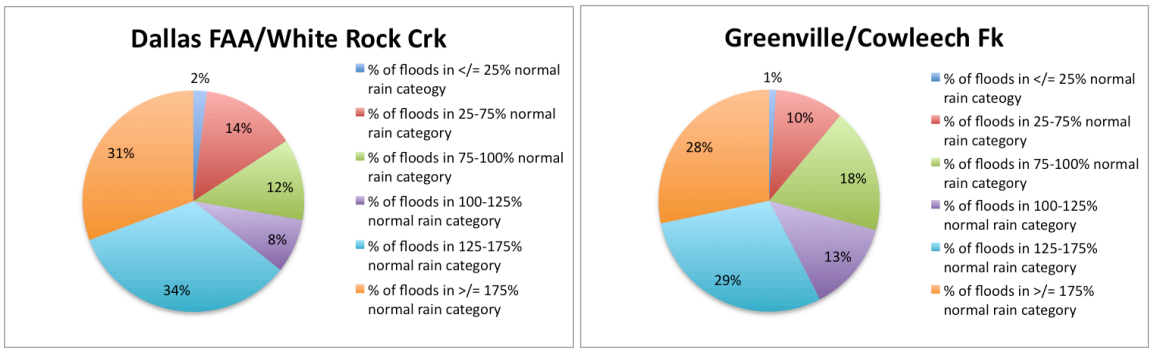

Figure 3.12: Flood occurrence distribution via monthly percent of normal categorical rainfall for Dallas FAA/White Rock Creek at Dallas, TX, the urban Dallas representative (left) and Greenville/Cowleech Fork of the Sabine River at Greenville, TX, the rural comparison site (right) from October 2001 through December 2014.

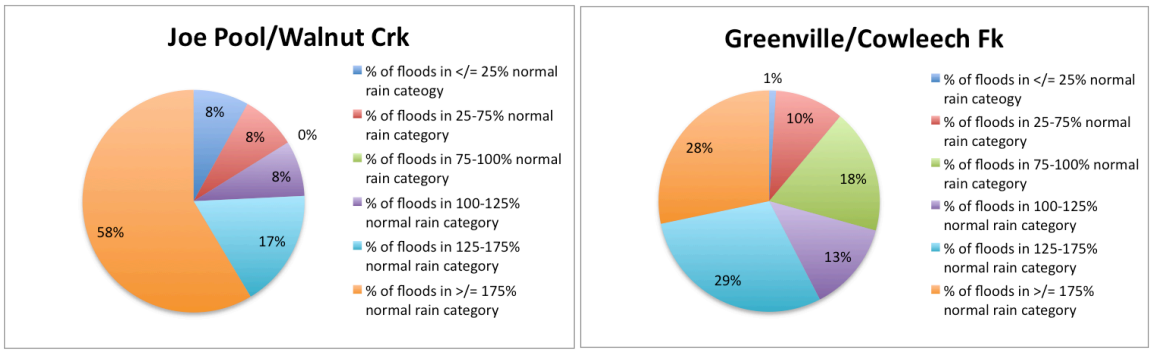

Figure 3.13: Flood occurrence distribution via monthly percent of normal categorical rainfall for Joe Pool Lake/Walnut Creek near Mansfield, TX, the urban Fort Worth representative (left) and Greenville/Cowleech Fork of the Sabine River at Greenville, TX, the rural comparison site (right) from October 2001 through December 2014.

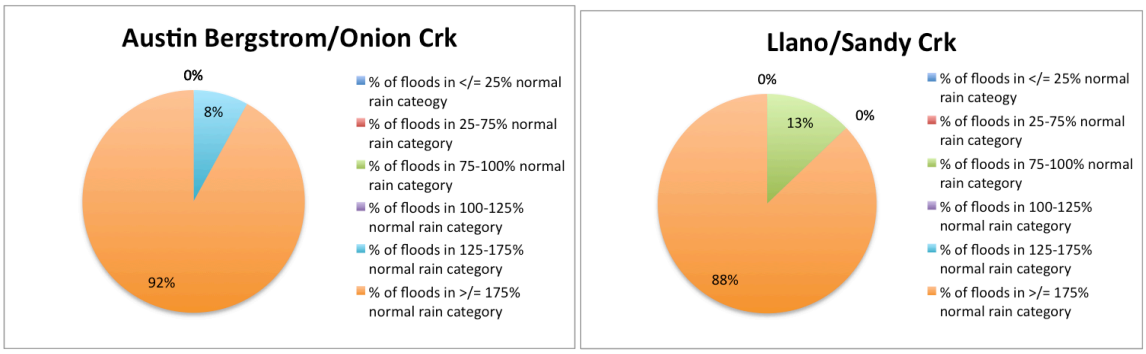

Figure 3.14: Flood occurrence distribution via monthly percent of normal categorical rainfall for Austin Bergstrom/Onion Creek at Austin, TX, the urban Austin representative (left) and Llano/Sandy Creek at Kingsland, TX, the rural comparison site (right) from October 2001 through December 2014.

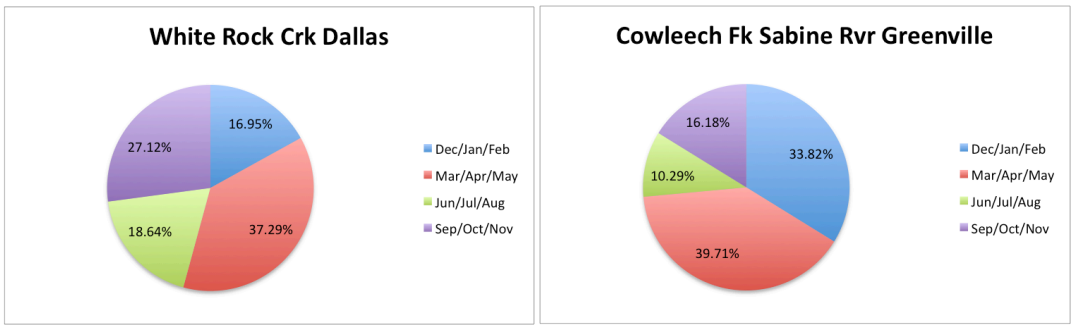

Figure 3.15: Seasonal distribution of flood occurrence for White Rock Creek at Greenville Ave, Dallas, TX (left) and Cowleech Fork of the Sabine River at Greenville, TX, the rural comparison site (right) from October 2001 through December 2014.

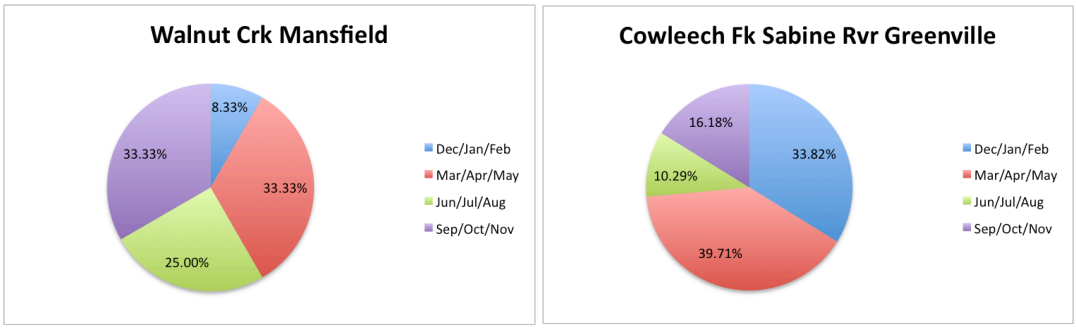

Figure 3.16: Seasonal distribution of flood occurrence for Walnut Creek near Mansfield, TX, the urban Fort Worth representative (left) and Cowleech Fork of the Sabine River at Greenville, TX, the rural comparison site (right) from October 2001 through December 2014.

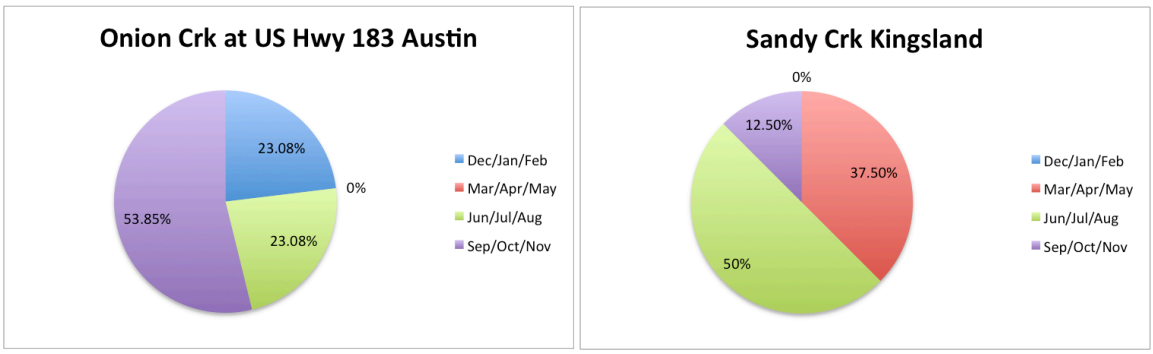

Figure 3.17: Seasonal distribution of flood occurrence for Onion Creek at US Hwy 183 in Austin, TX, (left) and Sandy Creek at Kingsland, TX, the rural comparison site (right) from October 2001 through December 2014.

CHAPTER 4

ATMOSPHERIC AND HYDROLOGIC CONTRIBUTORS TO THE 14 JUNE 2010 FLASH FLOOD EVENT IN OKLAHOMA CITY[3]

[3] Schroeder, A., J. Basara, and J. M. Shepherd. To be submitted to *Journal of Operational Meteorology*.

Abstract

Significant temporal and spatial differences exist for heavy rainfall events, and these events can lead to flash flooding, especially in urban areas. There are various hydrometeorological datasets available to assess flood events, and they have relative strengths and weaknesses. Building upon previous literature, this study analyzed the hydrometeorological aspects of the major flash flood event that affected Oklahoma City, OK on 14 June 2010 using a variety of datasets, including the high density, Oklahoma City Micronet (OKCNET). Results indicated that a classic meso-high flash flood scenario set up across the Oklahoma City metropolitan area during the morning hours of 14 June 2010, which led to copious amounts of rainfall occurring over the same localized area. Also, when the various in situ and remotely sensed datasets were compared to one another, it was discovered that the gage-biased radar mosaic QPE provided the best continuous representation of the rainfall distribution over the entire area. However, it did not adequately capture all details of the rainfall distribution observed by the OKCNET, especially within the central business district (CBD), where the average station spacing was less than 1 km.

4.1 Introduction

Recent research has shown that significant temporal and spatial inhomogeneities exist in heavy rainfall events for the Midwestern United States (Villarini et al. 2011). Furthermore, a slight increase in annual maximum daily rainfall over time was discovered for this same region. Schumacher and Johnson (2006) showed that for most of the eastern two-thirds of the United States (US), the primary weather system types causing the extreme rainfall events were mesoscale convective complexes (MCSs). Using NCDC Storm Data and radar image analyses, Ashley and Ashley (2008a) showed that deadly flood events were caused by MCSs only 36% of the time. However, that study was for the entire US and looked at a slightly different aspect of the problem when compared with the Schumacher and Johnson (2006) analysis that was only for the eastern two-thirds of the US. Likewise, in another study by Ashley and Ashley (2008b), they concluded that the majority of the fatalities occurred in automobiles and a significant percentage of the fatalities were due to persons intentionally walking through the floodwaters. These findings indicate that public awareness of the dangers associated with floods is still lacking.

Various hydrometeorological datasets have relative strengths and weaknesses, but higher spatial resolution data tend to resolve events with the most accuracy. Similar to the results from the Charlotte, North Carolina study conducted by Villarini et al. (2010), which concluded that:

> "the investigation of hydrologic response for extreme rainfall events is greatly enhanced when multiple datasets of good quality are available"

a combination of high spatial and temporal resolution gauge data and radar data will significantly enhance scientific understanding of the extent of an event and help explain the mechanisms behind an extreme urban flooding event, such as the flood event that affected the Oklahoma City metro area in June 2010, when compared to sparse gauge data and limited radar data availability. The current study is *particularly unique* because it leverages the intra-city Oklahoma City Micronet (OKCNET) and densely populated Oklahoma Mesonet, combined with high-resolution mosaic radar data from Arkansas-Red Basin River Forecast Center (ABRFC) to analyze a significant urban flood event, which, to date, has not been previously explored. Furthermore, the OKCNET has not been previously incorporated into any observational flooding research that takes a detailed look at identifying optimal observing methodologies, so the inclusion of this network adds another dimension to the analysis and will add to the current body of literature.

The study domain for this research is the city of Oklahoma City (Fig. 4.1). Located near the geographic center of the state of Oklahoma, Oklahoma City resides in the region known as the Red Bed Plains, an area of gently rolling plains with soft red sandstone and shale underneath fertile topsoil. This geographic area gently slopes upward towards the Rockies to the west; additionally, the density of trees diminishes from east to west in this region of the state. Also, the North Canadian River dissects the city (Bays and Fisher 2010), and many lakes and streams are located within the area as well.

Oklahoma City is a relatively young metropolitan area. However, founded in 1889 during the Land Run, Oklahoma City is a rapidly growing urban area. Since the 2000 United States Census, the population of Oklahoma City itself has increased by an

estimated 14.6% to a total of 579,999 residents (U.S. Census Bureau 2011). Furthermore, the Oklahoma City metropolitan area was ranked as the 31st most populated urban area in the US with over 1 million residents (U.S. Census Bureau 2009). Additionally, the spatial domain of the municipal boundaries of Oklahoma City had grown to span approximately 1570 km^2 and incorporated four counties within central Oklahoma (Oklahoma, Cleveland, Canadian, and Pottawatomie). This placed Oklahoma City within the top ten largest cities by land area in the US, and the largest city that was not a consolidated city-county. However, the portion of Oklahoma City that is currently urbanized is considerably less (approximately 630 km^2). Also noteworthy is that inland water covers approximately 36 km^2 of Oklahoma City (Kelley 2010). Figure 4.2 displays the land use/land cover for the area in and around Oklahoma City (MRLC 2014).

This high-resolution case study examined a flash flood that affected the Oklahoma City area on 14 June 2010 and used data from the OKCNET, Oklahoma Mesonet, NWS WSR-88D radar data, NWS ABRFC QPE hourly mosaic radar data, and other sources to assess the event. The key questions posed here are:

- What were the hydrometeorological factors associated with the June 2010 flooding event in OKC?
- What were the spatio-temporal characteristics of this extreme urban flooding event?
- How does the diagnosis of an extreme urban flooding event vary as a function of the spatio-temporal complexity of available observing methodologies?

It was expected that some aspects of the synoptic/mesoscale factors contributing to the event were unique, and that the impervious surface land cover enhanced runoff, significantly contributing to the flood event. The different datasets were expected to expose various elements of the event and provide for a unique, in-depth analysis. The combination of NWS radar data and in situ data from OKCNET and Oklahoma Mesonet likely provide enhanced resolution of the flood event, yet the inclusion of land use/land cover data likely enhanced the results beyond the capability of the meteorological data alone.

4.2 Data

To assess the land use/land cover characteristics for the area, National Land Cover Database 2011 data were downloaded from the Multi-Resolution Land Characteristics Consortium (MRLC) website. This dataset consisted of a 16-class land cover classification scheme at a spatial resolution of 30 meters across the US (MRLC 2014). To evaluate the antecedent conditions prior to the event, datasets included: Oklahoma Mesonet data, Palmer Drought Indices (NCDC 2013), and USGS streamflow data (USGS 2013).

Each Oklahoma Mesonet station deployed across the state of Oklahoma measures core parameters that include: air temperature and relative humidity at 1.5 m, wind speed and direction at 10 m, atmospheric pressure, downwelling solar radiation, rainfall, and bare and vegetated soil temperatures and moisture at multiple levels below ground level. Figure 4.3 shows the Oklahoma City West (OKCW) Mesonet site, located near N. Portland Avenue and Black Gold Drive in the western portion of Oklahoma City. All

Oklahoma Mesonet data are collected and transmitted to a central point every 5 minutes where they are quality controlled, distributed and archived (Brock et al. 1995, Shafer et al. 2000, McPherson et al. 2007).

The widely used Palmer Index, which refers to the 3 indices established by W. Palmer in the 1960s, provides a measure of the departure from normal moisture conditions in both the "wet" and "dry" sense (Heim 2002). The collaborative United States Drought Monitor, which incorporates numerous drought indices, is not included in this assessment because it only shows abnormally dry areas and does not show areas with abnormally wet conditions. To help explain the various Palmer indices, it should be noted that the opposite of flood, drought, has several types: agricultural, meteorological, hydrological, and socioeconomic, and they affect various entities and at different time scales. The Palmer Z-Index (Z Index) uses moisture anomalies to measure short-term drought conditions on a monthly scale and is typically used to get a sense of the effect of the moisture state on agriculture (i.e. agricultural drought). The Palmer Drought Severity Index (PDSI) illustrates long-term drought conditions with a focus on departure from normal cumulative meteorological conditions (i.e. meteorological drought) and incorporates duration and intensity of atmospheric circulation patterns. The Palmer Hydrological Drought Index (PHDI) provides a sense of the long-term drought conditions with a focus on departure from normal hydrological conditions (i.e. hydrological drought), and this method provides a good sense of the condition of groundwater and reservoir levels. While both PDSI and PHDI are a measure of the long-term conditions, PDSI tends to respond more quickly than PHDI, as meteorological conditions can change

very rapidly but the hydrologic response of the system tends to take longer to develop (NCDC 2013).

To assess the synoptic and mesoscale conditions leading up to and during the event that affected Oklahoma City, surface and upper air data were incorporated. The sounding data, available online from the University of Wyoming Department of Atmospheric Science (University of Wyoming 2013), were incorporated from the National Weather Service Weather Forecast Office in Norman, OK (OUN), which is located approximately 30 km south/southeast of downtown OKC. The climatological distribution of precipitable water for OUN, available from the National Weather Service Weather Forecast Office in Rapid City, SD (NWS UNR 2013), was also used. Surface and upper air data for the entire US that came from the National Weather Service Storm Prediction Center (NOAA SPC 2012) were also utilized, along with North American Regional Reanalysis (NARR) data (NOAA ESRL 2015). Finally, to address the event itself, the primary data sources came from the OKCNET, Oklahoma Mesonet, and various NWS radar products including: WSR-88D radar data from KTLX and ABRFC's hourly and 24-hour mosaic radar quantitative precipitation estimates (QPE), both the raw radar mosaic and the gage-biased mosaic products.

Deployed from 2008 through 2010, the OKCNET was a network of automated meteorological stations that measured atmospheric variables throughout Oklahoma City. The 40-station network consisted of four Oklahoma Mesonet stations (McPherson et al. 2007) and 36 traffic signal stations mounted on traffic signals at a height of approximately 9 m and station spacing of approximately 3 km (Basara et al. 2010). At each OKCNET traffic signal site, air temperature, humidity, pressure, rainfall, wind

speed, and wind direction at 9 m were measured and transmitted every minute to a central facility where they were quality controlled, distributed, and archived using the Oklahoma Mesonet infrastructure (Shafer et al. 2000). Furthermore, the OKCNET included a cluster of stations within the central business district (CBD), as well as stations dispersed throughout the city. Figures 4.4 and 4.5 provide further information regarding OKCNET. Finally, each Oklahoma Mesonet site deployed as part of OKCNET included sensors to measure air temperature at 9 m, as well as the routine variables provided by each Oklahoma Mesonet site.

The Arkansas-Red Basin River Forecast Center (ABRFC), an entity of NOAA's National Weather Service (NWS), aids the NWS with support regarding river and flood forecasts and warnings. Figure 4.6 shows the area of responsibility for the ABRFC, which is comprised of over 530,000 km^2 and includes portions of seven states, including the entire state of Oklahoma (ABRFC 2011). The raw radar mosaic quantitative precipitation estimate (QPE) and the adjusted radar mosaic QPE products provided by ABRFC were used in this study. Both of these products utilize the raw radar mosaic product, which incorporates rainfall estimates from all radars covering a given location. The gage-biased product goes a step further and adds quality control procedures, both automated and manually-adjusted, and includes in situ rainfall gage adjustments. It is important to note that this radar product incorporated the rainfall information from both the Oklahoma Mesonet and OKCNET. Both radar datasets are on a 4 km x 4 km grid and at a 1-hour time resolution. Figures 4.7 and 4.8 illustrate the ABRFC's 24-hr. total precipitation gage biased radar product for the time period used for this study.

4.3 Methods

In order to answer the first research question, the antecedent conditions leading up to the 14 June 2010 flood event in Oklahoma City were evaluated using a variety of hydrometeorological sources. Because the Palmer Index provides a measure of an area's departure from normal moisture conditions across the US, maps illustrating the spatial variability of the various Palmer indices can be quite useful in determining the broad preexisting conditions for an area at risk for flooding; therefore they were examined for the 5 ½ month period leading up to the event in question. An assessment of the streamflow patterns from multiple USGS streamflow sites in the area using time series plots was incorporated as well.

Next, soil moisture data from the Oklahoma Mesonet were included in the analysis to further contribute to the evaluation of the overall hydrologic state of the area leading up to the event. This evaluation was necessary due to the role antecedent soil moisture has on the occurrence of floods (Kunkel et al. 1999). Additionally, numerous spatial maps at various atmospheric heights, soundings from OUN, and time series plots of multiple Oklahoma Mesonet variables were used to determine the hydrometeorological set up. More specifically, a synoptic analysis using the surface and upper air maps at various levels was used to define the overall atmospheric conditions and mean prevailing wind direction for the region; also, the climatological distribution of surface to 300 mb precipitable water plotted with the precipitable water associated with the event taken from rawinsonde soundings from OUN was graphed, and multiple other factors, discussed in Chapter 2 of this dissertation, were evaluated. These detailed spatial plots,

soundings, graphs, and time series depicting the overall conditions prior to the event were used to illustrate the condition of the atmosphere and subsurface for the area.

To assess the event itself, data from both the OKCNET and Oklahoma Mesonet, coupled with KTLX radar data and the ABRFC radar mosaic products, were used to analyze the 14 June 2010 urban flooding case for Oklahoma City. The specific site metadata associated with the Oklahoma City Micronet (Schroeder et al. 2010) and NLCD 2011 land use/land cover data were also used to help address the land use/land cover characteristics for the area, allowing for a better understanding of the spatial variability of the imperious surface extent. A spatial plot of the urban land cover characteristics was then created to compare with the generated spatial plots of precipitation. Also, the mean prevailing flow was established using rawinsonde data at the 700 mb level from OUN to determine what region was considered "downwind" during the event to aid in the possible determination of urban influences.

To address the final research question, comparisons among the various datasets were performed. As stated earlier, the ABRFC adjusted radar mosaic product used in this study is a gage-biased QPE, and the in situ observations analyzed in the current study were incorporated into the generation of this particular radar mosaic product. Therefore, the addition of a radar-only QPE product was incorporated, along with the gage-biased QPE and in situ observations, to evaluate the variability between the datasets. Difference maps depicting the spatial distribution of differences among the various data types allowed for the diagnosis of optimal observing methodologies for an extreme urban flooding event, and incorporating root mean square error (RMSE) and Mann-Kendall

statistical analyses provided further quantitative assessments of the differences between the datasets.

To construct the difference maps, the Oklahoma Mesonet and OKCNET shapefiles were obtained from the Oklahoma Climatological Survey, along with the mts files containing the data for the event. Next, shapefiles of the ABRFC's gage-biased and raw radar mosaic QPE products for the event were obtained. While the radar mosaic shapefiles for the event were provided by ABRFC, the hourly rainfall accumulations for the various Oklahoma Climatological Survey datasets had to be constructed from the raw data and added to the shapefiles for those locations in order to perform a spatial comparison of rainfall for the event. Additionally, because all of the precipitation datasets were displayed as points, rasters had to be created for the spatial comparison, and this was done using the natural neighbor spatial interpolation scheme in ArcMap. Once all data sources were converted to raster format, several spatial differences were computed using the ABRFC's gage-biased mosaic QPE as the control. The other 3 data sources (ABRFC's raw radar mosaic QPE raster, an Oklahoma Mesonet raster, and a combined Oklahoma Mesonet and OKCNET raster) were subtracted from the control to determine how those datasets compared to the gage-biased product. Figure 4.9 provides the Model Builder created in ArcMap that was used to construct the above mentioned process.

Finally, root mean square error (RMSE) was calculated using the OKCNET, Oklahoma Mesonet, and ABRFC's gage-biased QPE for the event. Once the RMSE results were obtained, Mann-Kendall tests were then calculated from the results to draw inferences with respect to the RMSE calculations associated with the 3 datasets. Therefore, the ability of the gage-biased radar mosaic QPE to accurately capture the true

rainfall characteristics observed by the rain gauge networks could be quantitatively assessed through the examination of the p-value.

4.4 Results

Event Precursors

Several datasets were used to evaluate the soil conditions for central Oklahoma prior to the June 2010 flood event that affected Oklahoma City. First, the Palmer Indices were examined because they provide a measure of the departure from normal moisture conditions in both the "wet" and "dry" sense and on a broad spatial scale. Figure 4.10 shows the 3 different Palmer Drought indices for the month prior to the event, and Figure 4.11 provides the Z-index maps for the first 4 months of 2010 (NCDC 2013). According to the various Palmer Drought indices, central Oklahoma had been under normal subsurface moisture conditions since April 2010 for the PDSI and since March 2010 for the Palmer Z Index and the PHDI. The moisture conditions further back in time were only "moderately moist" for the area, and not extreme according to these metrics.

Another useful data source to evaluate the preexisting soil conditions came from the Oklahoma Mesonet. Fractional water index (FWI) is a unitless indicator of soil moisture that provides a sense of available plant water (divided into tenths) and, unlike many other variables, is independent of soil type. It is a normalized variable developed for the Campbell Scientific 229-L soil sensor (Schneider et al. 2003), which is used at Oklahoma Mesonet sites for obtaining soil moisture data. FWI has a range from 0.0 for very dry soil to 1.0 for saturated soil (Illston et al. 2008, Oklahoma Mesonet 2013). Long-term averages and departures from average for 2003-2012 were obtained through

the Mesonet website, and Figures 4.12 and 4.13 illustrate some of the results. Note that these average calculations only use data for a 10-year period, instead of the standard 30-year period of record to calculate normals. However, inferences can still be drawn from the time series plots regarding the state of the soil for both the central climate division, in which Oklahoma City is located within, as well as the Spencer, OK (SPEN) Mesonet site, one of the 4 Mesonet sites included in the OKCNET. Comparing the various FWI plots and the Palmer Index maps showed fairly good agreement on the state of the soil moisture in central OK, in that the conditions were not abnormally wet for the period leading up to the June 2010 flood event.

Finally, USGS streamgage data from various sites across the Oklahoma City metropolitan area were used to assess the trends in streamflow/gage height (i.e. discharge/stage). Figure 4.14 displays the locations of the 3 sites around the Oklahoma City metropolitan area that were assessed (NWS AHPS 2015). All 3 locations are situated along the North Canadian River, with the Yukon site located northwest of the CBD, the Britton Road location in the northern suburbs of the city, and the Harrah location in a rural section of eastern Oklahoma County. Gage height data were not available for download from the USGS website, but streamflow data were available for all 3 sites across the city and were used in conjunction with each site's individual rating curve and known NWS flood stage to evaluate the riverine hydrologic trends. Figures 4.15 and 4.16 (USGS 2013) provide information for one of the USGS locations important for the 2010 OKC flood event, the site located along the North Canadian River at Britton Road in Oklahoma City. For this USGS site, flood stage is 17 ft., and, based on the rating curve, the discharge value associated with this flood stage (minor flood stage) is approximately

8,000 cfs. Therefore, based on the discharge vs. time graph provided in Figure 4.16, the 14 June 2010 event was the first time that year that flood stage was met or exceeded, providing further evidence that the area was not abnormally wet. The other 2 locations (not shown) exhibited similar trends during the first 5 ½ months of 2010 as well. Therefore, this detailed antecedent subsurface moisture analysis showed that the area was not necessarily preconditioned for a major flood event to occur.

An upper air analysis from the morning of 14 June 2010 illustrated that central Oklahoma was downstream of a positively tilted trough. Little speed and directional shear was present between the low and mid levels of the atmosphere, and a shortwave was approaching from the west, evident from the 850 mb and 500 mb plots from 12 UTC on 14 June 2010 (Fig. 4.17). Additionally, a moist, low-level jet was injecting deep moisture into the region. This can be seen in the observed synoptic plots (Fig. 4.17), as well as in the North American Regional Reanalysis (NARR) data plots (Fig. 4.18). The NARR data displayed an abundant amount of moisture over Oklahoma, not only at 850 mb, but also at 700 mb, and this abundant mid-level moisture is likely one of the drivers behind the event. These NARR plots also display strong winds at 850mb, which continued to pump that moisture into the area, and upper level divergence (NOAA ESRL 2015). The sounding from OUN, located approximately 30 km south/southeast of downtown Oklahoma City, demonstrated that the atmosphere was uncapped with over 2000 J/kg of convective available potential energy (CAPE) and had a low level of free convection (557 m AGL). Further evidence of an extremely moist environment came from the 0-1 km and surface to 850 hPa mixing ratios, which were around 17 g/kg (Table 4.1). Furthermore, the precipitable water value was 54.79 mm (2.16 in.), which was

greater than the 99th percentile compared to climatology (Figs. 4.19 and 4.20). This assessment of precipitable water and resulting anomalously high value is similar to the precipitable water results observed in the catastrophic 2009 Atlanta flood (Shepherd et al. 2011).

When assessing the additional variables that were identified in Chapter 2 of this dissertation as being potential precursors for major urban flash flood events (Table 4.1), several additional aspects stood out for the Oklahoma City event. The atmosphere was very warm with a melting level located more than 4 km AGL and a -10°C level greater than 6 km AGL. With a lifted condensation level (LCL) of 469 m AGL, this led to a warm cloud depth (WCD) that was 5872 m thick, as WCD is defined here as the layer between the lifted condensation level (LCL) and the height of the -10°C level. This approach was taken because supercooled water is typically present when temperatures are above -10°C, yet below 0°C (WDTB 2014). Incidentally, this was the same definition used in Chapter 2 of this dissertation and the Vitale and Ryan (2013) study that examined low-echo centroid convection associated with high precipitation events. Warm rain precipitation processes governed by collision-coalescence instead of the Bergeron process, which requires the presence of ice in the cloud, is dominant if water is still in liquid form (Vitale and Ryan 2013), and warm rain processes are typically more efficient rainfall producers.

At the surface, a low was positioned over northeast KS and a pendent cold front was slowly creeping through Oklahoma during the early morning hours. The 12 UTC rawinsonde analysis from OUN showed that surface temperature and dewpoint were warm, 25°C and 22°C respectively, and the surface relative humidity was a soupy 79%.

Event Overview

During the evening hours of Sunday, 13 June 2010, thunderstorms developed over northwestern portions of Oklahoma ahead of a slowly advancing cold front. An outflow boundary from this early convection, oriented from northeast to southwest, which paralleled the orientation of the synoptic cold front, slowly propagated south toward Oklahoma City (OKC) during the overnight hours, with showers and thunderstorms scattered north of the boundary (Figs. 4.21 and 4.22). As the convection moved closer to OKC, enhancement of this convection occurred northeast of the city, allowing the outflow boundary orientation to change and become aligned in an east-west fashion. This led to the outflow boundary being positioned nearly perpendicular to the cold front as the outflow boundary passed through central OK. As stated earlier via the upper air map analysis, a moist, low-level jet also developed during overnight hours over the area, bringing moisture in from the south to feed the storms.

As the slow moving cold front continued to approach from the northwest, the outflow boundary stalled just south of the OKC metro. By 0900 UTC (4:00 a.m. CDT) on 14 June 2010, intense convection developed along the leading edge of the outflow boundary and moved into the Oklahoma City metropolitan area (Figs. 4.23 and 4.24). This setup led to continuous regeneration of thunderstorms in the same general area with propagation into central and northern portions of OKC for several hours on 14 June 2010 (Figs. 4.25 and 4.26). These training storms dumped over 250 mm (10 in.) of rain across portions of the metro by the next morning. The convection appears to continuously redevelop just SW of OKC in part because of the development of a strong easterly low-level jet behind the stalled outflow boundary that balanced the southerly nocturnal low

level jet (LLJ). Winds behind the outflow boundary were oriented E NE with a speed max of 35 kts around 2000 ft, and the nocturnal LLJ had winds from the S SW with speeds around 35 kts as well. The easterly jet behind the outflow boundary extended up to around 4200 ft and was present for several hours. Figure 4.27 provides schematic details of this setup.

As a result of the approaching upper level shortwave from the southwest, convection began to develop in south central Oklahoma by mid-morning, along the larger scale surface boundary. This convective development was on the warm side of the outflow boundary, and had a different origination point than the continuous convection that had been providing the OKC metro area with the copious amounts of rainfall through the morning hours. As the convection from south central Oklahoma approached Oklahoma City, it became more enhanced. It wasn't until this convection, originating along the larger-scale cold front southwest of OKC, moved through the city and developed a cold pool strong enough to disrupt the balance between the two low-level jets that the outflow boundary was able to nudge southward and take with it the major source of lift and resultant training thunderstorms that had plagued the area all morning.

Additionally, as the shortwave from the west approached central OK, and the larger scale cold front, originating from the low over KS, stalled just west of OKC, another weak surface low became evident southwest of OKC. This coupled with the stalled outflow boundary led to the setup of a classic meso-high event (Figure 4.28), described in further detail by Maddox et al. (1979). Figure 4.29 provides additional observational evidence of such a setup for the OKC event with plots of pressure (reduced

to sea level), as well as 10 m winds and the rainfall accumulation since midnight for 1600 UTC (11:00 a.m. CDT) on 14 June 2010.

Located in southwest OKC, Will Rogers World Airport, OKC's official observing station, recorded a daily total of 194 mm (7.64 in.), which was the largest value ever recorded for any day at that location since 1890 (NWS OUN 2015). However, even greater storm total rainfall values were measured by other automated sites, as well as human observers, including a measurement of 312 mm (12.3 in.) within the northern OKC suburb of Edmond. These observations were supported by estimated precipitation derived from surface and radar observations, as well as the rainfall distribution from the OKCNET and Oklahoma Mesonet sites (Fig. 4.30). The majority of the rain that fell over the area occurred within a 6-hr. period during the Monday morning rush hour. Dramatic rescues were needed but no fatalities were directly caused by the flood event. The precipitation frequency (PF) curves for northern Oklahoma City (Fig. 4.31), available from the NOAA Atlas 14, further illustrate the anomalous nature of this event (NOAA HDSC 2015). Based on the 24-hour rainfall reports across the northern extent of the city, this event had an average recurrence interval of at least 200 years (i.e. 0.5 % chance of occurring within any given year).

The hydrologic response to the excessive rainfall for the USGS sites was impressive as well. The USGS site located at Britton Road is a "flashy" urban watershed located in the northern part of the city, where the rainfall accumulation was the highest for the event. This site peaked with a discharge of 22,900 cfs and a stage value of approximately 22 ft. by 10:30 a.m. CDT on the 14th; which equated to moderate flood stage based on the NWS flood stage criteria for the location. The recovery for the gage to

minor flood stage occurred by 2 p.m. CDT the day after the event, with action stage being reached an hour later. However, the USGS site near Harrah, located downstream from the other two USGS sites, had a more dramatic and extended response. It had a peak discharge value of 17,400 cfs and a corresponding stage value of 19 ft. by 9:00 a.m. CDT on the 15th. Therefore, based on the local rating curve and NWS flood stage criteria, this location crested to major flood stage the morning after the event began, while the Britton Road location had crested within a few hours of the onset of the event. It wasn't until 2:30 a.m. CDT on the 16th that the site fell below minor flood stage and didn't fall below action stage until 9:30 p.m. on the 16th, nearly 30 hours after the Britton Road site reached action stage.

Hydrometeorological Dataset Analysis

As mentioned previously, several rainfall datasets were utilized in this study, including 2 in situ datasets (OK Mesonet and OKCNET) and 2 remotely sensed mosaic radar datasets (the gage-biased and raw mosaic QPE from ABRFC). To examine the differences between these datasets, difference maps were created to compare each type. Because the gage-biased mosaic product incorporated the OK Mesonet and OKCNET rainfall data in order to produce the final product, the gage-biased QPE was designated as the control, and all other datasets were compared to it (i.e.: test – control). In order to properly assess the differences, the analysis was divided into two time frames: the 24-hour rainfall accumulation ending at 12 UTC on 14 June 2010 and the 24-hour rainfall accumulation ending at 12 UTC on 15 June 2010. Figures 4.32-4.34 display the difference map results for the first time frame. The results comparing the raw radar

mosaic product to the control for the first time period show that the raw radar mosaic underestimated the rainfall totals for the majority of the OKC metro area. However, a small area of overestimation was present in the south central portions of the city, as seen by the warm colors. When viewing the difference map that utilizes the Oklahoma Mesonet sites, it becomes apparent that the gage-biased mosaic product was overestimating the rainfall accumulation for most of the OKC metro but underestimating over the area where the raw radar mosaic was overestimating. Finally, when assessing the results that compared the combined Oklahoma Mesonet/OKCNET raster with the gage-biased radar mosaic product, differences still existed but not to the same magnitude as previous comparisons showed. The gage-biased product was overestimating the rainfall accumulation for the OKC metro, with the exception of the area right around the OKCN site, where the gage-biased product was overestimating. These maps also bring to light that the RFC did not appear to take the in situ rainfall totals at face value for the majority of the sites because differences still existed for the bins where many of the sites were located.

When moving on to the second time frame, the 24-hour rainfall accumulation ending at 12Z on 15 June 2010, the differences among the datasets was magnified, likely because this time period incorporated the majority of the precipitation for the event. Figures 4.35-4.37 display the results from this time period. The raw radar mosaic vs. gage-biased mosaic difference map showed that, with the exception of a small area in the central business district (CBD), the raw mosaic product underestimated the rainfall accumulation for the OKC metro. Moving on to the Oklahoma Mesonet minus the gage-biased mosaic product difference map, the results showed that a broad area of gage-

biased underestimation existed within the CBD and an area of gage-biased overestimation existed for the southwestern and northeastern portions of the city. When assessing the final difference map, which compared the combined Oklahoma Mesonet/OKCNET raster to the gage-biased raster, the results showed that where a high concentration of OKCNET sites was located, relatively minor differences between the two rasters existed.

One of the unique characteristics of this study was this spatial comparison among the various datasets, which includes the high resolution, research quality urban network that was the OKCNET. This hydrometeorological dataset evaluation showed that when observations from a high-density in situ network are incorporated into the hydrometeorological analysis of a flood event, more realistic assessments of the rainfall distribution could be made. However, the gage-biased mosaic product was unable to capture all of the spatial variability of the rainfall distribution that the OKCNET provided. It was also apparent that the raw radar mosaic product continually underestimated the rainfall distribution for the Oklahoma City metro area. The sounding analysis showed that warm rain processes likely were the dominant convective scheme, and WSR-88D rainfall estimates during warm rain processes are often underestimated because the sensor cannot properly account for the high concentration of small droplets that lead to the rapid accumulation of rainfall observed at the surface (Smith et al. 1996; Petersen et al. 1999). This is due to the fact that algorithms used to estimate rainfall are based on the reflectivity factor (Z), which is dependent upon the number and diameters (raised to the sixth power) of what is being sampled in the radar volume scan (Rinehart 2004). With the diameters of the raindrops in warm rain processes being relatively small,

the corresponding reflectivity factors are dampened as well, resulting in an underestimation of rainfall.

Finally, the root mean square error RMSE calculations were performed for 2 comparisons: OKCNET vs. ABRFC's gage-biased radar mosaic QPE and Oklahoma Mesonet vs. ABRFC's gage-biased radar mosaic QPE. The average RMSE for the OKCNET vs. the gage-biased QPE was 0.56 in., and the average RMSE for the Oklahoma Mesonet vs. the gage-biased QPE was 0.14 in. These results showed that the RMSE associated with the OKCNET data were substantially greater than the RMSE associated with the Oklahoma Mesonet data. When the average RMSE was calculated for the CBD sites within the OKCNET, the value was even higher at 0.60 in. This demonstrates that the ABRFC gage-biased mosaic QPE was not accurately capturing the rainfall distribution observed by the OKCNET compared to the Oklahoma Mesonet when calculating their bias corrections applied to the raw radar product, especially for locations within the densely clustered CBD. With an average error of over half an inch calculated for the urban area, significantly underestimated impacts could result because much of the rainfall within an urban area is directly converted to runoff. Errors of over half an inch could be the difference between a minor "nuisance" flood and a major life-threatening flood.

When a right-tailed Mann-Kendall test was run on these data, it produced a p-value of less than 0.0001, thus providing very strong evidence that the OKCNET RMSE values were greater than the Oklahoma Mesonet RMSE values. This evidence showed that the gage-biased QPE was not accurately capturing the rainfall characteristics sampled by the OKCNET and strongly suggests this was not a random occurrence.

Part of the reason for this outcome is likely due to the difference in spatial resolution among the datasets. As stated earlier, the spatial resolution of the ABRFC mosaic QPE was on a 4 km x 4 km grid, but the average spacing between for the entire OKCNET was 3 km. The OKCNET was designed so that sites were clustered together tightly within the CBD and increased in spacing as distance from the CBD increased, much like the spokes of a bicycle wheel. Therefore, for the OKCNET sites located within the CBD, the average station spacing was even finer at less than 1 km. This illustrates how the gage-biased mosaic QPE would have a difficult time capturing the true rainfall characteristics measured by the OKCNET, especially within and near the CBD, where sites were more densely clustered. The rainfall distribution from the OKCNET was a sub-grid scale feature, unable to be captured by the coarser gage-biased radar mosaic QPE. This is similar to why traditional radar technology cannot resolve a tornado: it is typically a sub-grid scale feature that cannot be accurately sampled with the current technology, and without advances in the science and technology that lead to finer resolution sampling, will never be accurately depicted.

4.5 Conclusions

Record precipitation fell in the Oklahoma City metropolitan area on 14 June 2010, which led to a significant flash flood event. An analysis of the antecedent conditions revealed that central Oklahoma was not abnormally wet or dry, so the soils were not preconditioned to flooding. However, between 100 and 300 mm of rain fell over a 12 hr. period, with the peak falling during a 6-hr. period that included the Monday morning rush hour and led to a major flash flood event for the city. The detailed analysis

showed that the extremely heavy rainfall and flash flooding that ensued on 14 June 2010 was due to a number of critical factors including:

- A nearly stationary outflow boundary situated just south of Oklahoma City, providing focus for storm initiation and redevelopment with convection repeatedly moving over the urban area
- A strong low-level jet and weak speed and directional shear in the lower troposphere
- The development of an easterly jet that balanced the southerly low level jet, preventing the advancement of the outflow boundary for several hours
- Broad ascent through the lower troposphere evident by the conditionally unstable atmosphere (low LFC and CAPE values near 2000 J/kg)
- Very moist ambient environment evident in the extremely high precipitable water values and mixing ratios

Additionally, this flood event was a classic meso-high event, and the available observing systems allowed for the detailed identification of such. Furthermore, based on the evolution of the event, including the setup of both a southerly low-level jet and an easterly jet, it cannot be concluded that the urban area created an enhancement of the rainfall for the event. However, whether or not the urban area played a role in the distribution cannot be ruled out either.

Additionally, a comparison of the different observing methodologies was performed and revealed that the inclusion of high-density, research quality in situ networks, like the Oklahoma Mesonet and OKCNET, provide valuable information for the development of a more complete assessment of the spatial distribution of rainfall

across the area. Including such data was especially critical given the limitations of raw radar products regarding rainfall estimation during excessive rainfall events resulting from warm rain processes. The analysis also revealed that the gage-biased radar mosaic QPE was unable to capture all of the fine details of the rainfall distribution for the event that were observed by the OKCNET, likely due in part to the differences in spatial resolution between the two datasets, especially within the CBD. These results illustrated that the inclusion of rainfall observations from high spatial resolution networks, like the OKCNET, provide meso-urban scale rainfall information that the comparably course-resolution radar data often misses. Incorporating such data provides valuable small-scale details that could potentially make a substantial difference in observed impacts. Therefore, there is a need for use of high density in situ rainfall observations along-side more spatially continuous radar products for assessment of heavy rainfall events to get a more thorough picture of the rainfall distribution across an area.

This study can provide unique insight into a specific observed urban flooding event for Oklahoma City through the coupled analysis of high spatial and temporal resolution in situ data and robust radar mosaic data. This approach provides additional insight into the event, and understanding the details of such an event in Oklahoma City can aid urban planners, emergency managers, weather forecasters, and water resource management in preparing for future events.

4.6 References

ABRFC, cited 2011: About the ABRFC (Arkansas-Red Basin River Forecast Center). [Available online at http://www.srh.noaa.gov/abrfc/?n=aboutpage.]

Ashley, S. T. and W. S. Ashley, 2008a: The storm morphology of deadly flooding events in the United States. *Int. J. of Climatolo*., **28**, 493-503.

Ashley, S. T. and W. S. Ashley, 2008b: Flood fatalities in the United States. *J. Appl. Meteor. Climatolo.*, **47**, 805-818.

Basara, J. B., B. G. Illston, C. A. Fiebrich, P. Browder, C. Morgan, J. P. Bostic, A. McCombs, R. A. McPherson, A. J. Schroeder, and K. C. Crawford, 2010b: The Oklahoma City Micronet. *Meteorological Applications*, doi:10.1002/met.189

Bays, B. A. and D. K. Fisher, 2010: Oklahoma. The World Book Encyclopedia, **14**, 712-737.

Brock, F. V., K. C. Crawford, R. L. Elliott, G. W. Cuperus, S. J. Stadler, H. L. Johnson, M. D. Eilts, 1995: The Oklahoma Mesonet: A Technical Overview. J. Atmos. Oceanic Tech., **12**, 5-19.

Heim, Jr., R., 2002: A review of Twentieth-Century drought indices used in the United States. *Bull. Amer. Meteor. Soc.*, **83**, 1149-1165.

Illston, B. G., J. B. Basara, D. K. Fisher, R. Elliott, C. A. Fiebrich, K. C. Crawford, K. Humes, E. Hunt 2008: *Mesoscale Monitoring of Soil Moisture across a Statewide Network*. *J. Atmos. Oceanic Technol*., **25**, 167-181.

Kelley, E., 2010: Oklahoma City. The World Book Encyclopedia, **14**, 735-737.

Kunkel, K. E., R. A. Pielke, and S. A. Changnon, 1999: Temporal fluctuations in weather and climate extremes that cause economic and human heath impacts: A review. *Bull. Amer. Meteor. Soc*., **80**, 1077-1098.

Maddox, R. A., C. F. Chappell, and L. R. Hoxit, 1979: Synoptic and meso-alpha aspects of flash flood events. *Bull. Amer. Meteor. Soc., **60,*** 115–123.

McPherson, R. A., C. Fiebrich, K. C. Crawford, R. L. Elliott, J. R. Kilby, D. L. Grimsley, J. E. Martinez, J. B. Basara, B. G. Illston, D. A. Morris, K. A. Kloesel, S. J. Stadler, A. D. Melvin, A.J. Sutherland, and H. Shrivastava, 2007: Statewide Monitoring of the Mesoscale Environment: A Technical Update on the Oklahoma Mesonet. J. Atmos. and O. Tech., **24**, 301–321.

Multi-Resolution Land Characteristics Consortium, cited 2014: National Land Cover Database 2011 (NLCD 2011). [Available online at http://www.mrlc.gov/nlcd2011.php.]

National Climate Data Center, cited 2013: Historical Palmer drought indices. [Available online at http://www.ncdc.noaa.gov/temp-and-precip/drought/historical-palmers.php.]

National Oceanic and Atmospheric Administration (NOAA) Earth System Research Laboratory (ESRL), cited 2015: 3-hourly North American Regional Reanalysis (NARR) composites. [Available online at http://esrl.noaa.gov/psd.]

National Oceanic and Atmospheric Administration (NOAA) National Weather Service Storm Prediction Center (SPC), cited 2012: Surface and upper air maps. [Available online at http://www.spc.noaa.gov/obswx/maps/]

National Oceanic and Atmospheric Administration (NOAA) National Weather Service Hydrometeorological Design Studies Center (HDSC), cited 2015: NOAA Atlas 14 point precipitation frequency estimates: OK. [Available online at http://hdsc.nws.noaa.gov/hdsc/pfds/pfds_map_cont.html?bkmrk=ok.]

National Weather Service (NWS) Advanced Hydrologic Prediction Service (AHPS), cited 2015: WFO OUN Observations. [Available online at http://water.weather.gov/ahps2/index.php?wfo=oun.]

National Weather Service (NWS) Weather Forecast Office: Norman OK (OUN), cited 2015: Climatological Averages and Records. [Available online at http://www.srh.noaa.gov/oun/?n=climate-records.]

National Weather Service (NWS) Weather Forecast Office: Rapid City, SD (UNR), cited 2013: Precipitable water plots. [Available online at http://www.crh.noaa.gov/unr/?n=pw.]

Oklahoma Mesonet, cited 2013: Fractional Water Index. [Available online at http://www.mesonet.org/images/site/Fractional%20Water%20Index%20User%20Info%20Aug2013.pdf.]

Petersen, W. A., L. D. Carey, S. A. Rutledge, J. C. Knievel, N. J. Doesken, R. H. Johnson, T. B. McKee, T. V. Haar, J. F. Weaver, 1999: Mesoscale and radar observations of the Fort Collins flash flood of 28 July 1997. *Bull. Amer. Soc*. **80**(2), 191-216.

Rinehart, R. E., 2004: *Radar for Meteorologists, 4th Ed*. Rinehart Publications, 482 pp.

Schneider, J. M., D. K. Fisher, R. L. Elliott, G. O. Brown, and C. P. Bahrmann, 2003: Spatiotemporal variations in soil water: First results from the ARM SGP CART network. *J. Hydrometeor*., **4**, 106–120.

Schroeder, A. J., J. B. Basara, and B. G. Illston, 2010: Challenges Associated with Classifying Urban Meteorological Stations: The Oklahoma City Micronet Example. *The Open Atmos. Sci. J.,* **4**, 88-100.

Schumacher, R. S. and R. H. Johnson, 2006: Characteristics of U.S. extreme rain events during 1999-2003. *Weather and Forecasting*, **21**, 69-85.

Smith, J. A., D. J. Sao, M. L. Baeck, M. D. Hudlow, 1996: An intercomparison study of NEXRAD precipitation estimates. *Water Resour. Res*., **32**(7), 2035-2045.

Shafer, M. A., C. A. Fiebrich, D. S. Arndt, S. E. Fredrickson, and T. W. Hughes, 2000: Quality assurance procedures in the Oklahoma Mesonetwork, *J. Atmos. Oceanic Technolo*., **17**, 474-494.

Shepherd, J. M, T. Mote, J. Dowd, M. Roden, P. Knox, S. C. McCutcheon, and S. E. Nelson, 2011: An overview of synoptic and mesoscale factors contributing to the disastrous Atlanta flood of 2009. *Bull. Amer. Meteor. Soc*., **92**, 861-870.

United States Census Bureau, cited 2009: Metropolitan and micropolitan statistical area population and estimated components of change: April 1, 2000 to July 1, 2008. [Available online at http://www.census.gov/popest/metro/files/2008/CBSA-EST2008-alldata.csv.]

United States Census Bureau, cited 2011: State and county quickfacts. [Available online at http://quickfacts.census.gov/qfd/index.html.]

United States Geological Survey, cited 2013: WaterWatch. [Available online at http://waterwatch.usgs.gov/index.php?r=ok&id=pa01d.]

University of Wyoming, College of Engineering, Dept. of Atmospheric Science, cited 2013: Weather. [Available online at http://weather.uwyo.edu/upperair/sounding.html.]

Villarini, G., J. A. Smith, M. L. Baeck, P. Sturdevant-Rees, and W. F. Krajewski, 2010: Radar analysis of extreme rainfall and flooding in urban drainage basins. *J. of Hydro*., **381**, 266-286.

Villarini, G., J. A. Smith, M. L. Baeck, R. Vitolo, D. B. Stephenson, and W. F. Krajewski, 2011: On the frequency of heavy rainfall for the Midwest of the United States. *J. of Hydro*., **400**, 103-120.

Vitale, J. D. and T. Ryan, 2013: Operational recognition of high precipitation efficiency and low-echo-centroid convection. *J. Operational Meteor*., **1**, 128-143.

WDTB, cited 2014: Introduction to the Top-Down Methodology, Topic 6, Lesson 1, AWOC Winter Weather Track. Warning Decision Training Branch, Norman, OK. [Available online at www.wdtb.noaa.gov/courses/winterawoc/IC6/lesson1/player.html.]

Table 4.1: Statistical analysis of important surface and moisture parameters, vertical levels, stability parameters, and upper level wind changes for the events used in Chapter 2 with the addition of the values from the June 2010 OKC event examined in the current Chapter.

	Ch. 2 Average	**Ch. 2 Standard Deviation**	**Ch. 2 Max**	**Ch. 2 Min**	**12z 14 June 2010 value**
Surface T [°C]	22.3	4.7	31.4	9.0	25.4
Surface Td [°C]	19.6	3.7	25.5	6.4	21.7
Surface RH [%]	85	12	100	53	79
Surface - 850 hPa mean mixing ratio (g kg^{-1})	14.05	2.36	18.21	7.59	17.17
0 - 1 km mean mixing ratio (g kg^{-1})	14.60	2.70	19.45	7.60	17.52
0 - 3 km mean mixing ratio (g kg^{-1})	11.99	1.83	14.61	6.78	13.80
Melting Level [m AGL]	4108	502	4791	2734	4285
Height of -10 °C Level [m AGL]	6213	466	6782	5021	6341
WCD (m)	5866	522	6680	4691	5872
LCL [m AGL]	346.27	299.95	1262.93	17.02	469.37
MUCAPE	1817	1155	5146	76	2537
MUCIN	-16	23	0	-85	0
700-500 hPa lapse rate [°C/km]	5.95	0.79	7.47	3.61	6.58
850-500 hPa lapse rate [°C/km]	6.17	0.54	7.23	4.79	6.33
0-3 km lapse rate [°C/km]	5.97	0.93	7.79	3.79	6.14
3-6 km lapse rate [°C/km]	5.94	0.72	7.56	3.86	6.60
K Index	37.3	4.1	44.5	26	43.2
700 hPa wind speed [kts]	24	16	70	3	22
Wind speed change btw 700 and lowest MAN hPa level [kts]	5	14	52	-20	0
Wind speed change btw 500 and lowest MAN hPa level [kts]	11	16	64	-13	11
Wind direction change btw 700 and lowest MAN hPa level [deg]	44	50	200	-16	30
Wind direction change btw 500 and lowest MAN hPa level [deg]	67	57	210	-45	50

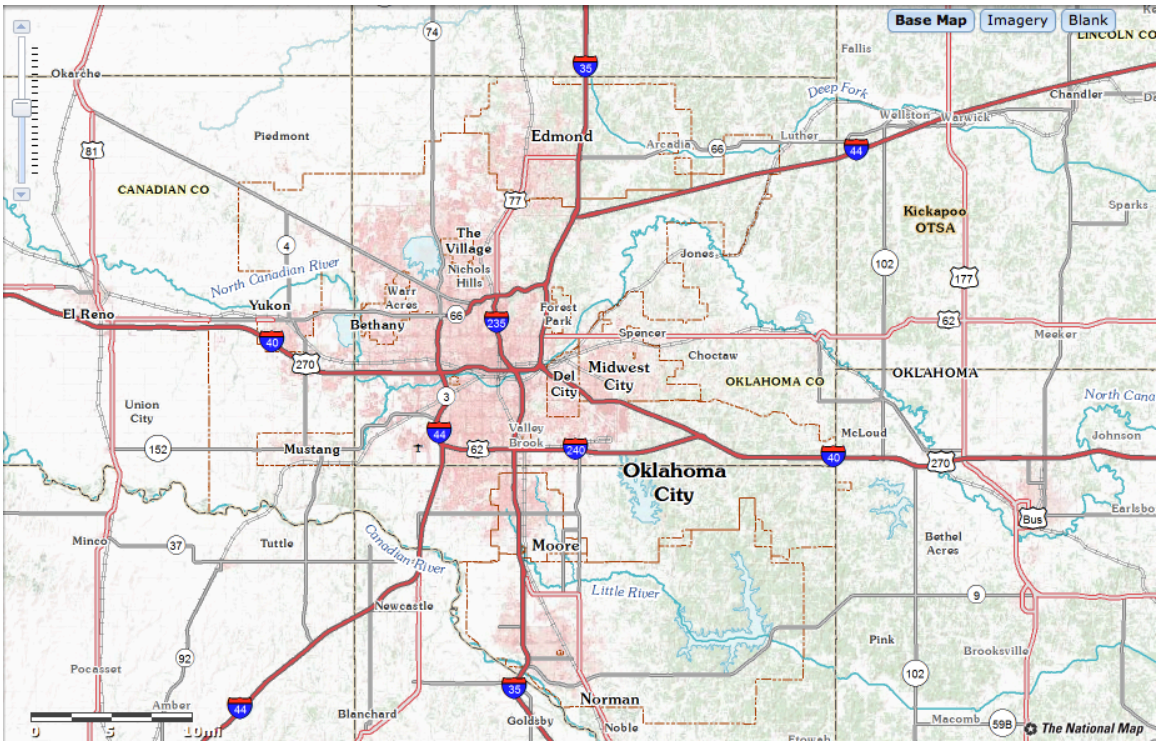

Figure 4.1: Map of Oklahoma City, OK (generated from http://viewer.nationalmap.gov/viewer/).

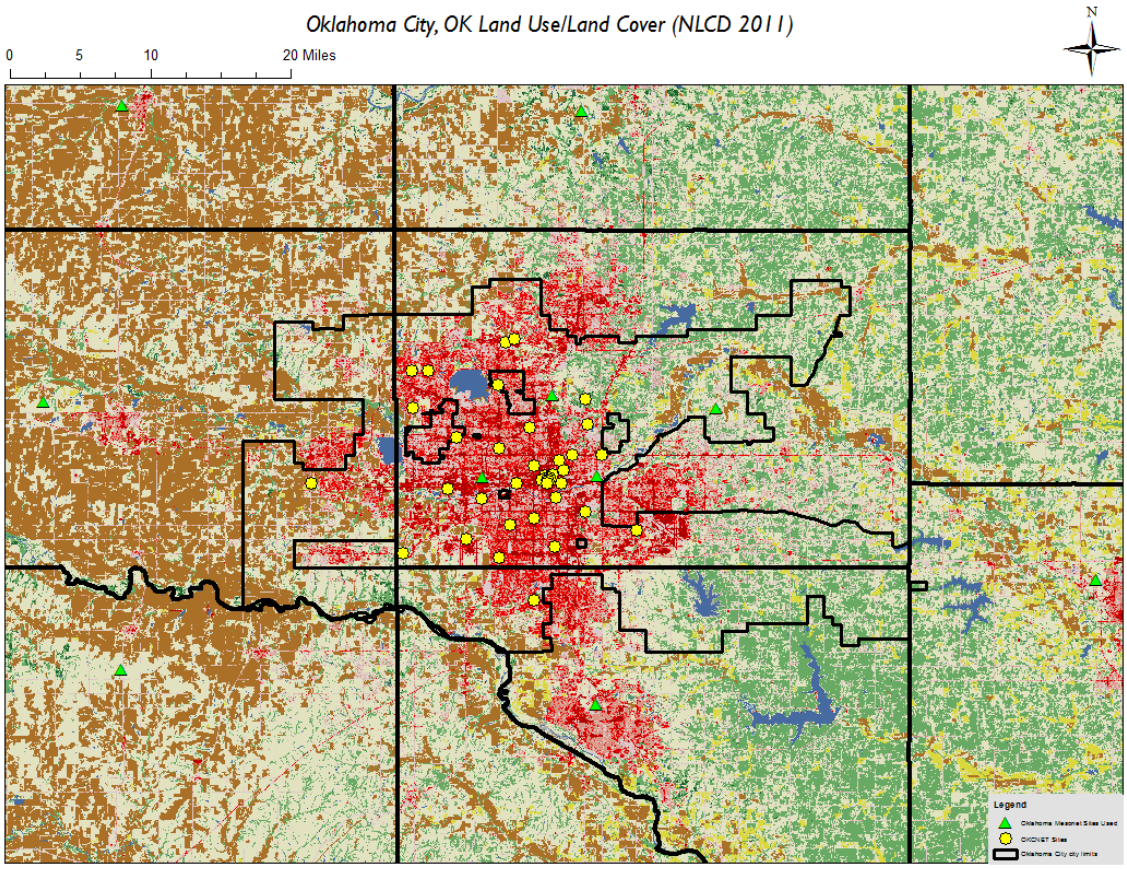

Figure 4.2: NLCD 2011 land use/land cover characteristics for the Oklahoma City metropolitan area (MRLC 2014).

Figure 4.3: OKCW Mesonet site, located near N. Portland Ave. and Black Gold Dr. in the western portion of Oklahoma City.

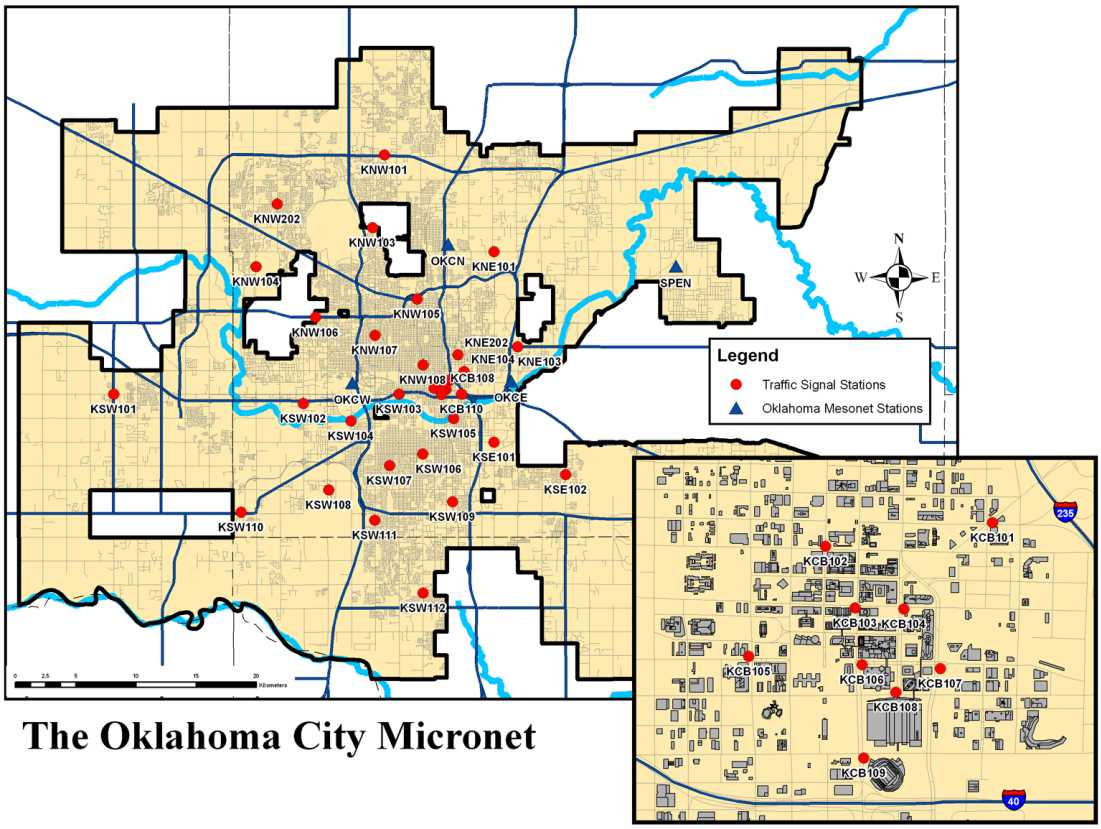

Figure 4.4: Distribution of OKCNET sites (red circles indicate traffic light sites and blue triangles indicate Oklahoma Mesonet sites associated with the OKCNET network; *courtesy of the Oklahoma Climatological Survey*).

a) 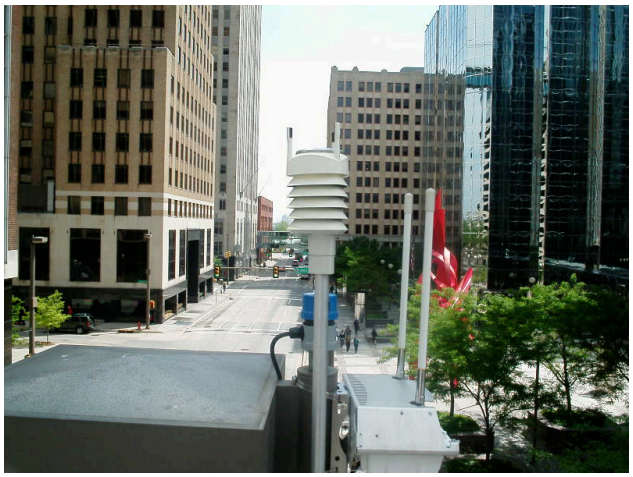 b) 

Figure 4.5: a) “Bird’s eye view” and b) street view of KCB103, the OKCNET site located at Robert S. Kerr Ave. and N. Robinson Ave. in downtown Oklahoma City (*courtesy of the Oklahoma Climatological Survey*).

Fig. 4.6: Area of responsibility (shaded in green) for the ABRFC (ABRFC 2011).

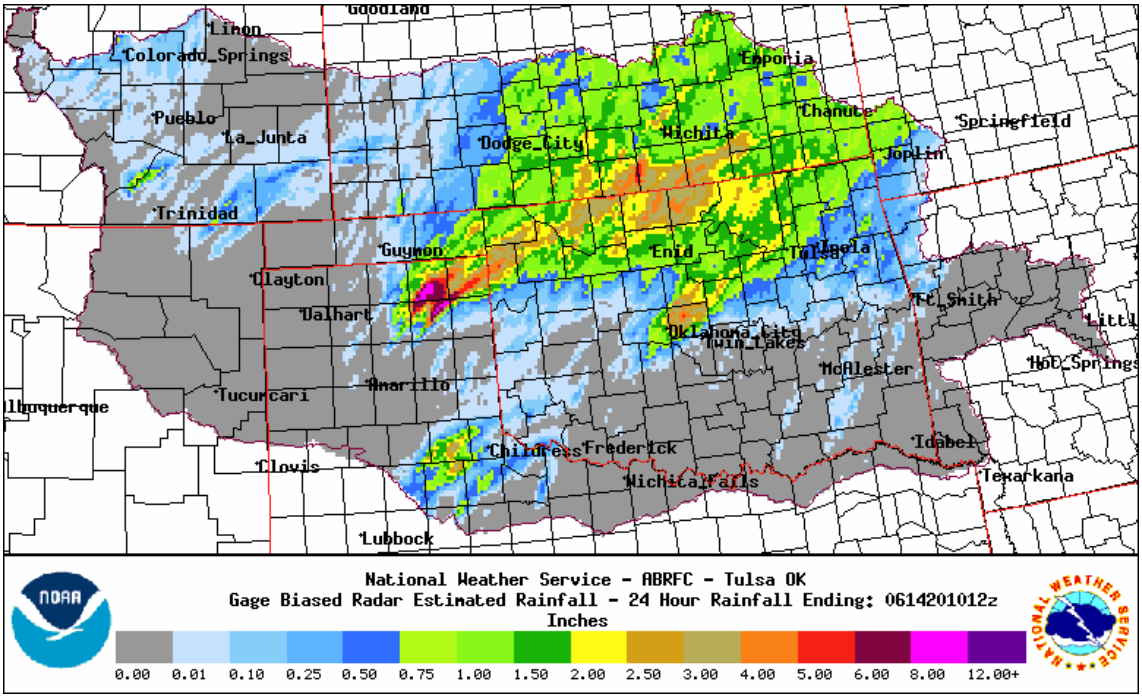

Figure 4.7: 24-hr. total gage biased radar estimated rainfall for the ABRFC area for time ending 14 June 2010 at 0000 UTC (http://www.srh.noaa.gov/abrfc/arc_search.php).

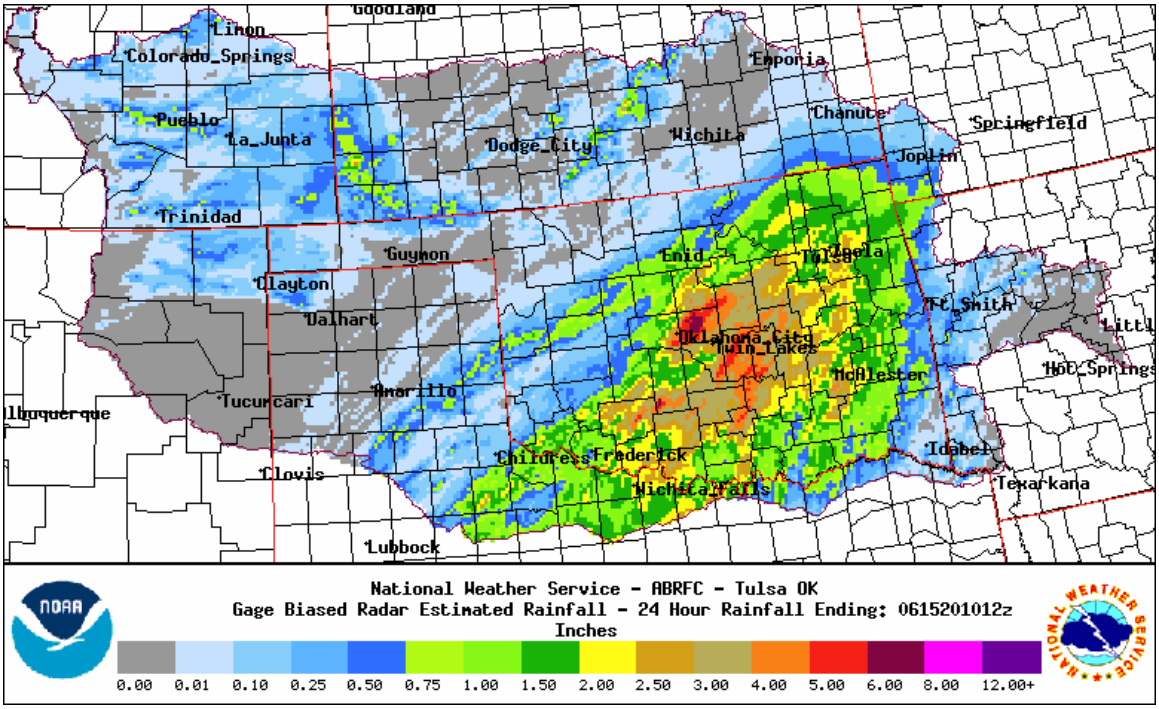

Figure 4.8: 24-hr. total gage biased radar estimated rainfall for the ABRFC area for time ending 15 June 2010 at 0000 UTC (http://www.srh.noaa.gov/abrfc/arc_search.php).

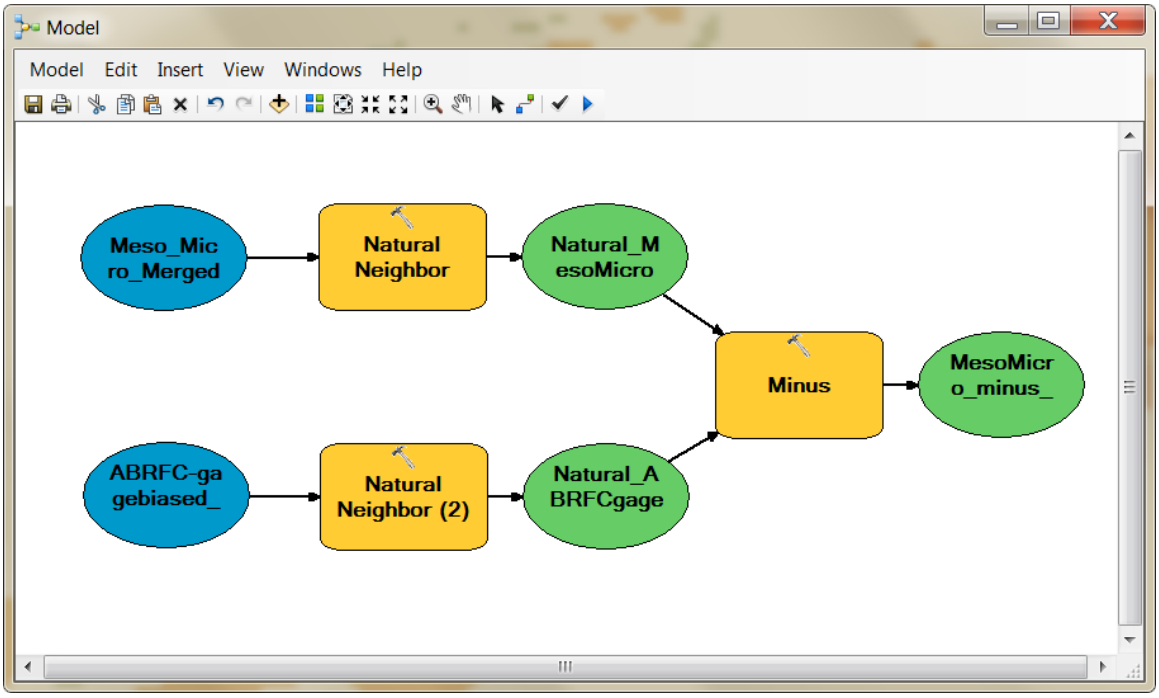

Figure 4.9: Model Builder created for the construction of the difference maps used in this study to compare the various observing systems.

(a)

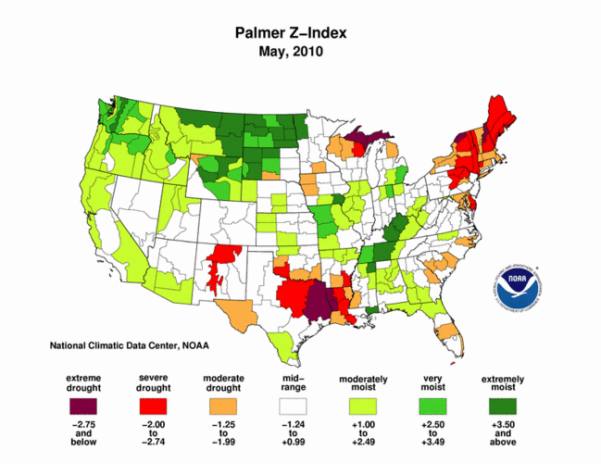

(b)

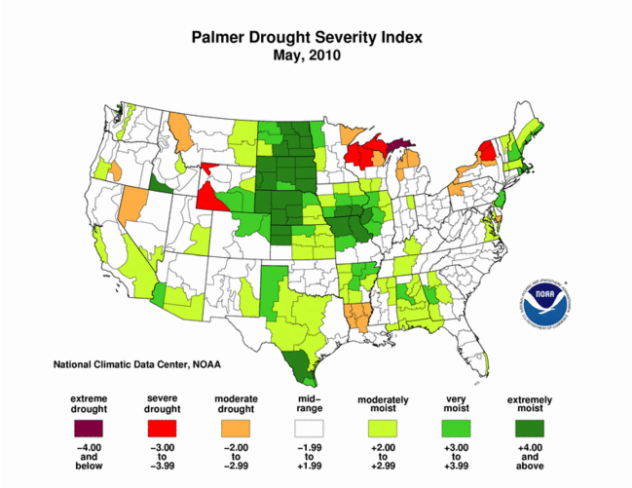

(c)

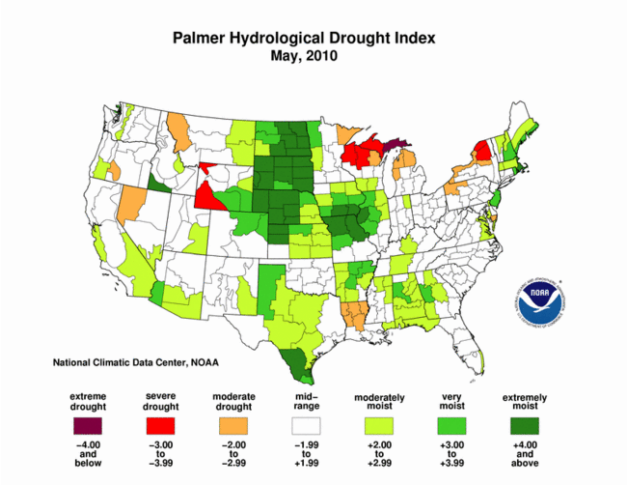

Figure 4.10: May 2010 Palmer Drought indices for the contiguous United States divided into climate division (a) Palmer Z-Index, (b) Palmer Drought Severity Index, (c) Palmer Hydrological Drought Index (NCDC 2013: http://www.ncdc.noaa.gov/oa/climate/research/prelim/drought/palmer.html).

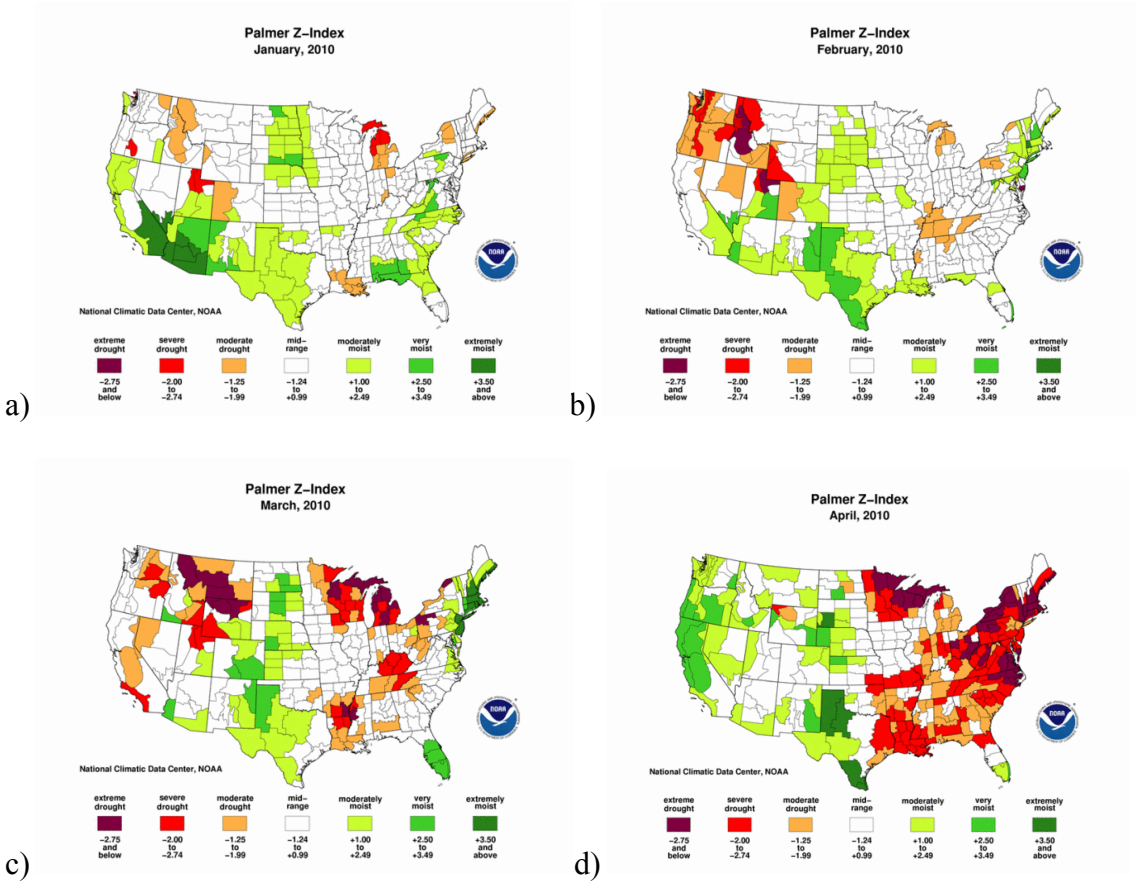

Figure 4.11: Palmer Z-Index maps for the contiguous United States divided into climate division for a) January 2010, b) February 2010, c) March 2010, and d) April 2010 (NCDC 2013: http://www.ncdc.noaa.gov/oa/climate/research/prelim/drought/palmer.html).

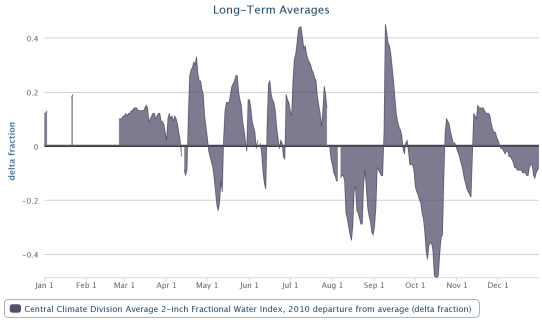

a)

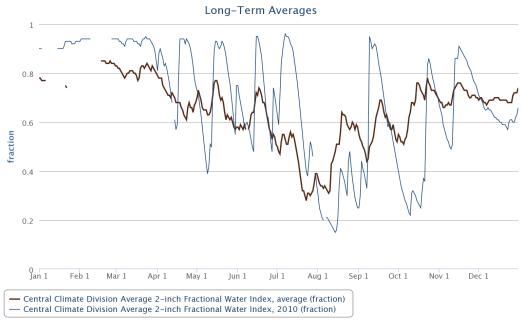

b)

Figures 4.12: a) 2-inch FWI departure from the long-term average for 2010 for the central climate division and b) time series of the 2-inch FWI for the central climate division for 2010 and the long-term average (Oklahoma Mesonet 2013).

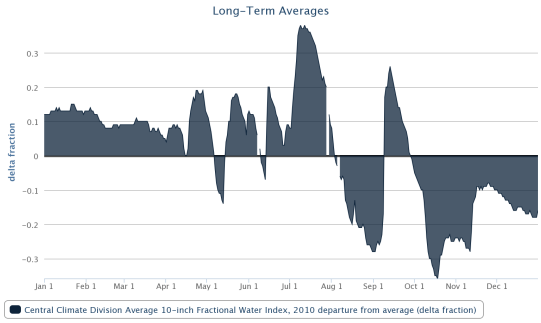

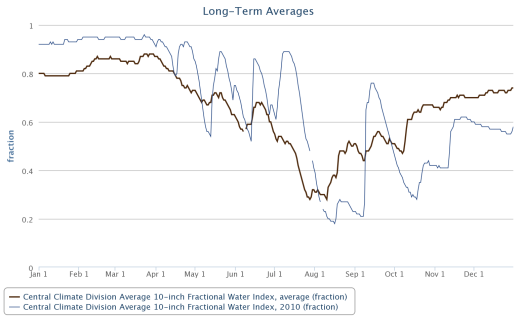

a) b)

Figures 4.13: a) 10-inch FWI departure from the long-term average for 2010 for the central climate division and b) time series of the 10-inch FWI for the central climate division for 2010 and the long-term average (Oklahoma Mesonet 2013).

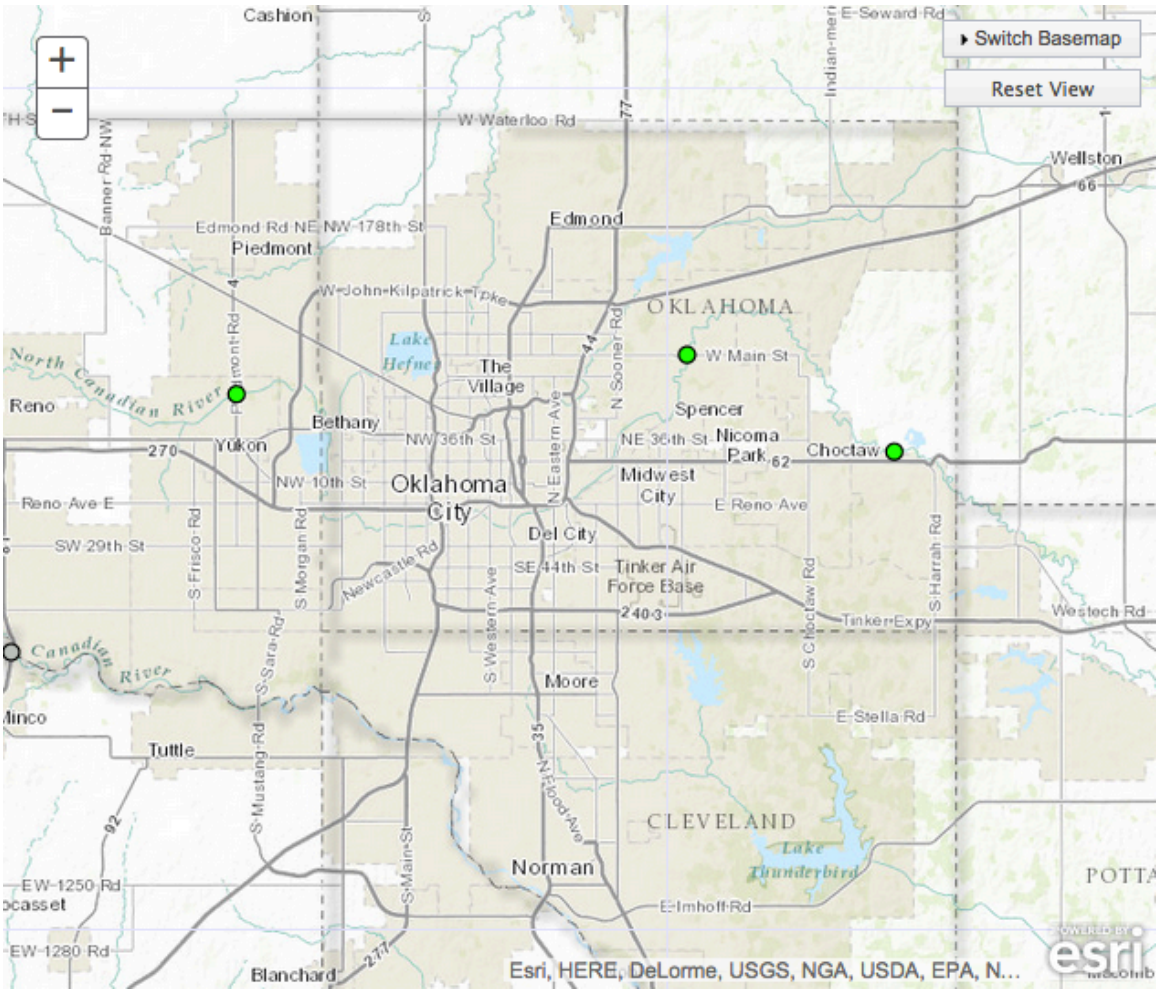

Figure 4.14: USGS streamgage sites utilized in the Oklahoma City 14 June 2010 flood event (NWS AHPS 2015 http://water.weather.gov/ahps2/index.php?wfo=oun).

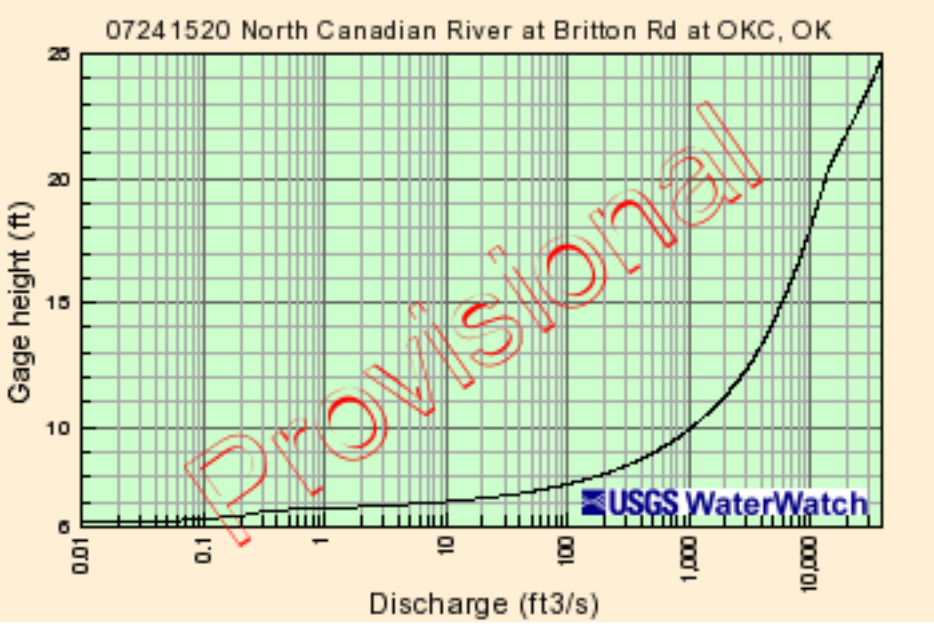

Figure 4.15: USGS rating curve for the USGS gage located on the North Canadian River at Britton Rd. in Oklahoma City, OK (USGS 2013).

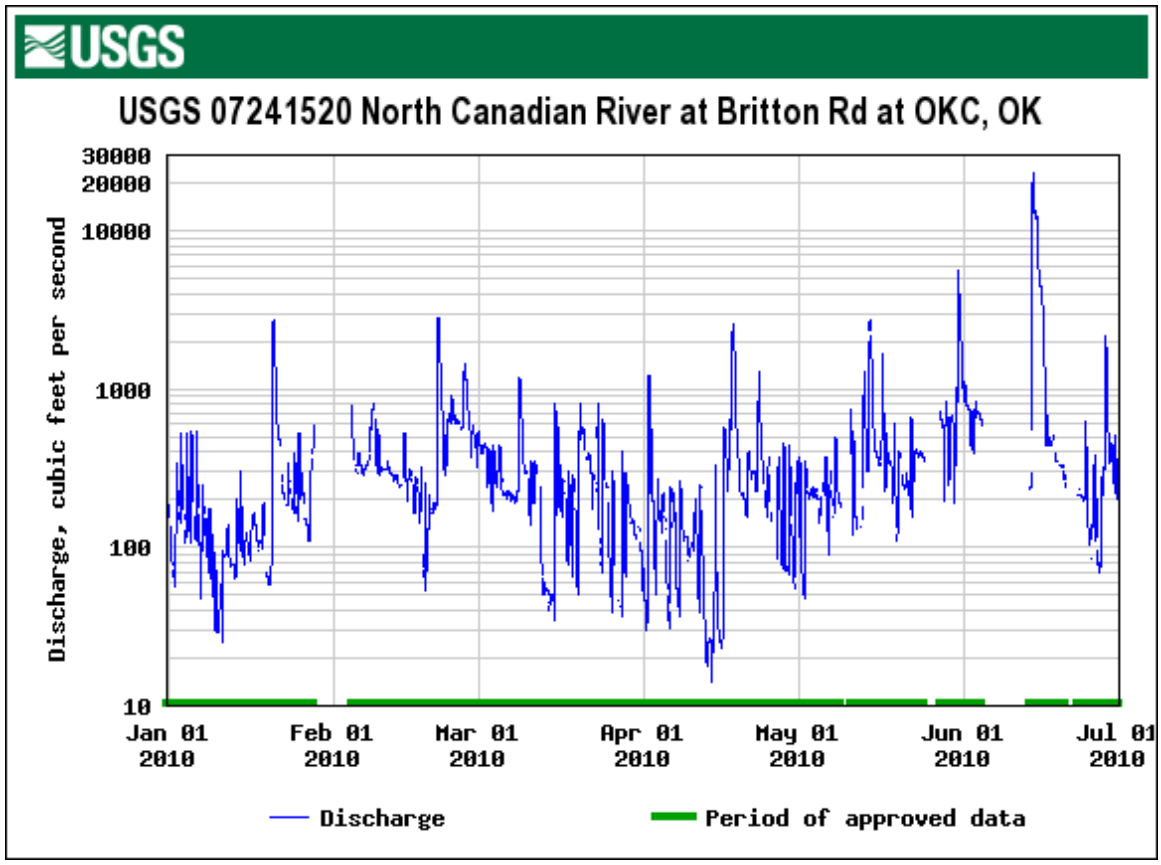

Figure 4.16: Discharge data from 1 January 2010 through 1 July 2010 for the USGS gage site located on the North Canadian River at Britton Rd. in Oklahoma City, OK (USGS 2013).

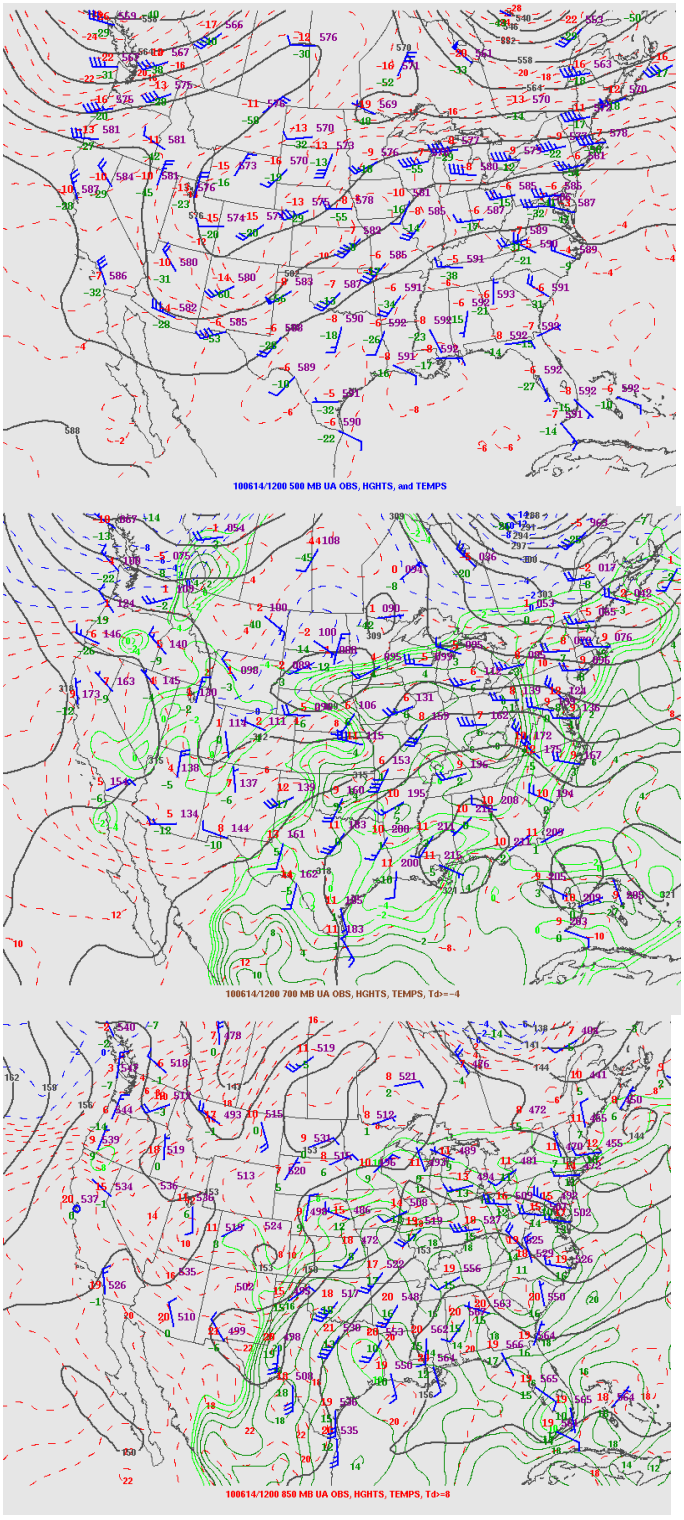

Figure 4.17: Upper air analysis at 1200 UTC on 14 June 2010 (top) 500 mb (middle) 700 mb and (bottom) 850 mb (NOAA SPC 2012 http://www.spc.noaa.gov/obswx/maps/).

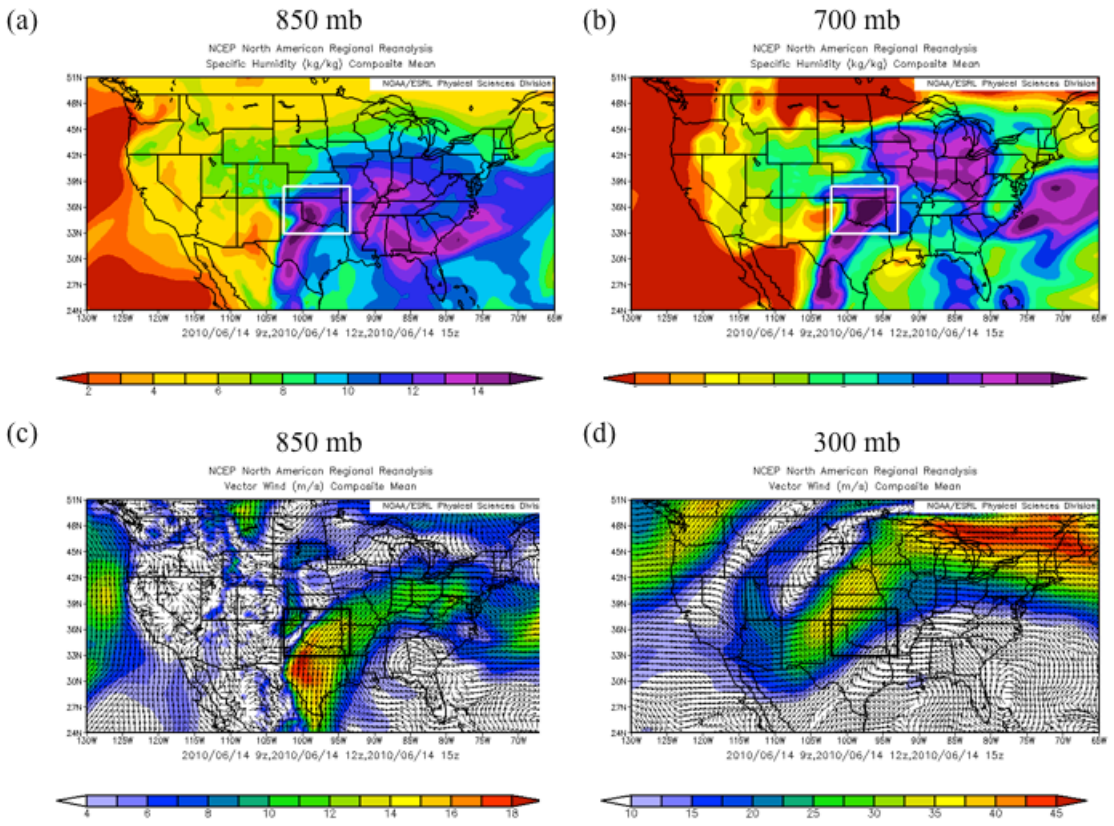

Figure 4.18: North American Regional Reanalysis (NARR) displaying composite maps of (a) 850 mb specific humidity, (b) 700 mb specific humidity, (c) 850 mb winds, and (d) 300 mb winds from 14 June 2010 (Image provided by NOAA/ESRL Physical Science Division, Boulder, CO from their website at http://www.esrl.noaa.gov/psd/).

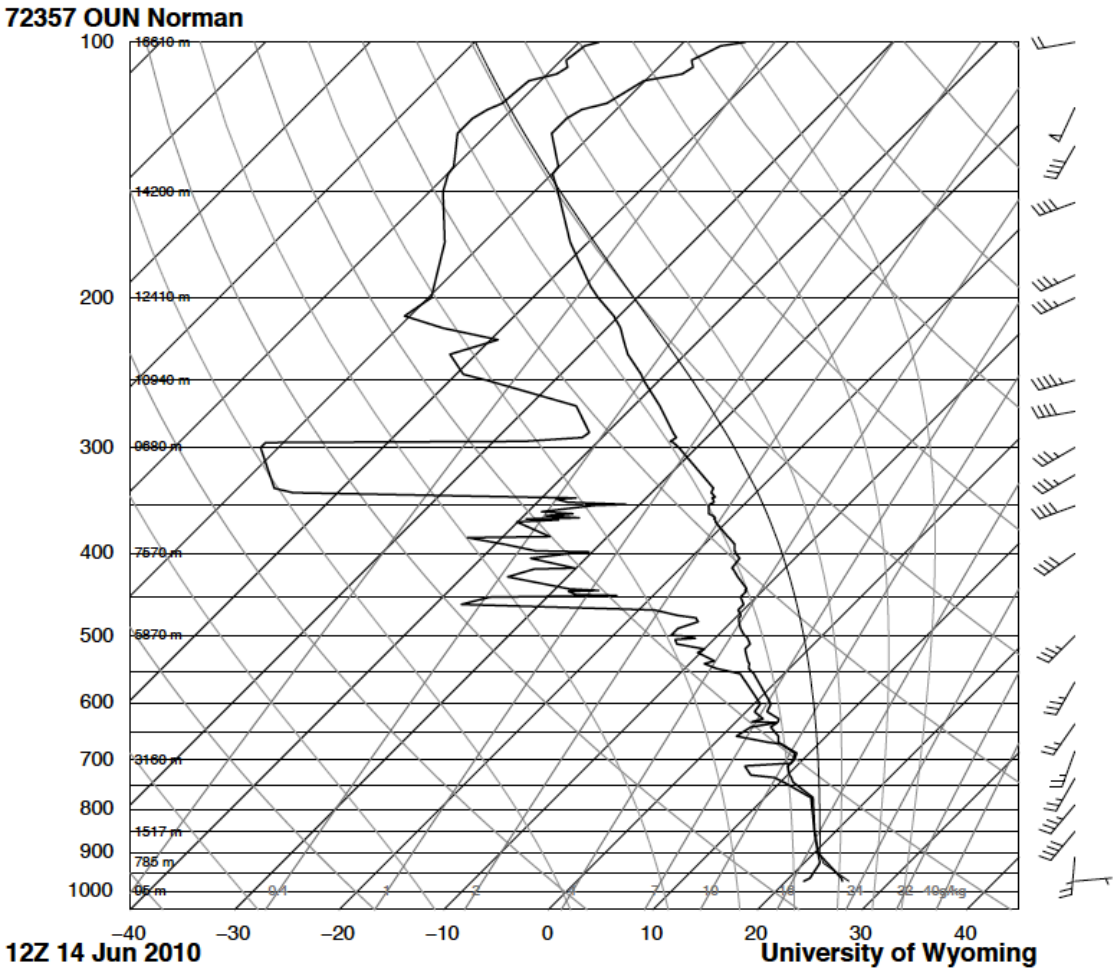

Figure 4.19: Sounding from the NWS Weather Forecast Office in Norman, OK (OUN) for 1200 UTC on 14 June 2010 (University of Wyoming 2013).

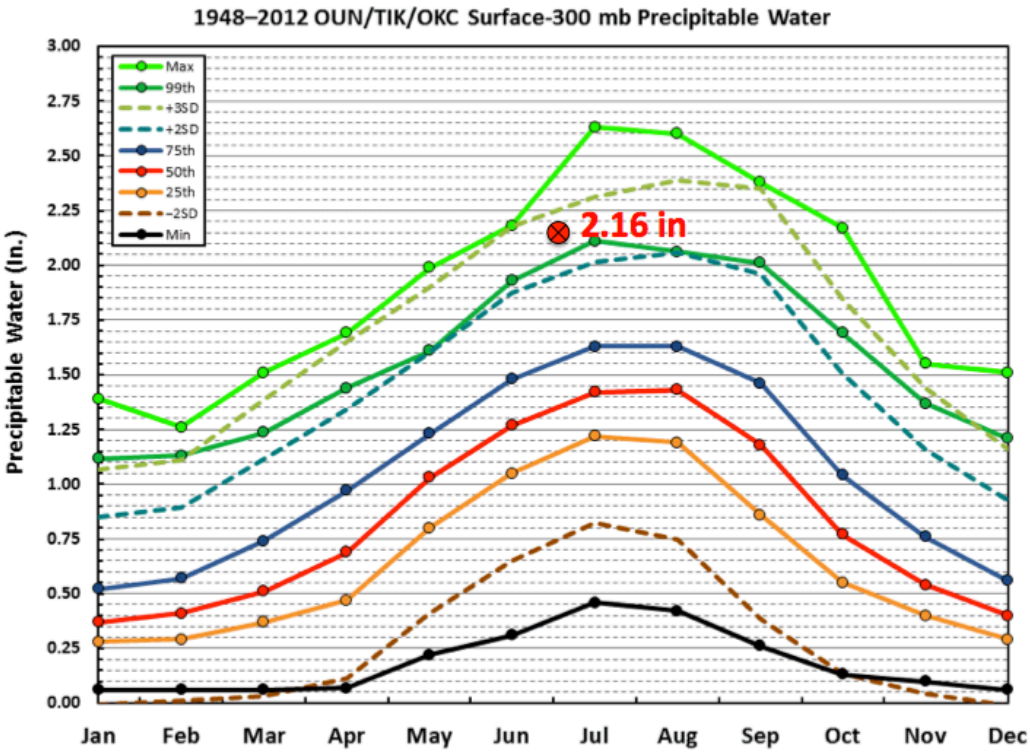

Figure 4.20: Annual climatology of precipitable water (PW) values for the Oklahoma City area (NWS UNR 2013) with the PW value for 1200 UTC on 14 June 2010 superimposed on the graph.

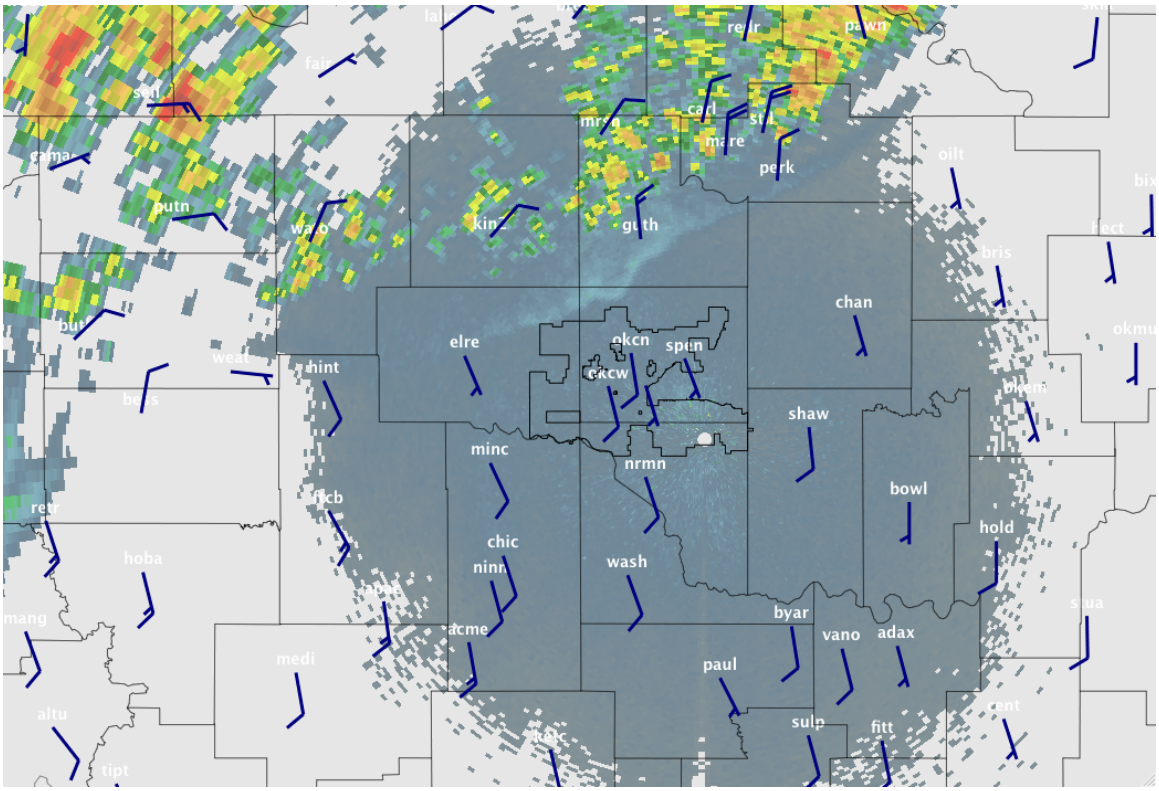

Figure 4.21: KTLX reflectivity and OK Mesonet 10 m winds at 0500 UTC (12:00 a.m. CDT) on 14 June 2010.

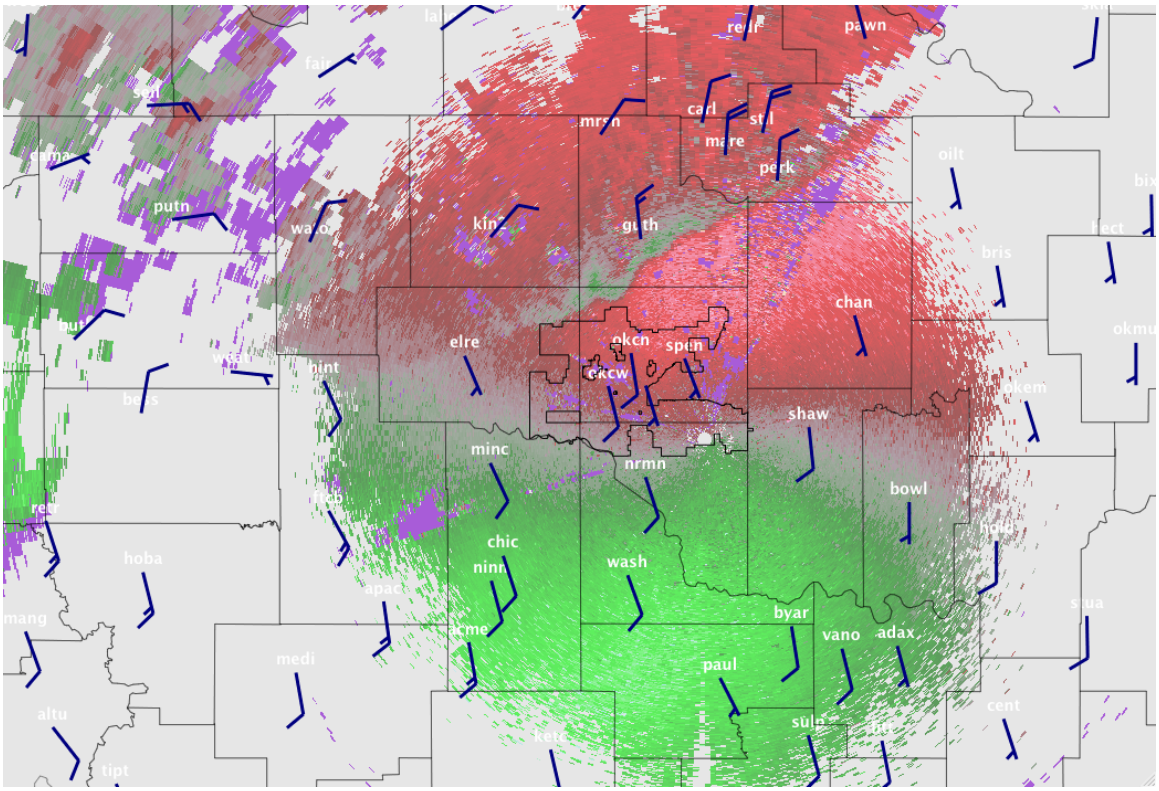

Figure 4.22: KTLX velocity and OK Mesonet 10 m winds at 0500 UTC (12:00 a.m. CDT) on 14 June 2010.

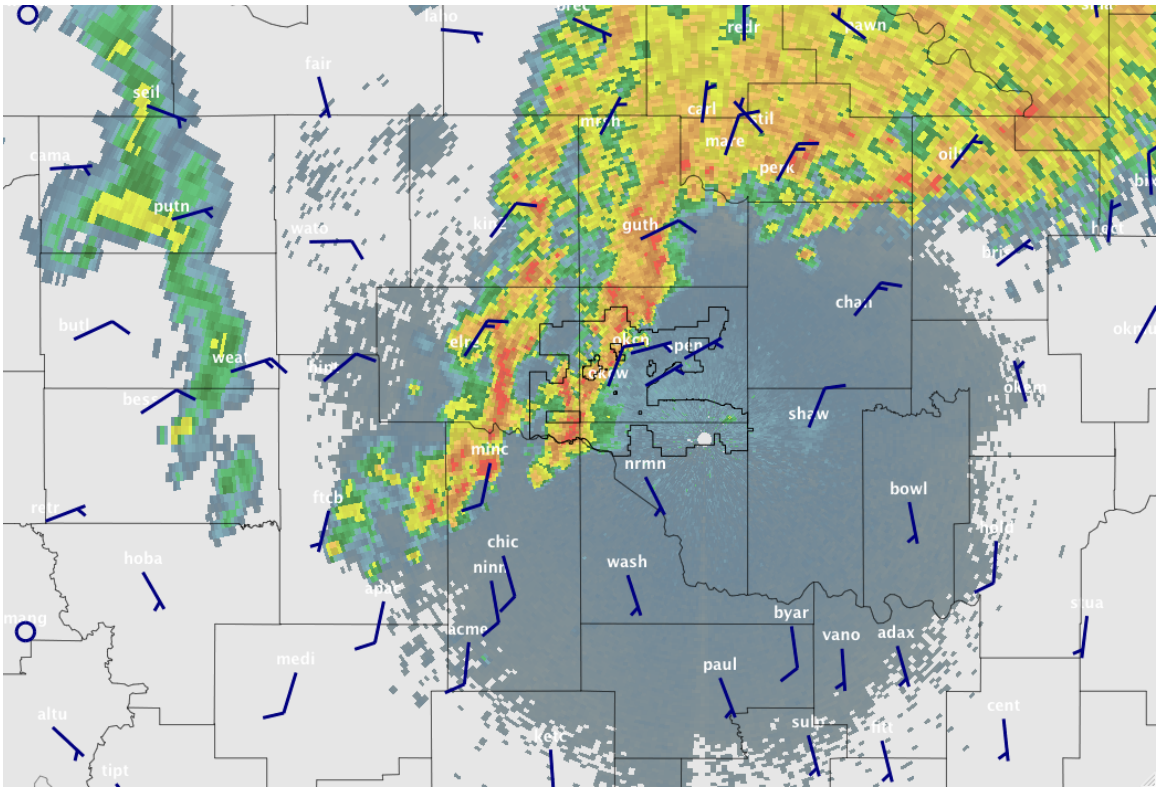

Figure 4.23: KTLX reflectivity and OK Mesonet 10 m winds at 0900 UTC (4:00 a.m. CDT) on 14 June 2010.

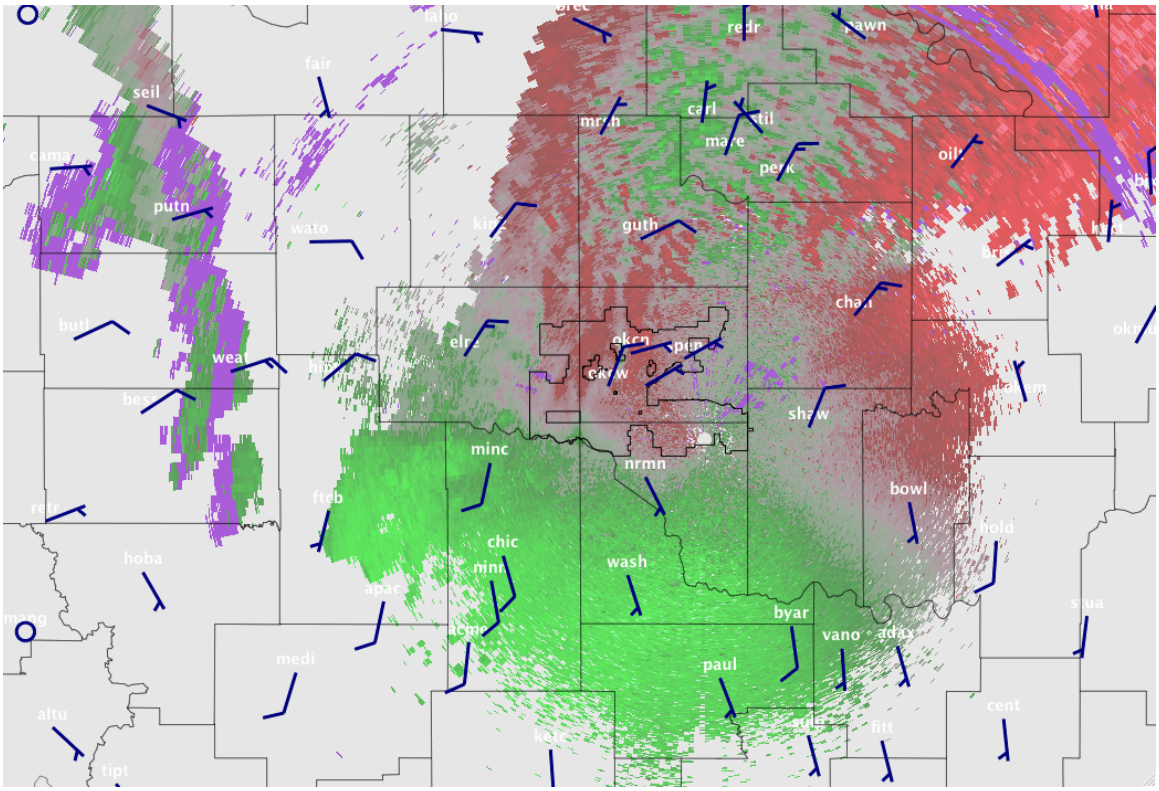

Figure 4.24: KTLX velocity and OK Mesonet 10 m winds at 0900 UTC (4:00 a.m. CDT) on 14 June 2010.

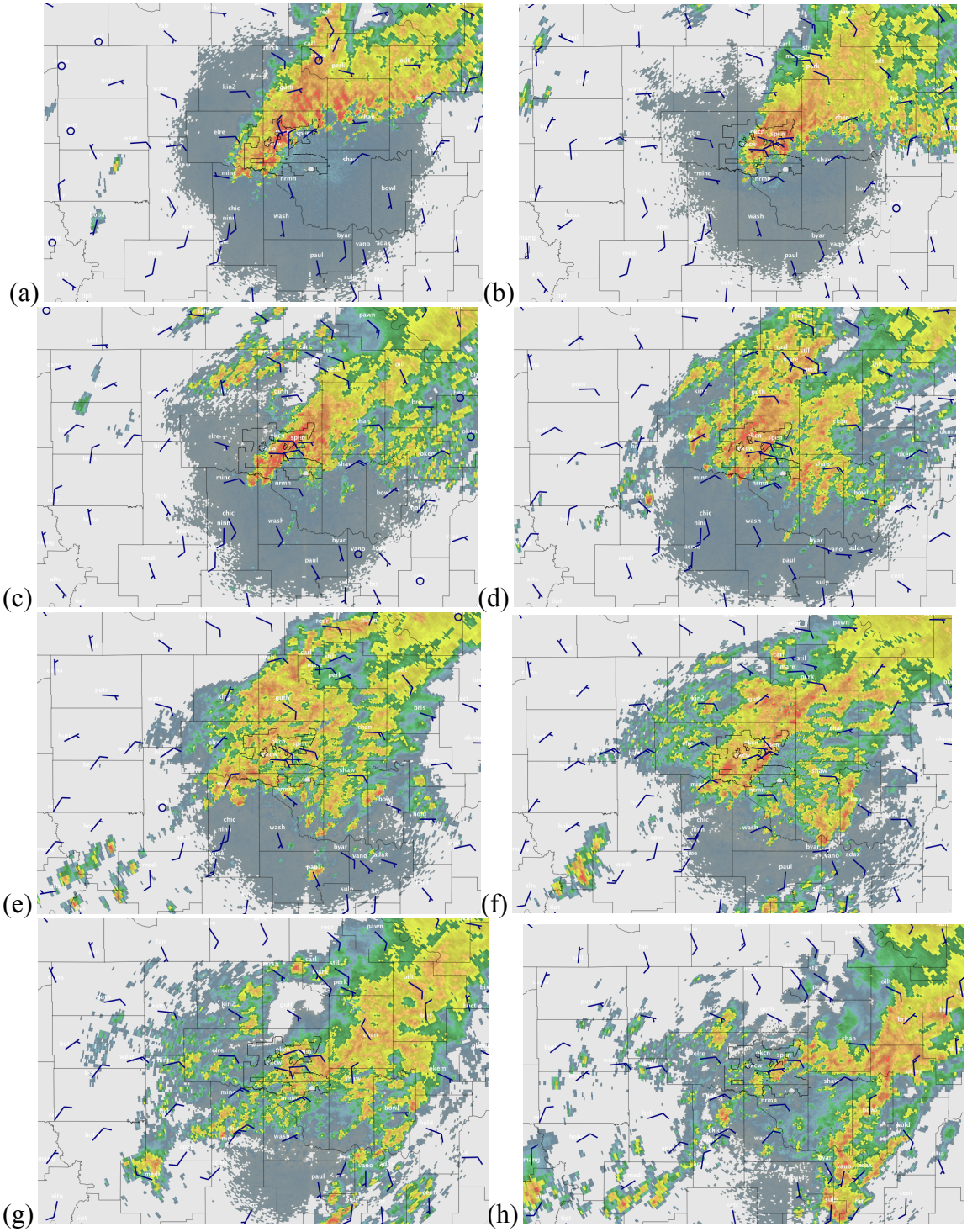

Figure 4.25: KTLX reflectivity and OK Mesonet 10 m winds at (a) 1000 UTC (5:00 a.m. CDT), (b) 1100 UTC (6:00 a.m. CDT), (c) 1200 UTC (7:00 a.m. CDT), (d) 1300 UTC (8:00 a.m. CDT), (e) 1400 UTC (9:00 a.m. CDT), (f) 1500 UTC (10:00 a.m. CDT), (g) 1600 UTC (11:00 a.m. CDT), (h) 1700 UTC (12:00 p.m. CDT) on 14 June 2010.

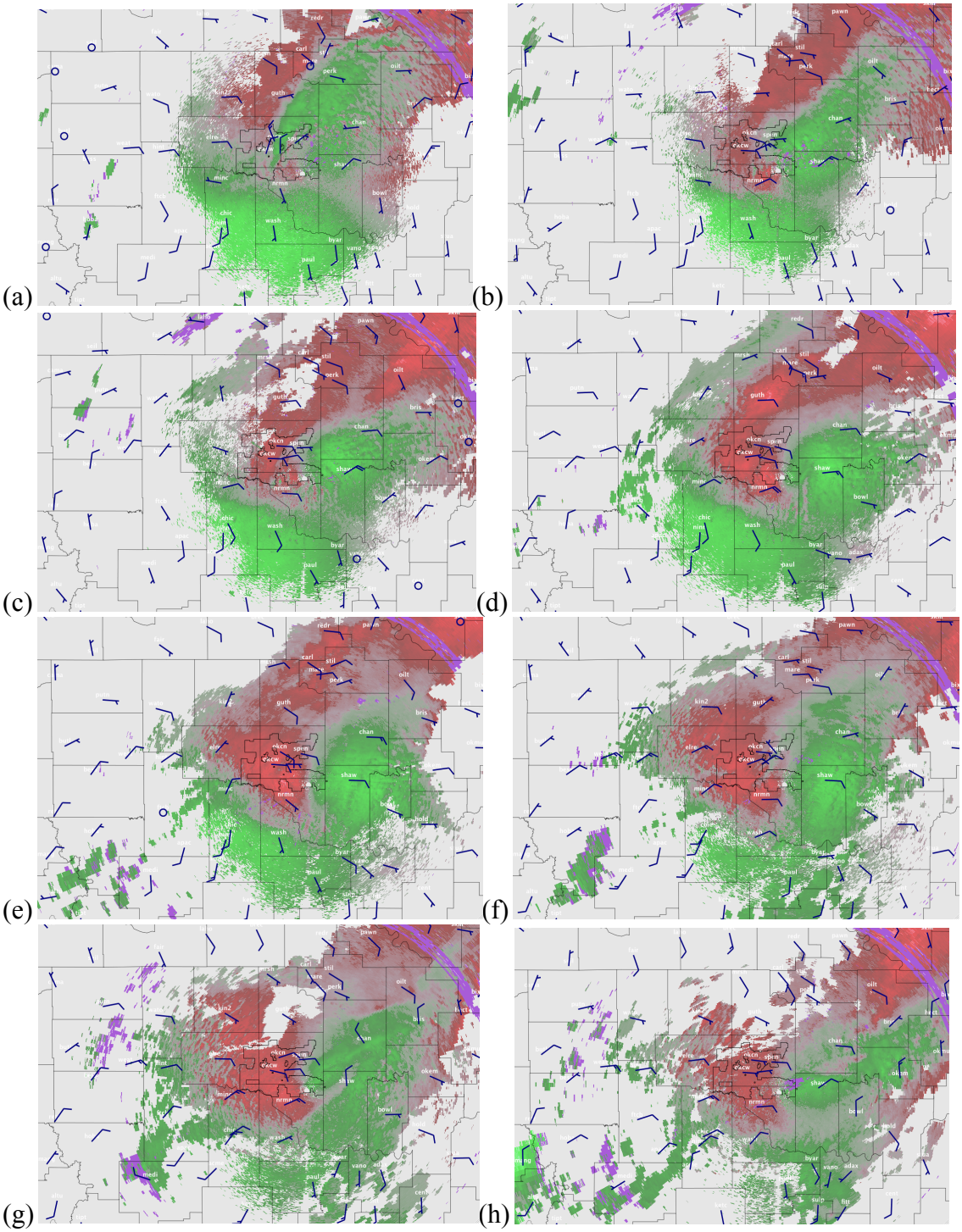

Figure 4.26: KTLX velocity and OK Mesonet 10 m winds at (a) 1000 UTC (5:00 a.m. CDT), (b) 1100 UTC (6:00 a.m. CDT), (c) 1200 UTC (7:00 a.m. CDT), (d) 1300 UTC (8:00 a.m. CDT), (e) 1400 UTC (9:00 a.m. CDT), (f) 1500 UTC (10:00 a.m. CDT)), (g) 1600 UTC (11:00 a.m. CDT), (h) 1700 UTC (12:00 p.m. CDT) on 14 June 2010.

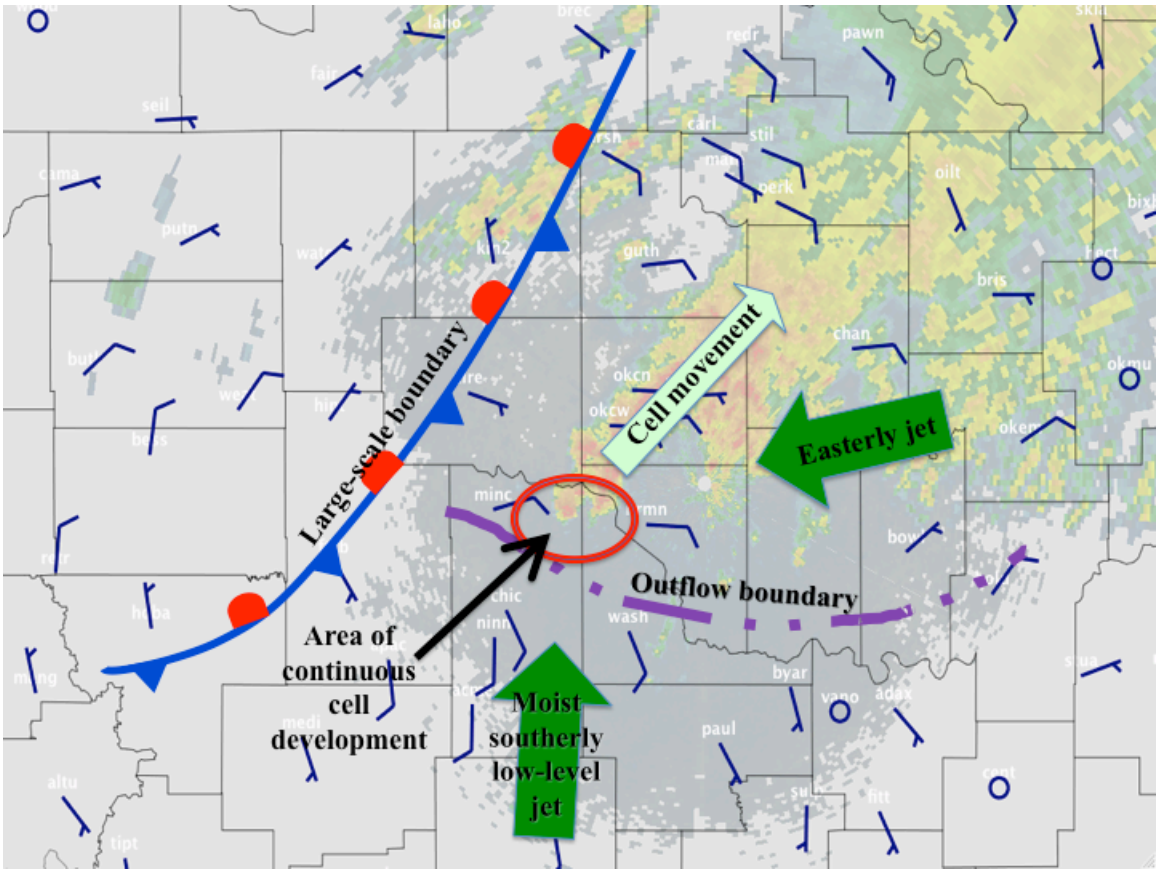

Figure 4.27: Schematic diagram that displays what led to the evolution of the 14 June 2010 Oklahoma City flood event.

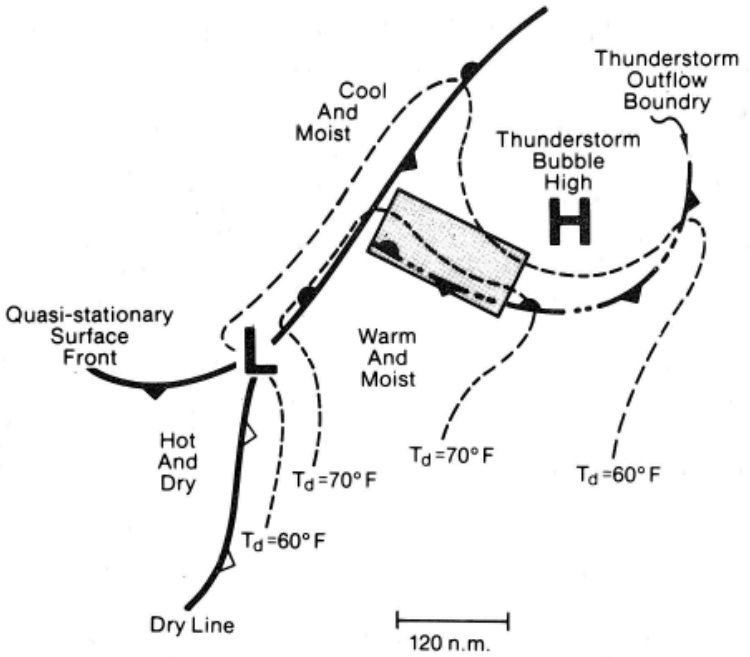

FIG. 10a. Surface pattern for a typical mesohigh event with details as in Fig. 6.

Figure 4.28: Schematic of a typical meso-high event that leads to flash flooding (Maddox et. al 1979).

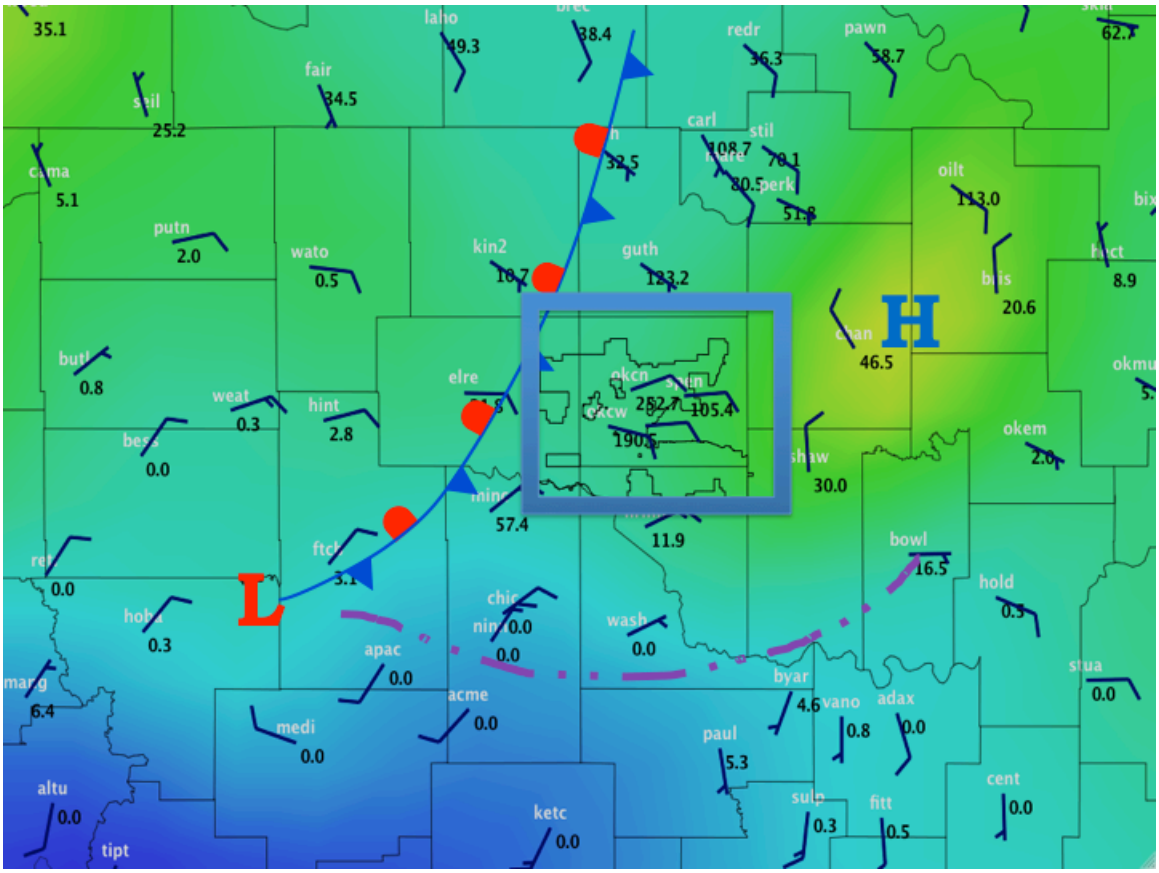

Figure 4.29: Spatial interpolation of OK Mesonet pressure reduced to sea level with plotted OK Mesonet 10 m winds and accumulated rainfall since midnight (mm) at 1600 UTC (11:00 a.m. CDT) on 14 June 2010.

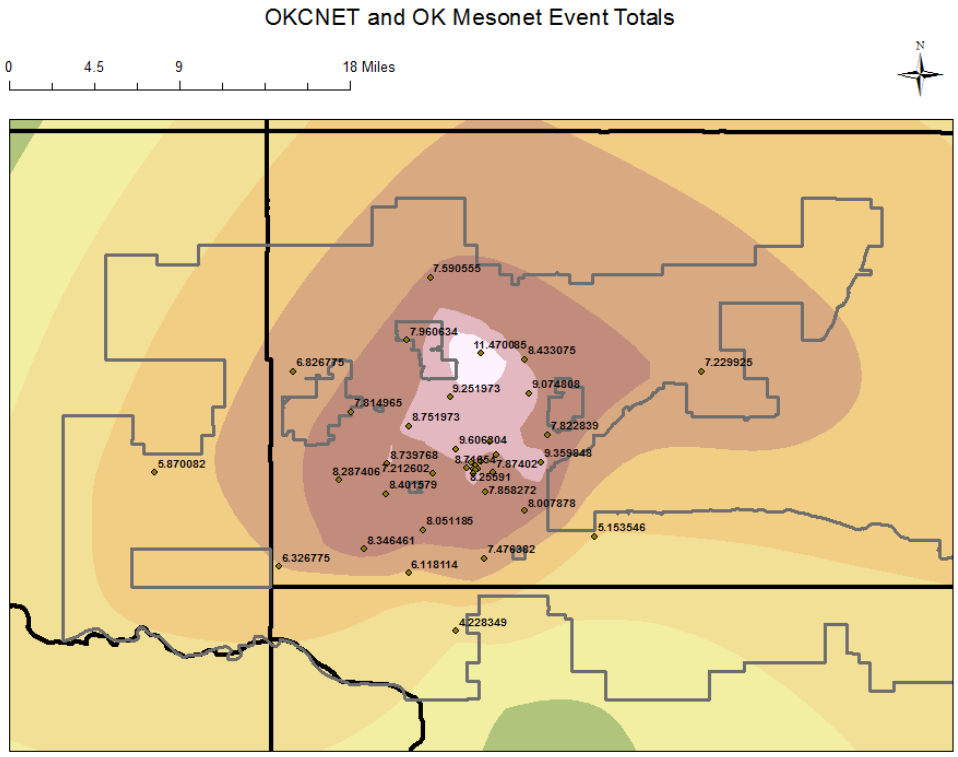

Figure 4.30: Rainfall distribution (inches) of the combined OKCNET and Oklahoma Mesonet observations.

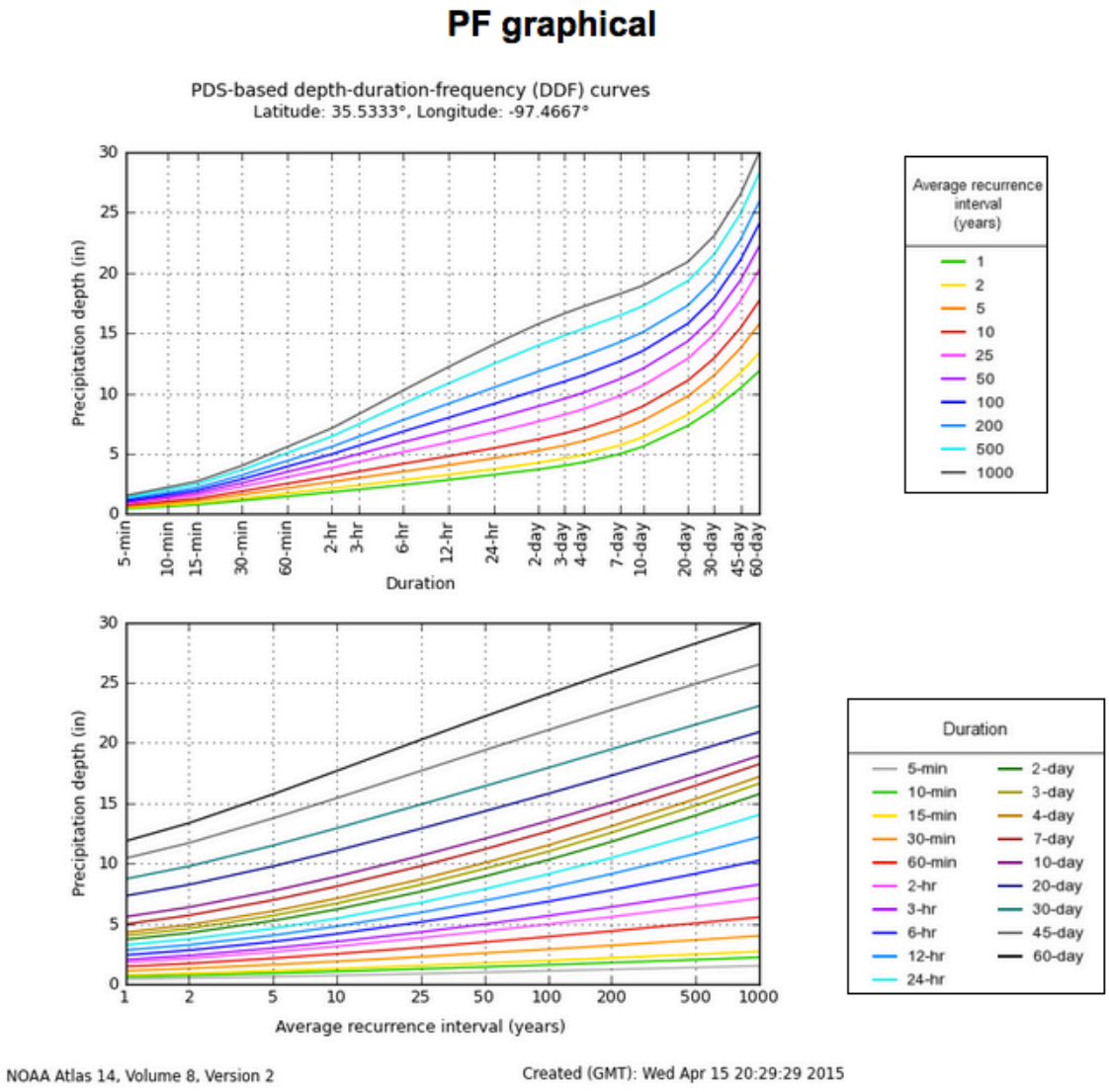

Figure 4.31: Precipitation frequency curves for north Oklahoma City, OK (NOAA HDSC 2015).

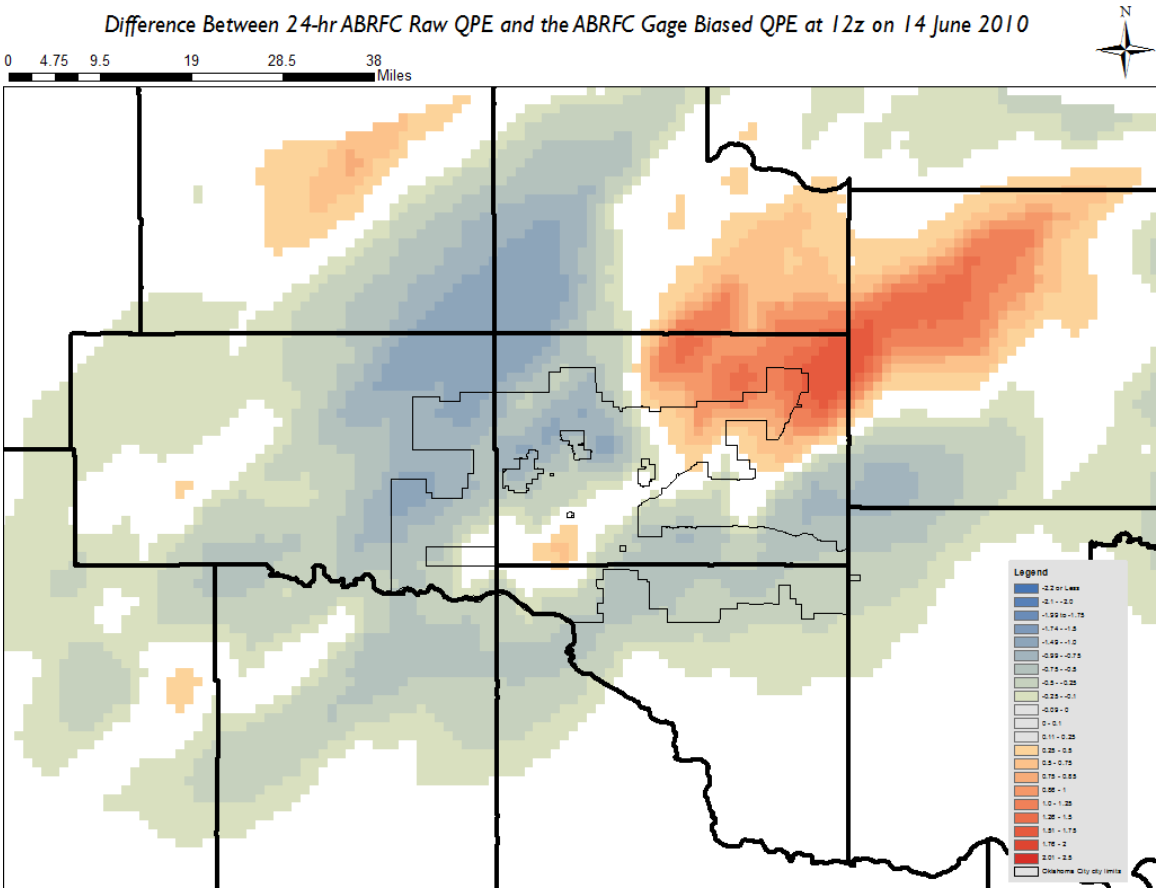

Figure 4.32: 24-hr. rainfall accumulation difference from the ABRFC's raw radar QPE 24-hr. rainfall accumulation minus the ABRFC's gage-biased QPE 24-hr. rainfall accumulation ending at 12z on 14 June 2010.

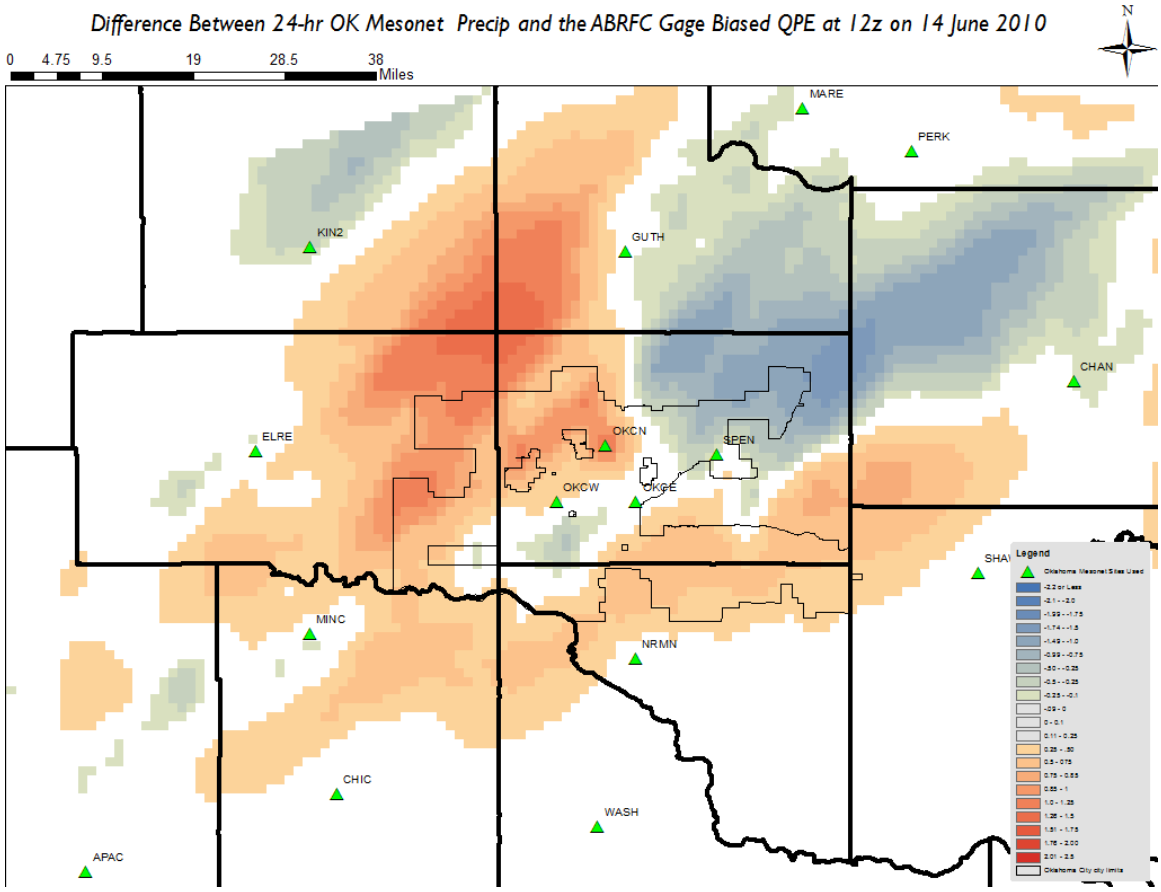

Figure 4.33: 24-hr. rainfall accumulation difference from the Oklahoma Mesonet 24-hr. rainfall accumulation minus the ABRFC's gage-biased QPE 24-hr. rainfall accumulation ending at 12z on 14 June 2010.

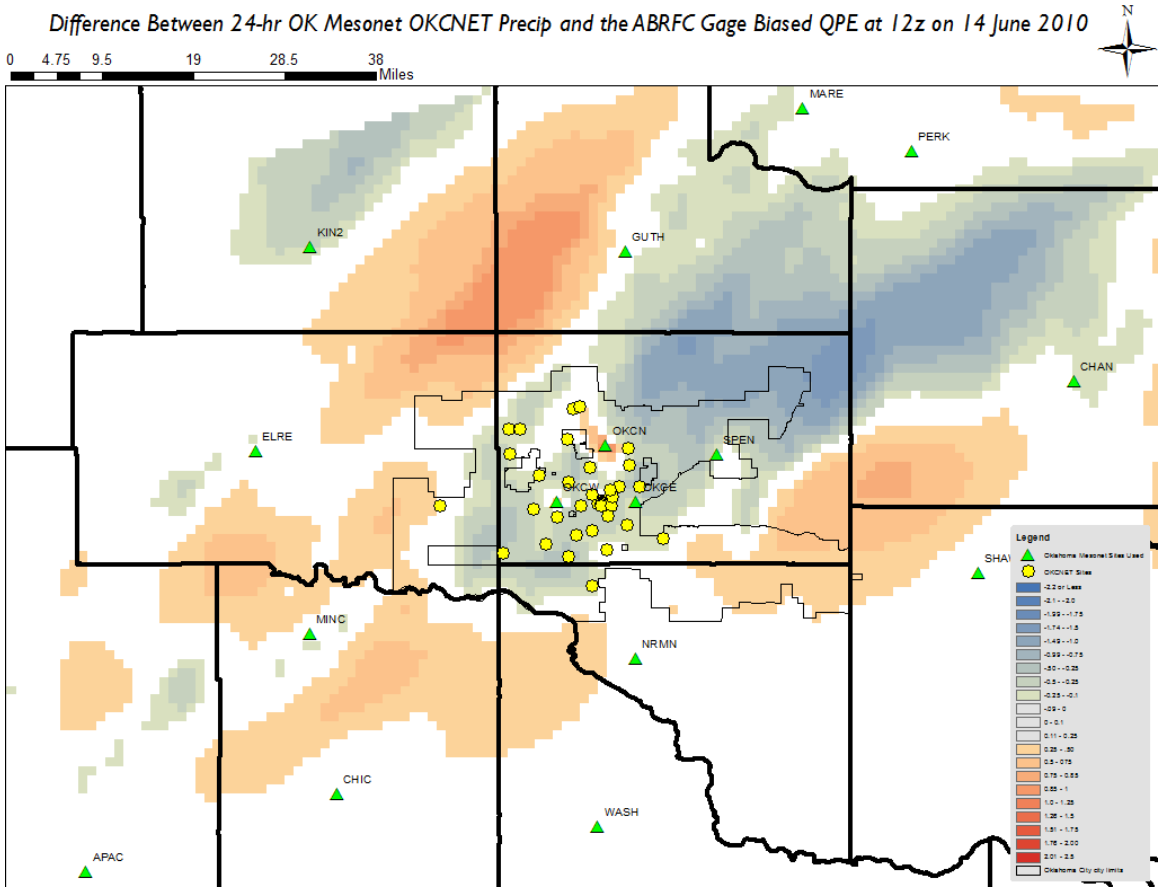

Figure 4.34: 24-hr. rainfall accumulation difference from the combined Oklahoma Mesonet/OKCNET 24-hr. rainfall accumulation minus the ABRFC's gage-biased QPE 24-hr. rainfall accumulation ending at 12z on 14 June 2010.

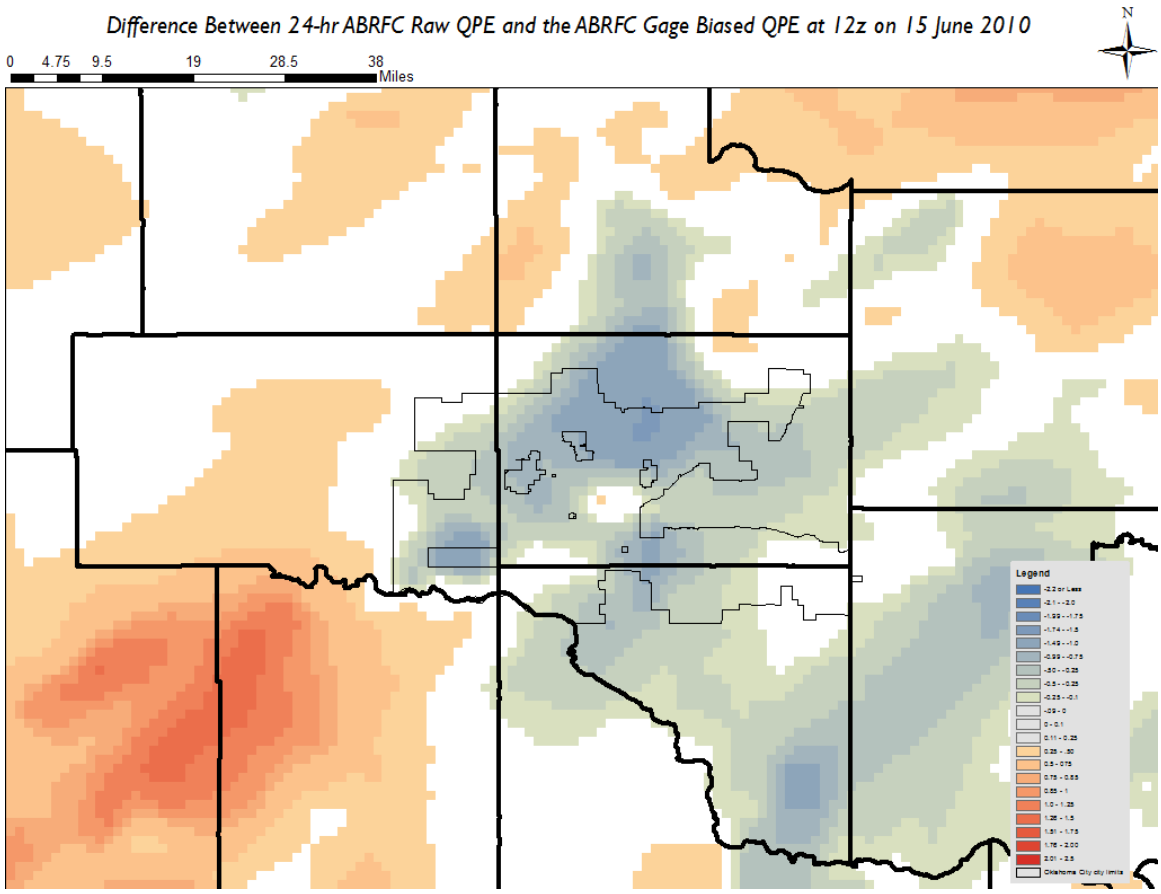

Figure 4.35: 24-hr. rainfall accumulation difference from the ABRFC's raw radar QPE 24-hr. rainfall accumulation minus the ABRFC's gage-biased QPE 24-hr. rainfall accumulation ending at 12z on 15 June 2010.

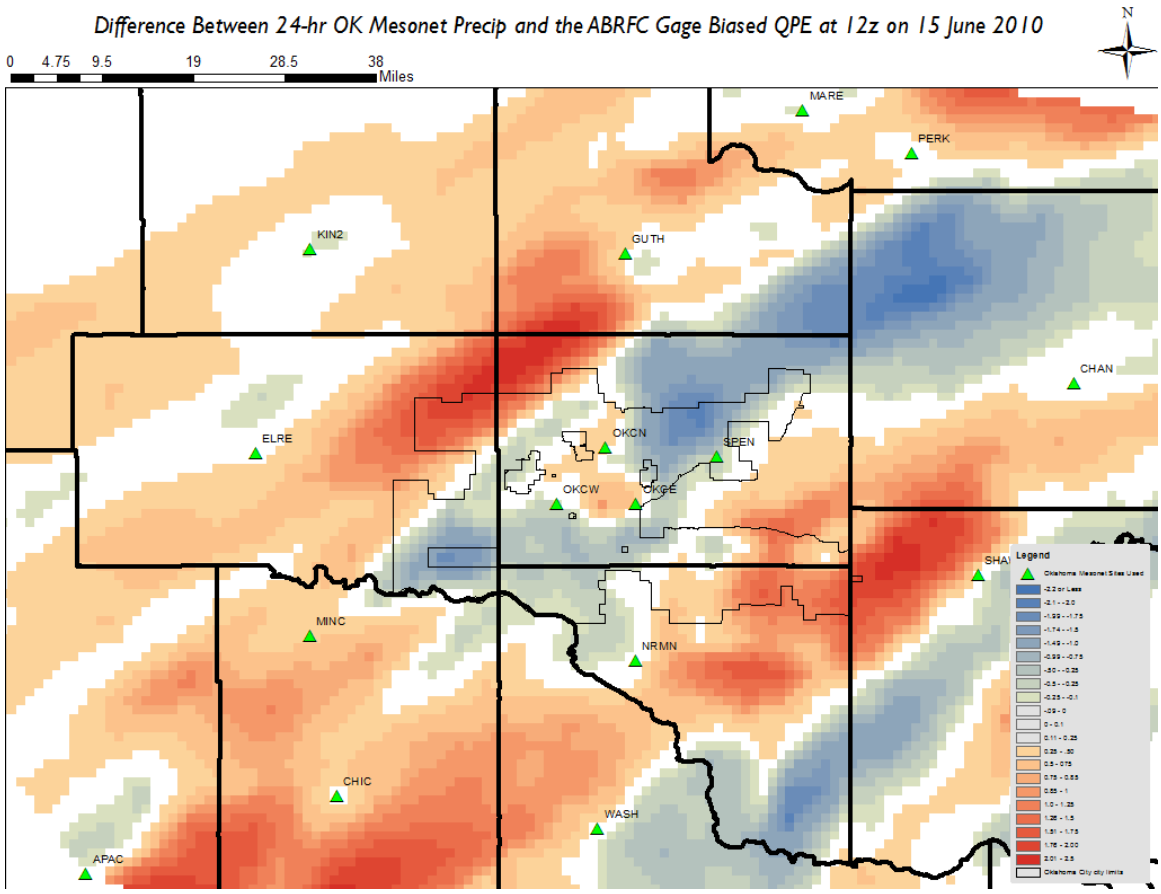

Figure 4.36: 24-hr. rainfall accumulation difference from the Oklahoma Mesonet 24-hr. rainfall accumulation minus the ABRFC's gage-biased QPE 24-hr. rainfall accumulation ending at 12z on 15 June 2010.

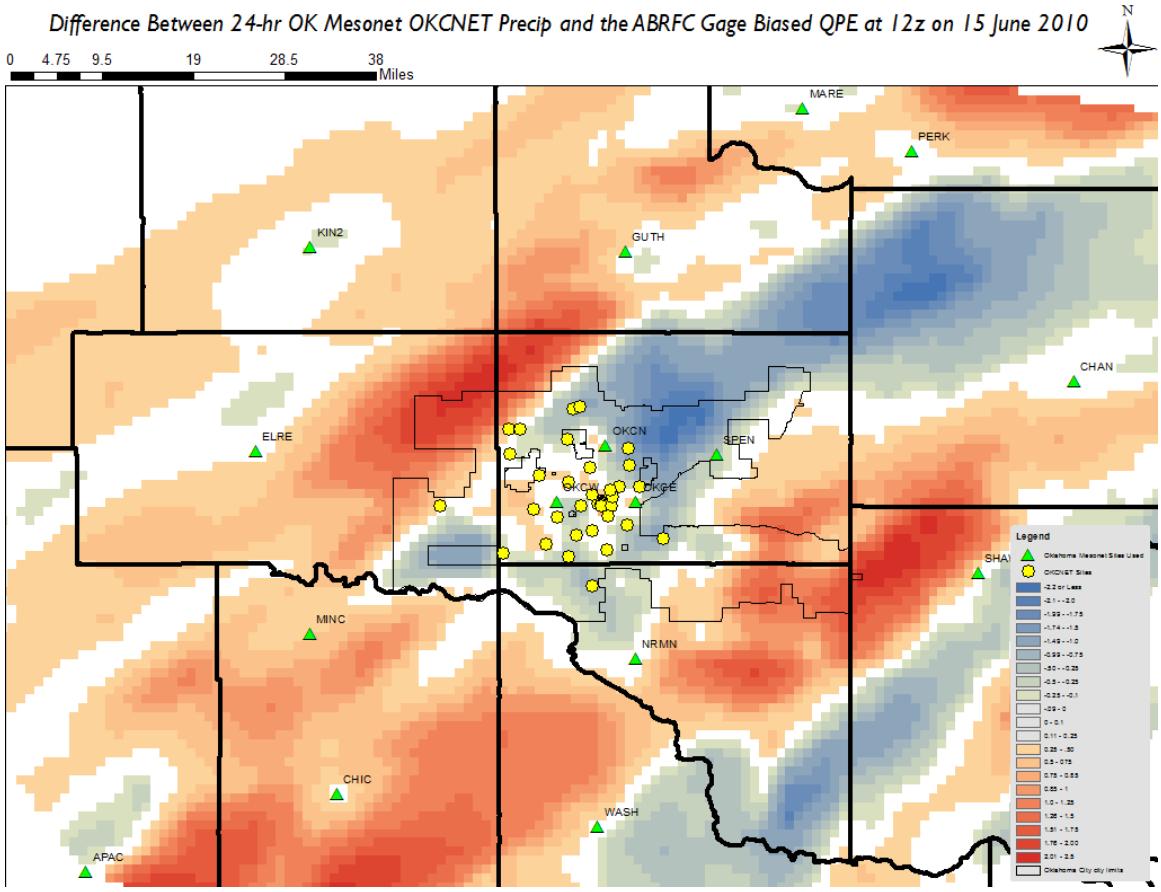

Figure 4.37: 24-hr. rainfall accumulation difference from the combined Oklahoma Mesonet/OKCNET 24-hr. rainfall accumulation minus the ABRFC's gage-biased QPE 24-hr. rainfall accumulation ending at 12z on 15 June 2010.

CHAPTER 5

SUMMARY AND CONCLUSIONS

5.1 Overview

Changes in surface characteristics have led to urban areas possessing different climates when compared to nearby rural areas (Voogt and Oke 1997), and urban hydroclimates are no exception. Flooding is one specific altered process related to urban hydroclimates. There are several important atmospheric and hydrologic components that play a role in whether flooding will occur in an area and to what degree. Some of these ingredients include: rainfall rate, duration of rainfall, antecedent precipitation and soil moisture, as well as size, topography, and land use/land cover of the drainage basin. Given the complexity of the urban hydroclimate, this dissertation directly addressed 3 of the main components that contribute to urban flood events: atmospheric conditions, hydrologic response, and land surface characteristics.

To explore the atmospheric component, quantitative analyses were performed on many thermodynamic variables and parameters that play a role in heavy rainfall episodes that can give rise to major urban flood events. This was assessed via rawinsonde analyses of forty past flood events that impacted numerous urban areas across the US. This approach took a broad geographical and temporal look at flash floods, as the spatial extent spanned the contiguous US over a 37-year period. To address the hydrologic response and land use/land cover factors, spatio-temporal trends of urban flooding, from

a hydroclimatological perspective, and characteristics associated with urban flooding events for several cities of within the state of Texas were examined. This was carried out through a partial duration series (PDS) approach using maximum daily discharge for five basins over a 13-year period. The thresholds needed to perform the PDS were identified and validated using a variety of sources including: established National Weather Service (NWS) flood stage, United States Geological Survey (USGS) rating curves, NWS local storm reports (LSRs), and the unique and cutting-edge National Severe Storms Laboratory's (NSSL's) Severe Hazards Analysis and Verification Experiment (SHAVE) data. Additionally, land use/land cover characteristics were obtained from the high-resolution National Land Cover Database (NLCD) 2011 created by the Multi-Resolution Land Characteristics (MRLC) Consortium. This approach zoomed in to a regional geographic scale and was assessed over a shorter temporal period (daily assessments over a 13-year period) than the earlier atmospheric assessment.

Finally, the 3 components (atmospheric, hydrologic, and land use/land cover) were brought together via the assessment of a 2010 flood event the occurred in Oklahoma City to gain a better understanding of the hydrometeorological factors that led to a specific event and to identify what urban-atmospheric-hydrologic interactions played a role in the event's evolution. Therefore, this final objective of the dissertation fine-tuned the geographic and temporal extent of the flash flood assessment through the examination of a local flood event, with an event duration of less than 48-hours in length. A combination of remotely sensed and in situ observation data were incorporated into this study, including the high-resolution Oklahoma City Micronet (OKCNET). Additionally,

the various observational networks were examined in order to assess whether or not optimal observing methodologies exist for urban flash flood events.

5.2 Summary

For the first objective, a synergistic study was conducted to analyze hydrometeorological aspects of forty major urban flood events in the US from 1977 through 2014 that were caused by locally heavy precipitation. Nearly two-thirds of the cases occurred during the summer months of JJA, the climatological peak in flash flood events for the US. Additionally, approximately 75% of the urban flash flood cases were associated with precipitable water (PW) values that were at least 2SD above the mean for that location and time of year, and all forty were above the 75th percentile (150% of the mean). A key point from this finding was that a universal threshold is not an appropriate way to analyze PW. With only 15 of the 40 cases (38%) examined in the study having PW values that exceeded 50.8 mm (2 inches), the common "broad brush" value often used by forecasters to heighten their awareness of flash flooding potential, over half of the devastating floods examined in this study may have been missed by forecasters had PW been a primary indicator for heightened flash flood potential. This clearly demonstrates the need to include the PW climatology for the location in question to attain proper perspective of the degree to which the value is anomalous.

However, it is the assembly of multiple ingredients that leads to flash flood-producing heavy rainfall events. While the PW anomaly appears to be a strong indicator that could be used to alert forecasters to the potential of a heavy rainfall event, that condition alone is not sufficient to produce a flash flood event for any location.

Additionally, these events revealed that, despite geographic location and time of year, most events had a warm cloud depth (WCD) of at least 6 km, which was defined here as the layer between the lifted condensation level (LCL) and the height of the -10°C level. These conditions lead to warm rain processes, which are known heavy rainfall producers. Current results have also shown that instability and wind shear play an important role, with MUCAPE between 1000 and 2200 J kg^{-1} and weak to moderate speed and directional wind shear present for the events in question. Finally, a composite flood sounding was also calculated and revealed a characteristically tropical thermodynamic structure, despite cases related to tropical cyclones being excluded from the study.

For the second objective, a partial duration series (PDS) approach was performed to examine daily maximum discharge values from five watersheds across North and Central Texas to identify urban flooding trends from 2001 through 2014. NWS COOP rainfall data were also examined to assess the precipitation component of the water cycle. This objective showed that the rural locations' flood occurrences were tied to how anomalously wet that year was. However, that trend was not equaled for the urban locations because, while the urban basins did experience a high number of floods during wet years, they also experienced a relatively high percentage of flood events during abnormally dry years, but their rural counterparts did not. By stratifying the analysis into months, it was revealed that urban locations had a higher percentage of floods occur during months when 75% or less of normal rainfall was observed than did the rural locations. Additionally, when the seasonal breakdown of flood occurrence was examined, it was revealed that the urban locations had a higher percentage of floods occur during the climatological summer months of JJA, which, as mentioned earlier, has been

identified as the climatological peak in flash flood events for the US. This finding also echoes the seasonal breakdown finding outlined in the previous chapter of this dissertation that demonstrated the peak occurrence of urban flood cases examined were during JJA as well.

Finally, various right-tailed Mann-Kendall tests were conducted on the data in order to assess statistical significance through the examination of the p-value. It was concluded that it was statistically significant to the 90^{th} percentile that 5 of the 6 basins experienced more flood events as the monthly % of normal rainfall increased. However, when a Mann-Kendall test was run comparing urban and rural basin flood occurrence during months that experienced only 0-75% of normal rainfall, the test failed for all comparisons, so no statistical significance could be concluded for that particular statistical test. This was likely due in part to the relatively small number of flood events that occurred for all locations in the "driest" months category. However, when the urban vs. rural Mann-Kendall test comparing the number of flood days instead of the number of flood events was run, some statistical significance could be concluded for 2 of the comparisons: Dallas FAA/White Rock (urban basin) vs. Greenville/Cowleech (rural basin) and Joe Pool/Walnut (urban basin) vs. Greenville/Cowleech (rural basin). Because the Dallas FAA/White Rock vs. Greenville/Cowleech comparison also had a similar number of total flood events for the period of record, this Mann-Kendall result suggested that the urban basin (White Rock Creek) was more "flashy" than the rural basin (Cowleech Fork) because it had a faster response and recovery than the rural location. This finding adds to the current body of urban flood research by highlighting the

"flashy", quick response nature of urban drainage basins through an observational trend analysis using a challenging, non-trivial approach (PDS) and a robust statistical analysis.

For the third objective, a high-resolution observational case study was performed for a June 2010 Oklahoma City flash flood event. Record precipitation fell in the Oklahoma City metropolitan area on 14 June 2010, which led to a significant flash flood event for the area. An analysis of the antecedent conditions revealed that central Oklahoma was not abnormally wet or dry, so the soils were not necessarily preconditioned to flooding. However, between 100 and 300 mm of rain fell over a 12 hr. period, with the peak falling during a 6-hr. period that included the Monday morning rush hour, and numerous flash flood reports ensued as a result. Like the previous objective demonstrated, this indicates that flash floods can and do occur during dry antecedent conditions. The detailed analysis of the event itself showed that the extremely heavy rainfall and resultant flash flooding on 14 June 2010 was due to a number of critical factors including:

- A nearly stationary outflow boundary situated just south of Oklahoma City, providing focus for storm initiation and redevelopment with convection repeatedly moving over the urban area
- A strong low-level jet and weak speed and directional shear in the lower troposphere
- The development of an easterly jet that balanced the southerly low level jet, preventing the advancement of the outflow boundary for several hours
- Broad ascent through the lower troposphere evident by the conditionally unstable atmosphere (low LFC and CAPE values near 2000 J/kg)

- Very moist ambient environment evident in the extremely high precipitable water values and mixing ratios

This event was a classic meso-high event, and the available high spatial and temporal resolving observation systems allowed for the detailed identification of such. Despite the maximum precipitation being concentrated in and downwind of the city, it cannot be concluded that the urban area created an enhancement of the rainfall for the event because the mesoscale evolution of the event, including the setup of both a southerly low level jet and an easterly low level jet, appeared to be the driving force behind cell development and the resultant rainfall distribution. However, whether or not the urban area played a role in the rainfall distribution cannot be ruled out either.

Additionally, a comparison of the different observing methodologies was performed and revealed that the inclusion of high-density, research quality in situ networks, like the Oklahoma Mesonet and OKCNET, provided valuable information for the development of a more complete assessment of the spatial distribution of rainfall across the area. Including such high spatial and temporal resolution data was especially critical given the limitations of raw radar products regarding rainfall estimation during excessive rainfall events resulting from warm rain processes. This finding suggests that augmenting radar-based hydrometeorological products with high-density ground-truth observational networks increases the accuracy of the final radar product. However, the analysis also revealed that the gage-biased radar mosaic QPE was unable to capture all of the fine details of the rainfall distribution for the event that were observed by the OKCNET, likely due in part to the differences in spatial resolution between the two datasets, especially within the central business district (CBD). These results illustrate that

the inclusion of rainfall observations from high spatial resolution networks, like the OKCNET, provide rainfall information that the comparably course-resolution radar data often misses. Incorporating such data provides valuable small-scale details that could potentially make a substantial difference in observed impacts. Therefore, there is a need for use of high density in situ rainfall observations along-side more spatially continuous radar products for assessment of heavy rainfall events to get a more thorough picture of the rainfall distribution across an area.

This study provides unique insight into a specific observed urban flooding event for Oklahoma City through the coupled analysis of high spatial and temporal resolution in situ data and robust radar mosaic data. This approach has the potential to provide additional insight into the event, and understanding the details of such an event in Oklahoma City can aid urban planners, emergency managers, weather forecasters, and water resource management in preparing for future events.

5.3 Conclusions

Results from this dissertation demonstrated the complex nature of urban flash flood events but provided clear guidelines to help anticipate and more accurately observe future events. Detailed assessments of the atmospheric conditions *and* the surface/subsurface conditions (from both a hydrologic and land use perspective) are crucial in order to obtain accurate assessments of the potential for, and resultant magnitude of, urban flash flood events. Based on these findings, a conceptual framework to maximize proper anticipation and detection of flash flood events can be formulated and summarized as follows. First, from a hydrologic and land use/land cover perspective,

it is important for scientists to identify which basins have a considerable urban footprint because it has been demonstrated that increased impervious surface percentage common in cities puts urbanized areas at increased risk for flood events. Urban areas tend to have more runoff and faster hydrologic response times when heavy rainfall affects urban basins, which can catch people off guard if they are unaware of the land use/land cover of the watershed. Therefore, knowing which areas have significant urban footprints will help during flash flood warning situations because meteorologists can hone in to those areas and anticipate "flashy" responses, thus providing additional lead time to the public. Furthermore, it is extremely important for those entrusted with flash flood forecasting, warning, messaging, and response to have an *up-to-date* and complete understanding of the hydrologic and land use/land cover characteristics for the area they are responsible for protecting because continued urban growth will change the fabric of the US landscape, and the observed hydrologic response is magnified with increased urban land cover.

Additionally, previous research has shown that antecedent precipitation and soil moisture are important, but Objectives 2 and 3 demonstrated that just because an area is not "primed" (i.e. "wet" conditions in place before the heavy rain event begins) does not mean that flash floods are not still a distinct possibility. Therefore, knowing the current hydrologic state of the area is important but should not warrant discounting the potential for a flash flood event just because the antecedent conditions happen to be "dry". Furthermore, Objectives 1 and 2 showed that a higher number of floods occurred during the summer, which is typically thought of as a relatively "dry" season for many parts of the country. Being unaware of these trends and/or being complacent only breeds a reactive response instead of a proactive response, which can have adverse affects and

leave the public feeling “caught off guard” or having “little to no warning”, a phrase no meteorologist, emergency manager, or first responder likely wants to hear.

From an atmospheric perspective, Objective 1 demonstrated that when an upper level system approaches, forecasters need to include in their forecasting arsenal a continuous assessment of the PW *anomaly for their specific area and time of year*, as well as the projected WCD, MUCAPE, and wind shear. Once an event has begun, continued situational awareness of the environment, both on the mesoscale and microscale, is imperative because, as Objective 3 showed, the evolvement of the various surface boundaries and progression of the various convective cells led to the birth and eventual demise of the heavy rainfall that caused the flash flooding in Oklahoma City. Furthermore, this analysis showed that radar velocity products can provide utility for flash flood monitoring as well by displaying subtle boundary interplay above the surface, which was critical for the evolution of the OKC event, thus demonstrating that this base product has more uses than just identifying rotational couplets associated with severe thunderstorms.

The Oklahoma City case study examined here also provided evidence that including *both* in situ observational data, like the Oklahoma Mesonet and OKCNET, and remotely sensed data, like the radar mosaic QPE products available from River Forecast Centers, is imperative in order to have a continual and more-thorough picture of the evolvement of a flash flood event. Leveraging all available products and understanding the limitations of those datasets will help provide a more accurate picture of a flood event.

Unfortunately, solving the "flash flood problem" will need to go beyond the meteorology and hydrology of events and dive into better education of the public. Additional work has already begun in this area; namely, a flash flood severity index (FFSI) is being developed by an interdisciplinary group of researchers from the 2013 Studies of Precipitation, flooding, and Rainfall Extremes Across Disciplines (SPREAD) workshop, hosted by Colorado State University. The FFSI project will eventually shed more light on flash flood events and help meteorologists and the public better understand past events and plan for future ones. This endeavor is important because multiple statistics have demonstrated the deadly nature of flash flood events over the past several decades, and public response does not appear to be substantially improved because floods remain one of the deadliest natural hazards.

The research presented in this dissertation has provided additional insight into the problem through the assessment of past urban flash flood events. However, because a high percentage of US residents already reside in urban areas and that percentage is only expected to increase over the coming decades, the risk associated with flash floods is only expected to increase as well. Rainfall is usually such a benign occurrence, but under the right conditions, it can be deadly. The knowledge gained from this dissertation and planned future work has the potential to provide insight and help forecasters, emergency managers, urban planners, and the public prepare for future events.